



**Institute of
Applied Physics**

Friedrich-Schiller-Universität Jena

Optical System Design Fundamentals

Lecture 4: Optical Imaging with Diffraction

2024 / 05 / 28

Vladan Blahnik

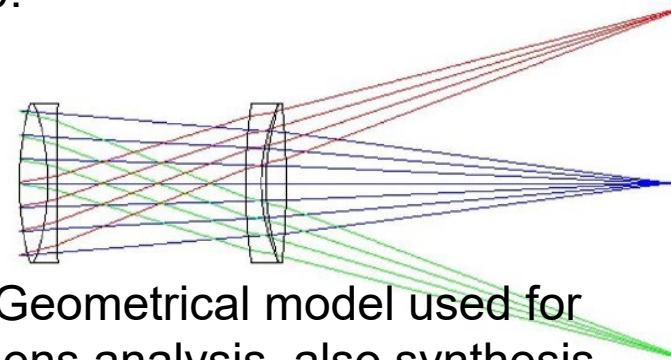
Preliminary Schedule - OSDF 2024

1	07.05.2024	Optical Imaging Fundamentals	Fermat principle, modeling light propagation with ray and wave model; diffraction; Snell's law, total internal reflection, light propagation in optical system, raytracing; ray and wave propagation in optical systems; pinhole camera; central perspective projection; étendue, f-number and numerical aperture, focal length; ideal projection laws; fish-eye imaging; anamorphic projection; perspective distortion, Panini projection; massive ray-tracing based imaging model	(S) (optional)
2	14.05.2024	The ideal image	Paraxial approximation, principal planes, entrance and exit pupil, paraxial imaging equations; Scheimpflug condition; paraxial matrix formulation; Delano diagram; Aplanatic imaging: Abbe sine condition, numerical aperture, sine scaled pupil for microscope imaging	(S)
3	21.05.2024	First order layout, system structures and properties	application of imaging equations; examples: layout of visual imaging system; layout of microscope lens and illumination system; telecentricity, "4f-setups"; tele and reversed tele (retrofocus) system; depth of field, bokeh; equivalence to multi-perspective 3D image acquisition; focusing methods of optical systems; afocal systems; connecting optical (sub-)systems: eye to afocal system; illumination system and its matching to projection optics); zoom systems; first order aberrations (focus and magnification error) and their compensation: lens breathing, aperture ramping; scaling laws of optical imaging	S
4	28.05.2024	Imaging model including diffraction	Gabor analytical signal; coherence function; degree of coherence; Rayleigh-Sommerfeld diffraction; optical system transfer as complex, linear operator; Fraunhofer-, Fresnel-approximation and high-NA field transfer wave-optical imaging equations for non-coherent, coherent and partially coherent imaging; isoplanatic patches, Hopkins Transfer Function for partially coherent imaging, optical transfer functions for non-coherent and coherent imaging; ideal wave-optical imaging equations; Fourier-Optics; spatial filtering; Abbe theory of image formation in microscope, phase contrast microscopy	S
5	04.06.2024	Wavefront deformation, Optical Transfer Function, Point Spread Function and performance criteria	wave aberrations, Zernike polynomials, measurement of system quality; point spread function (PSF), optical transfer function (OTF) and modulation transfer function (MTF); optical system performance criteria based on PSF and MTF: Strehl definition, Rayleigh and Marechal criteria, 2-point resolution, MTF-based criteria, coupling efficiency / insertion loss at photonics interface	S
6	11.06.2024	Aberrations: Classification, diagrams and identification in real images	measurement of wave front deformation: Shack-Hartmann sensor, Fizeau interferometer Symmetry considerations as basis for aberration theory; Seidel polynomial, chromatic aberrations; surface contributions and Pegel diagram, stop-shift-equation; Longitudinal and transverse aberrations, spot diagram; computing aberrations with Hamilton Eikonal Function; examples: defocus, plane parallel plate longitudinal and lateral chromatic aberration, Abbe diagram, dispersion fit; achromat and apochromat aberration in real images of (extended) objects	no
7	18.06.2024	Optimization process and correction principles	pre- and post-computer era correction methodology, merit function, system specification, initial setups, opto-mechanical constraints, damped-least-square optimization; symmetry principles, lens bending, aplanatic surface insertion, lens splitting, aspheres and freeforms	S
8	25.06.2024	Aberration correction and optical system structure	Petzval theorem, field flattening, achromat and apochromat, sensitivity analysis, diffractive elements; system structure of optical systems, e.g. photographic lenses, microscopic objectives, lithographic systems, eyepieces, scan systems, telescopes, endoscopes	(S)
9	02.07.2024	Tolerancing and straylight analysis	optical technology constraints, sensitivity analysis, statistical fundamentals, compensators, Monte-Carlo analysis, Design-To-Cost; false light; ghost analysis in optical systems; AR coating; opto-mechanical straylight prevention	S

Imaging model

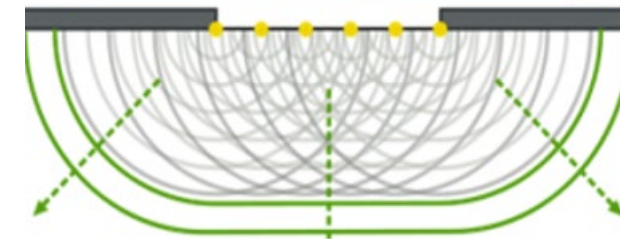


Situation in year 1870:



Geometrical model used for lens analysis, also synthesis (e.g. Petzval)

$$V(x, y, z) = \iint_P V(x_s, y_s, 0) \left[\frac{1}{2\pi\rho} \frac{z}{(1 - ik\rho)} \frac{e^{ik\rho}}{\rho^2} \right] dx_s dy_s$$



diffraction known, regarding circular area (Airy) as well as periodic structures / gratings (Fraunhofer)

Obstacles for systematic application to optical microscope theory: diffraction both at aperture as well as object structures, treatment of light source / illumination setup / coherence, multiple element ray tracing with higher incidence angles incl. glass dispersion

Today we have a statistical theory of image formation spatially-temporally partially coherent illumination including the coherent and non-coherent case (also incl. polarization, spectral dependences,...). First of all **due to computational effort** (numerical integration) and sometimes also due to limitations of statistical models those imaging models are **approximations** of the propagation equations as well as the boundary conditions of real optical systems.
Although today optical imaging is applied very successfully in excellent accuracies for specific applications it is important to keep that in mind and being aware of the approximation for the problem at hand.

Anamorphic lens effects in animation: The Lego Movie (2013)



Animation by
Animal Logic

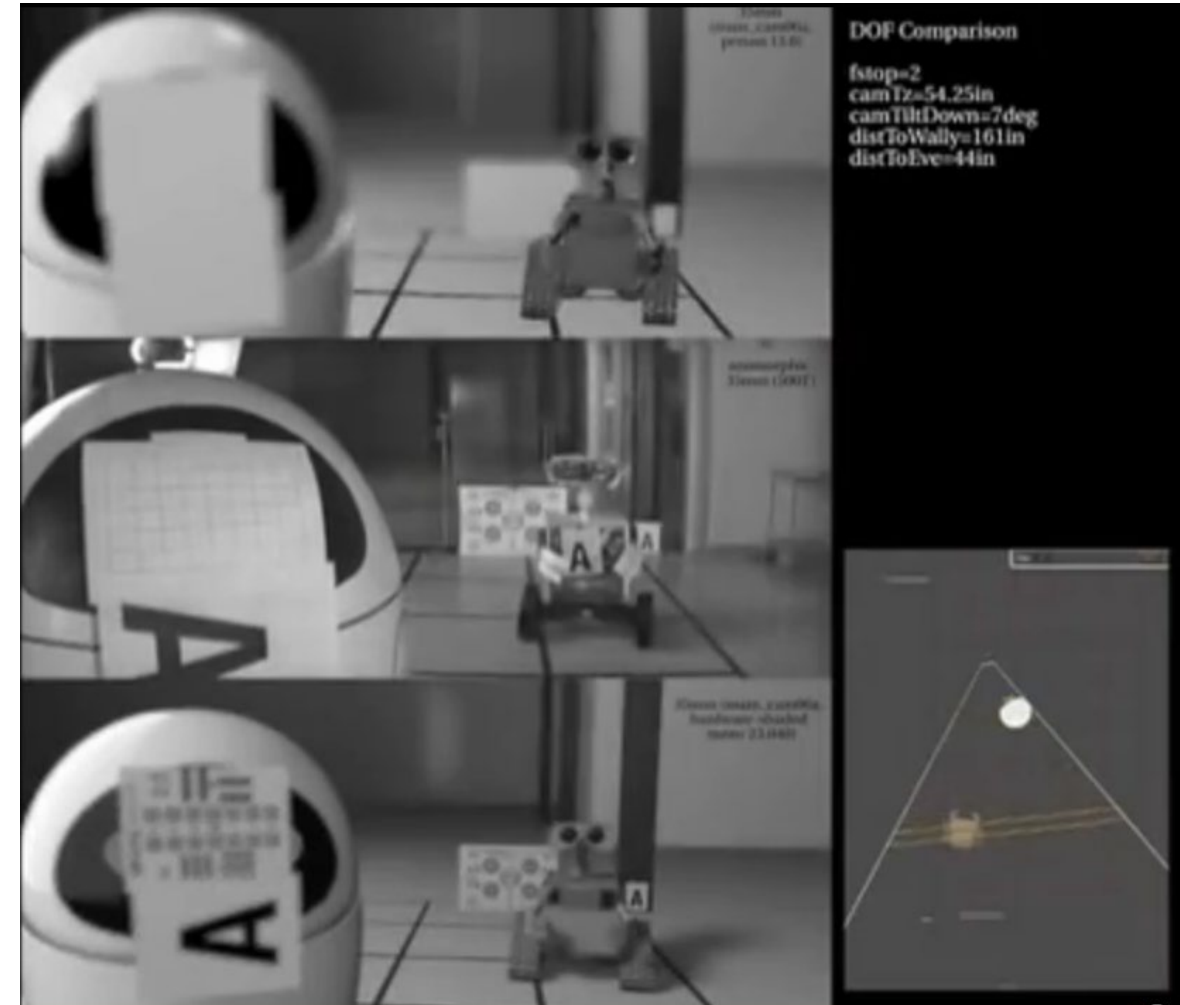
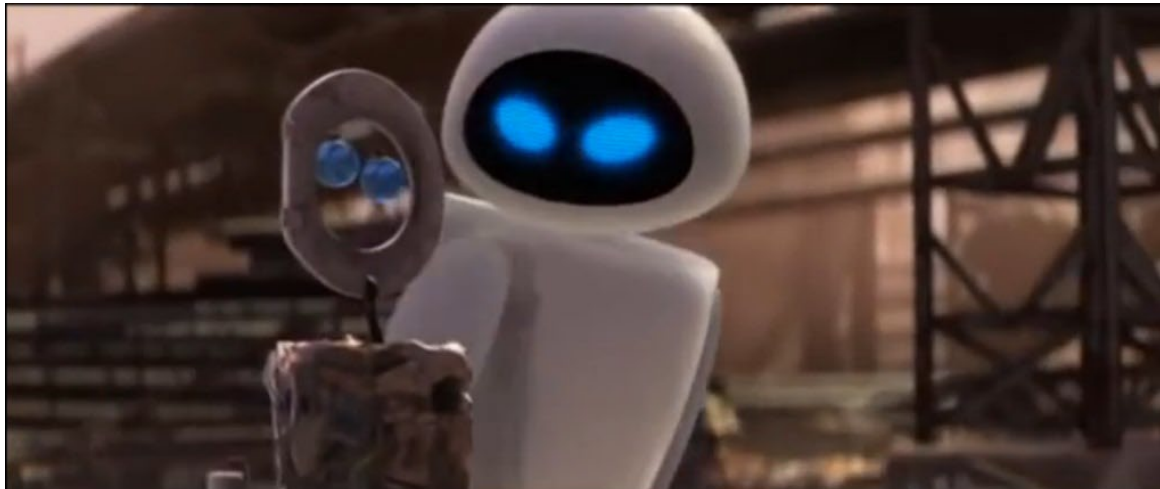


Depth of field in animation: Wall-e (2008), Disney/Pixar

<http://www.engadget.com/2015/08/02/disney-explains-hyperion-renderer/>

The Imperfect Lens - Creating the Look of WALL•E, Pixar/Disney

https://www.youtube.com/watch?v=IjKntxS_WlY

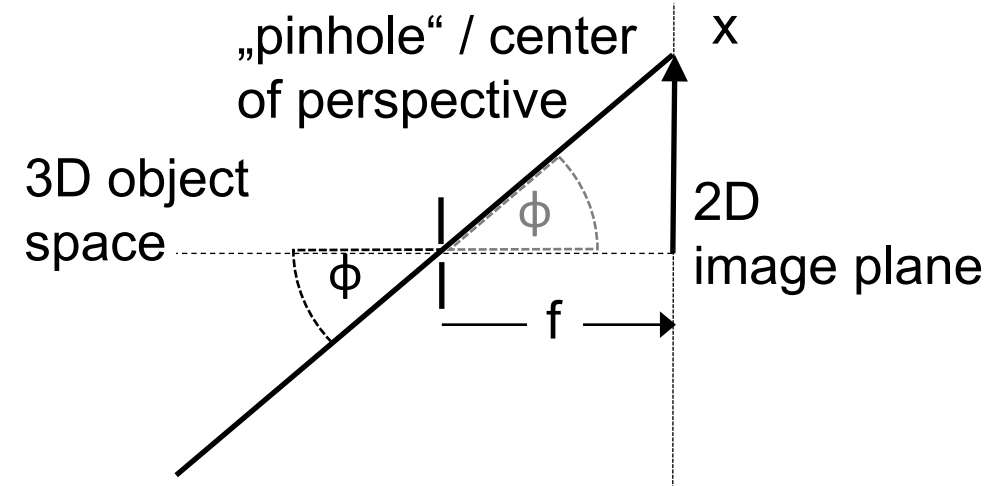


DOF Comparison
fstop=2
camTz=54.25in
camTiltDown=7deg
distToWally=161in
distToEve=44in

The central projection in computer vision

Central projection using homogeneous coordinates / „pinhole model“

$$\begin{pmatrix} X \\ Y \\ Z \\ 1 \end{pmatrix} \rightarrow \begin{pmatrix} fX \\ fY \\ fZ \\ 1 \end{pmatrix} = \underbrace{\begin{pmatrix} f & 0 & 0 \\ 0 & f & 0 \\ 0 & 0 & 1 \\ 1 & 0 & 0 \end{pmatrix}}_{\text{Camera projection matrix}} \begin{pmatrix} X \\ Y \\ Z \\ 1 \end{pmatrix}$$



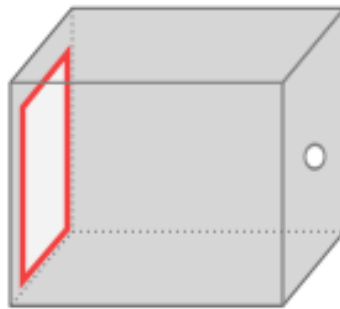
„Pinhole model“ with „principal point“ offset

$$\begin{pmatrix} X \\ Y \\ Z \\ 1 \end{pmatrix} \rightarrow \begin{pmatrix} fX + p_x Z \\ fY + p_y Z \\ fZ \\ 1 \end{pmatrix} = \underbrace{\begin{pmatrix} f & p_x & 0 \\ 0 & f & p_y \\ 0 & 0 & 1 \end{pmatrix}}_{\text{Camera calibration matrix}} \begin{pmatrix} X \\ Y \\ Z \\ 1 \end{pmatrix}$$

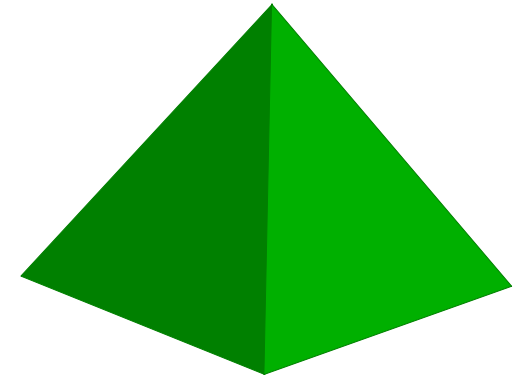
In computer vision literature those shift factors are usually called „principal points“, but in optics terminology the center of projection corresponds to the entrance pupil position (and not the principal or nodal points).



**Light
source**

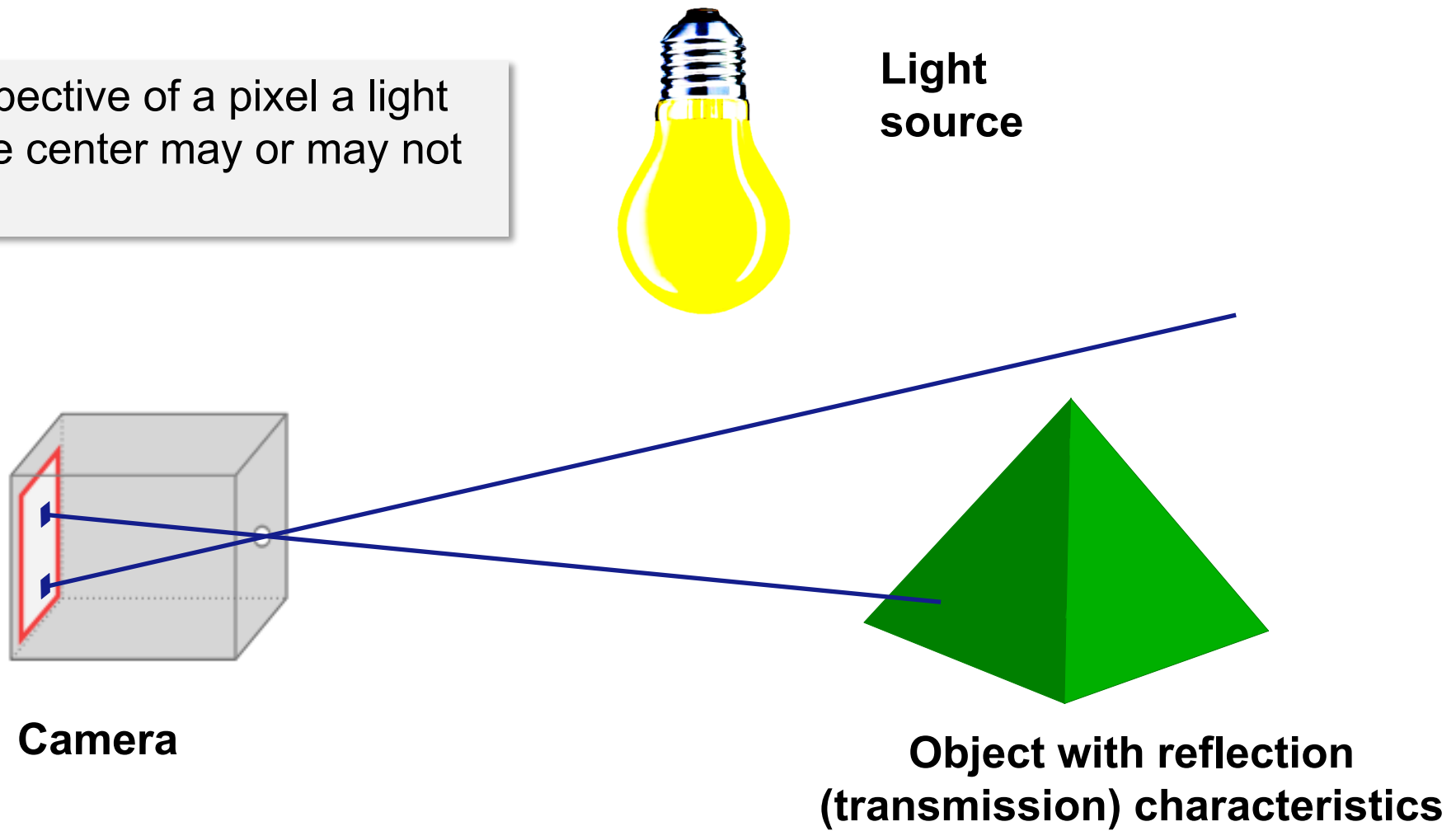


Camera

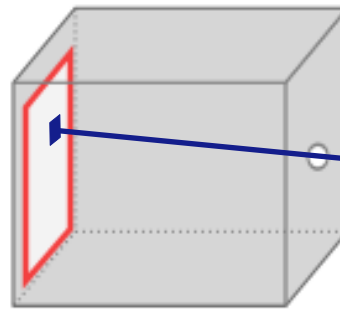


**Object with reflection
(transmission) characteristics**

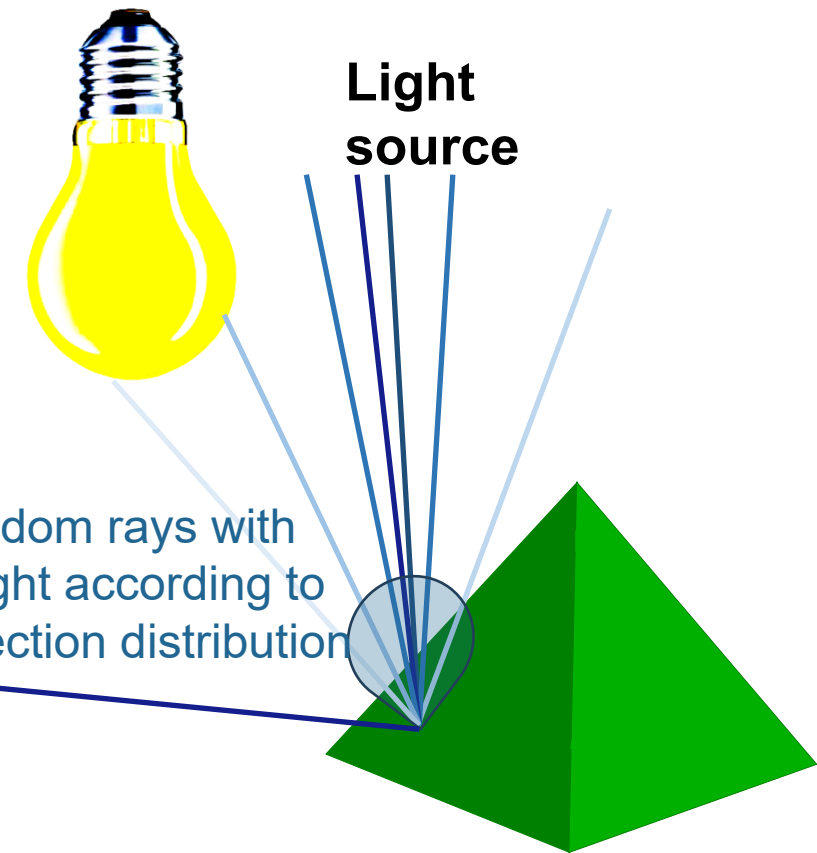
From the perspective of a pixel a light ray through the center may or may not hit the object.



If the object is hit according to the incidence position and angle a random bundle of rays is generated (weighted) according to reflection distribution (Monte-Carlo approach).

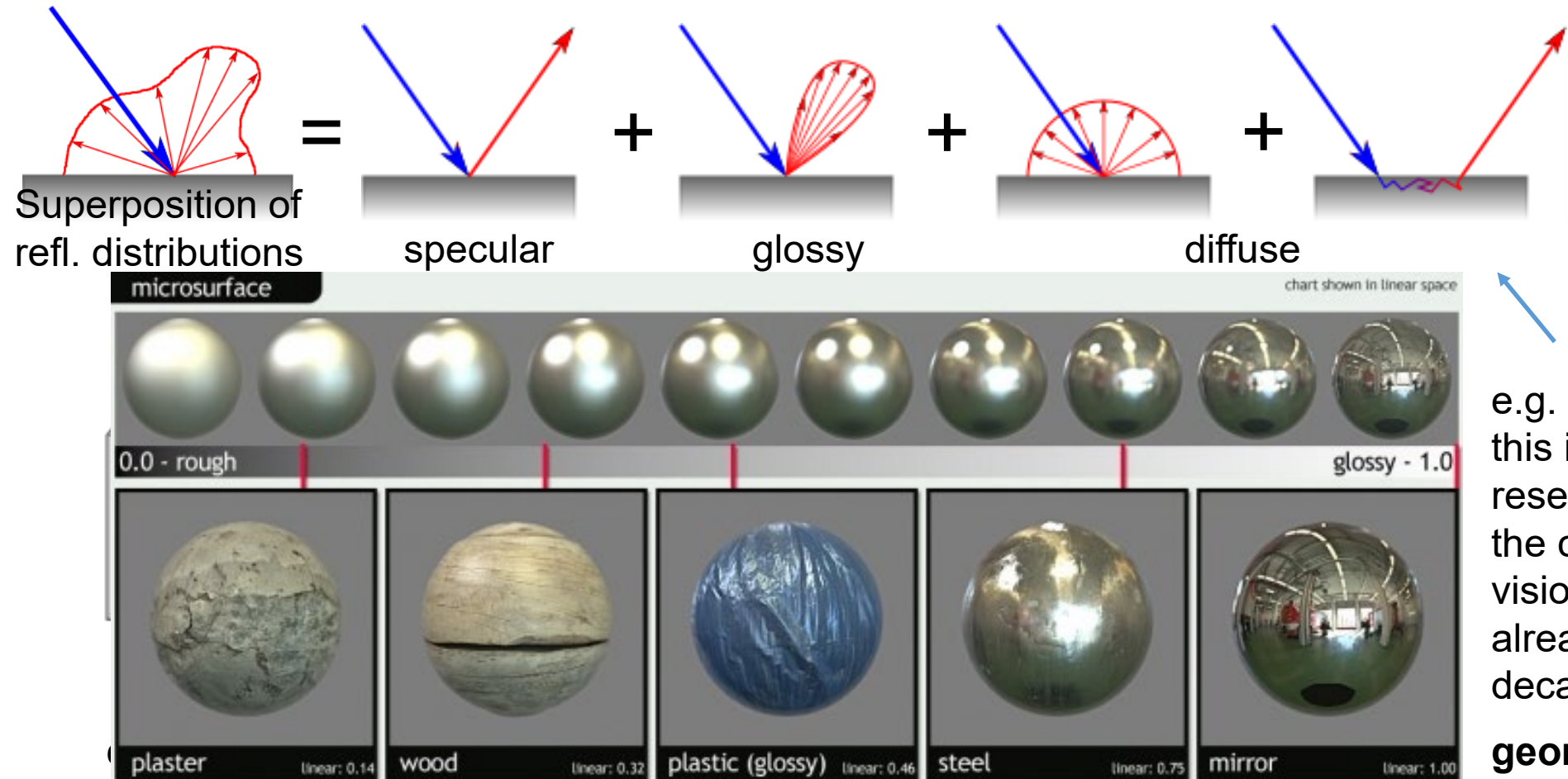


Camera



Object with reflection (transmission) characteristics

Bidirectional reflection distribution function (BRDF)



e.g. human skin,
this is a central
research topic in
the computer
vision community
already for
decades!

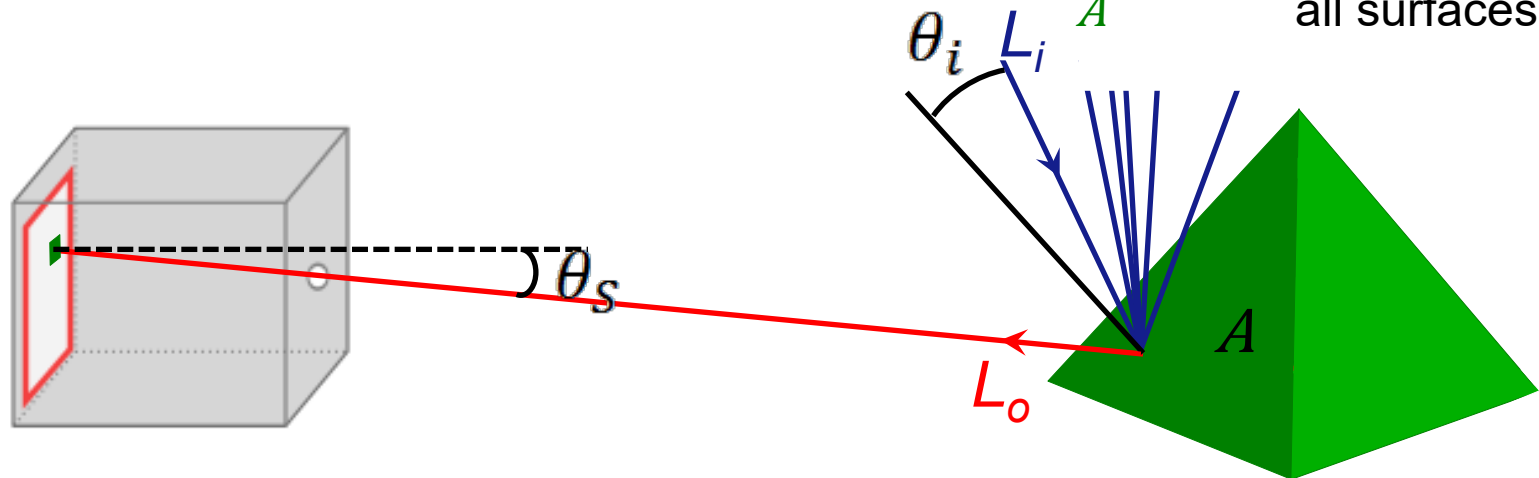
**geometry/
reflection
properties**

Bidirectional reflection distribution depends on the angle of incidence, angle of exit, wavelength, polarization... Whether the simulated scene appears realistic depends on detailed assumptions!

Rendering equation

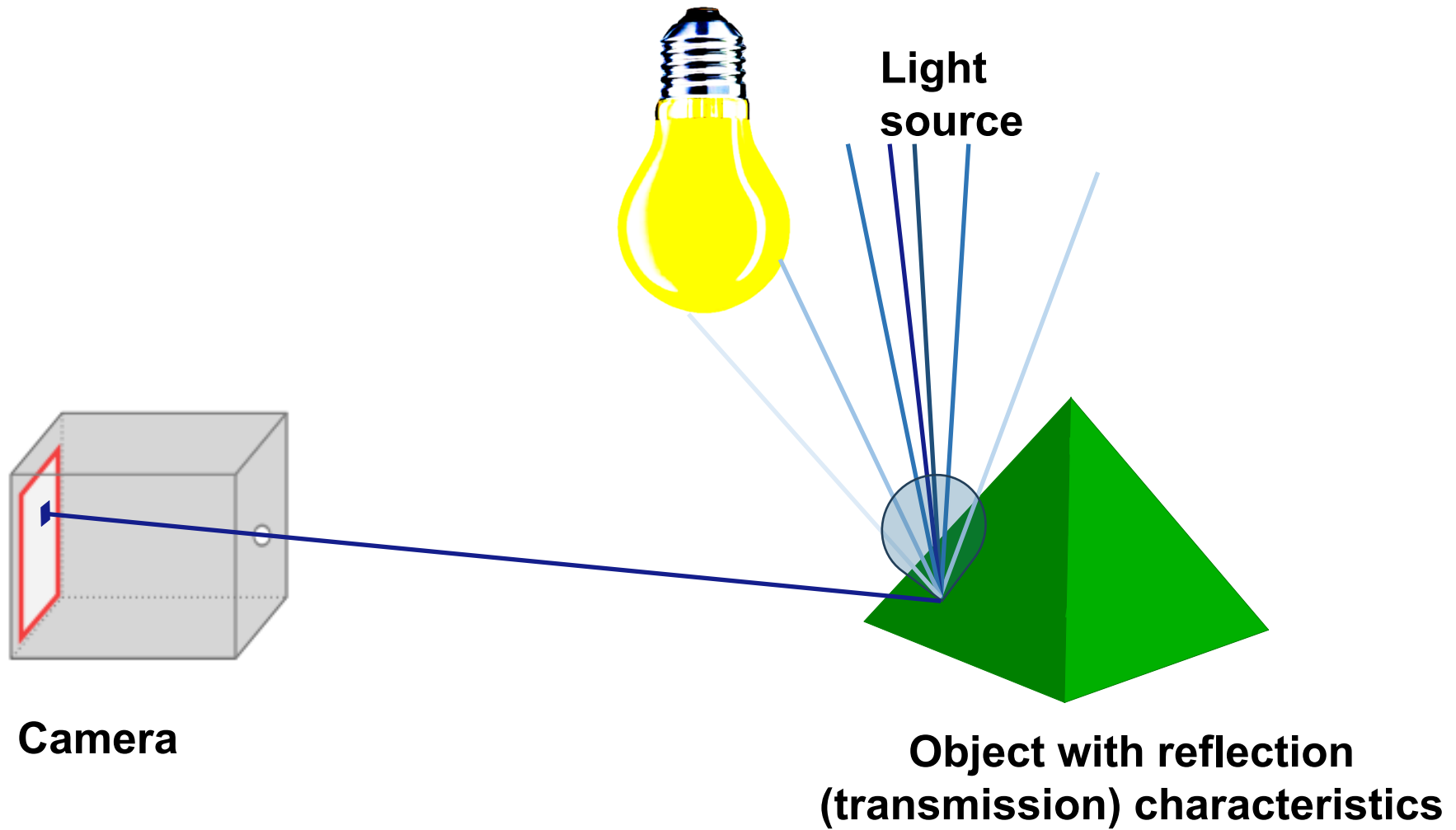
$$\begin{aligned} L_o &= L_e + \int_A f_o L_i V \frac{\cos \theta_i \cos \theta_s}{\|p - p_A\|^2} dA \\ &\approx L_e + \sum_n f_o L_i V \frac{\cos \theta_i \cos \theta_s}{\|p - p_A\|^2} \end{aligned}$$

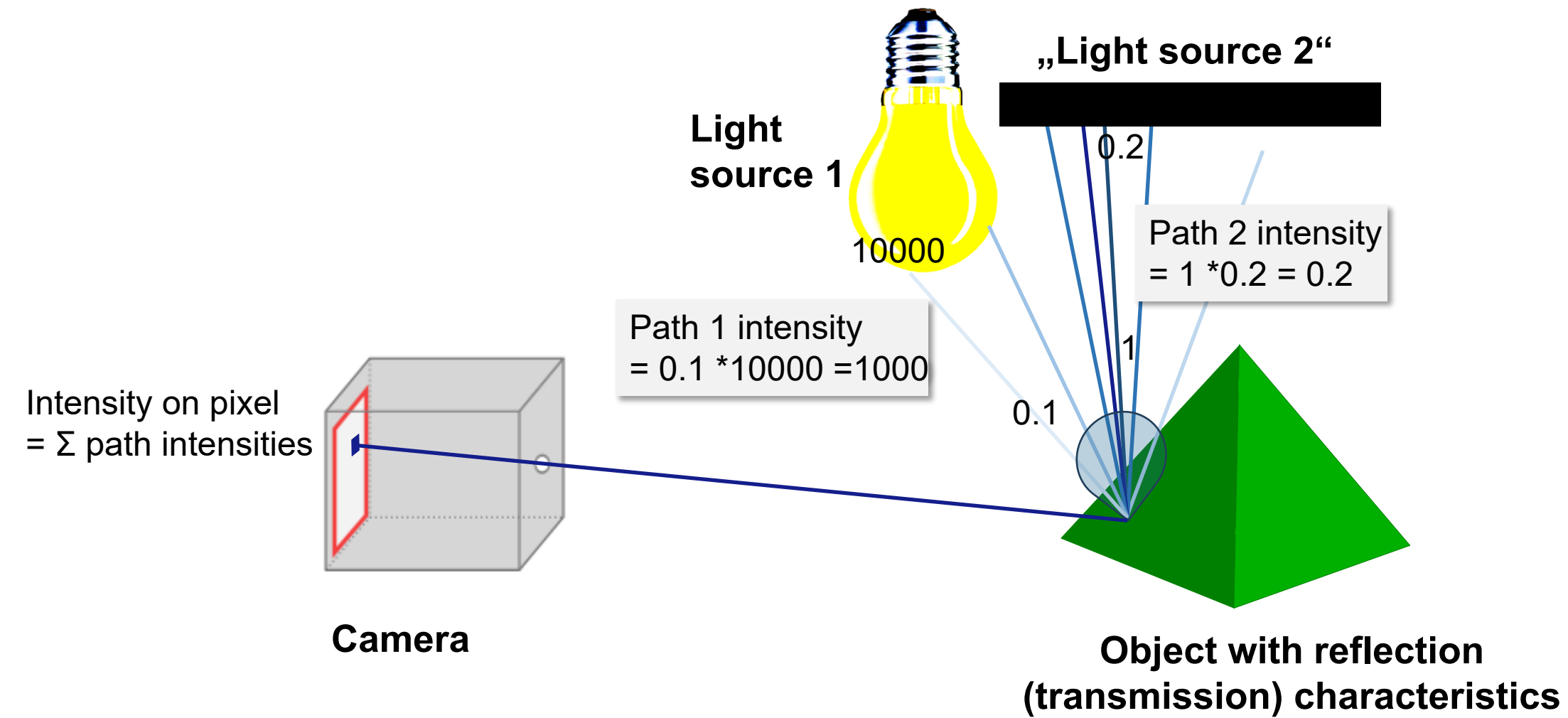
$L_o(p_A; \theta_s)$ outgoing radiance
 $L_i(p_A; \theta_i)$ incident radiance
 $L_e(p_A; \theta_s)$ emitted radiance
 $f_o(p_A; \theta_i, \theta_o)$ bidirectional
reflection distribution function
 $V(p, p_A)$ visibility
 A all surfaces



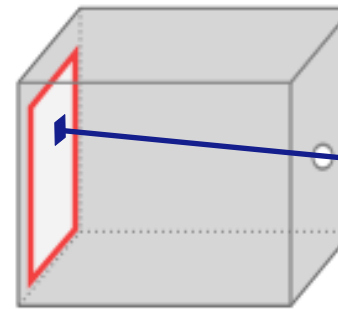
camera model

geometry/
reflection properties

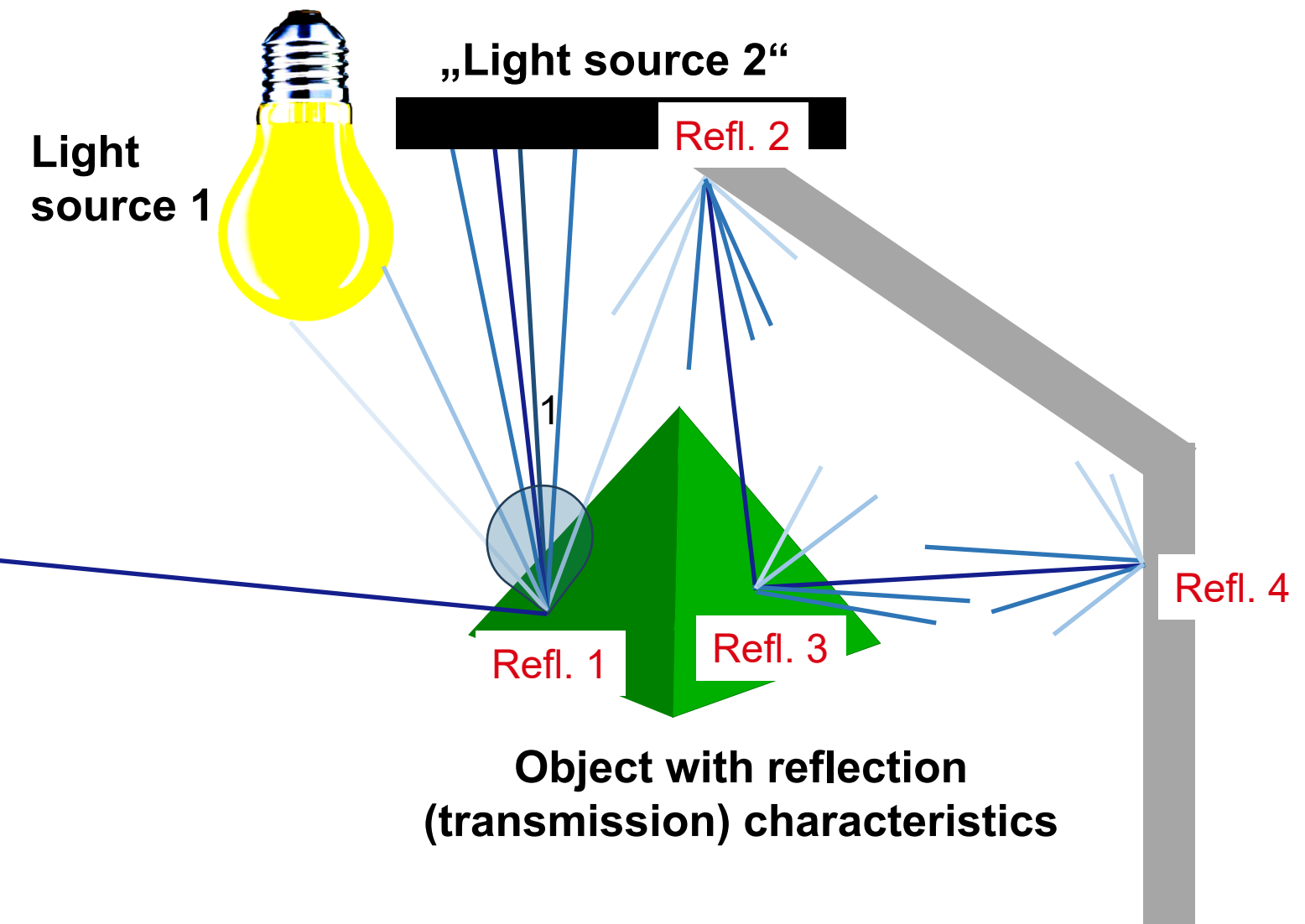




For complex scenes considering several reflections significantly increases the number of paths. For the realism of scene rendering, it is required and crucial to model multi reflections.

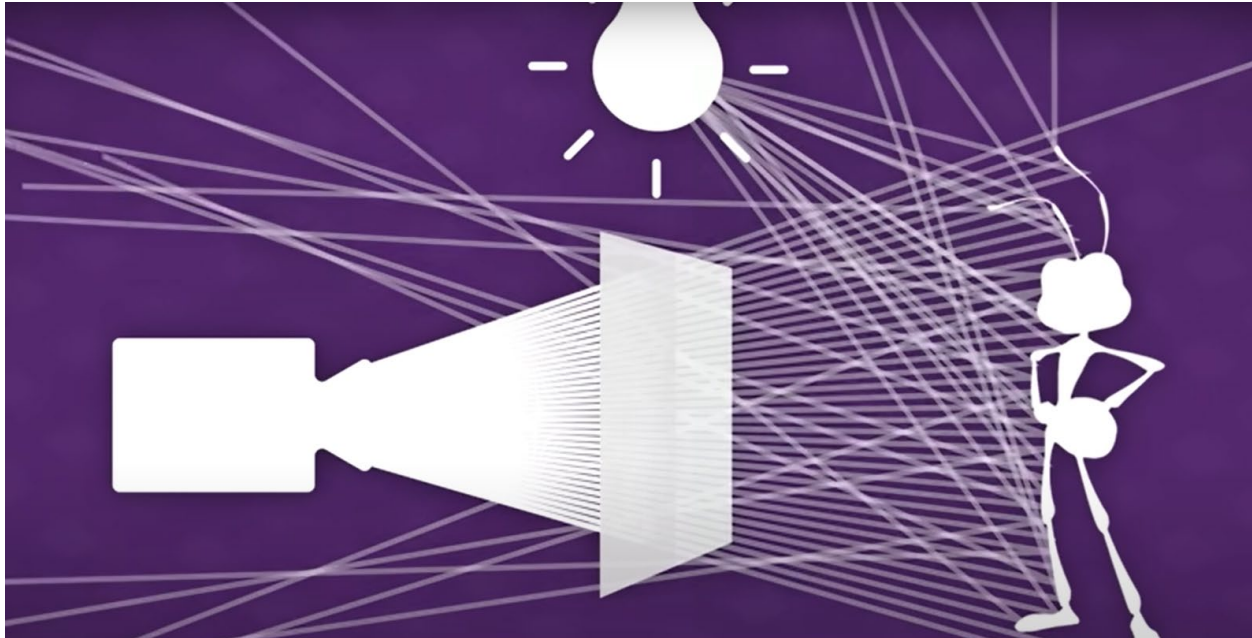


Camera

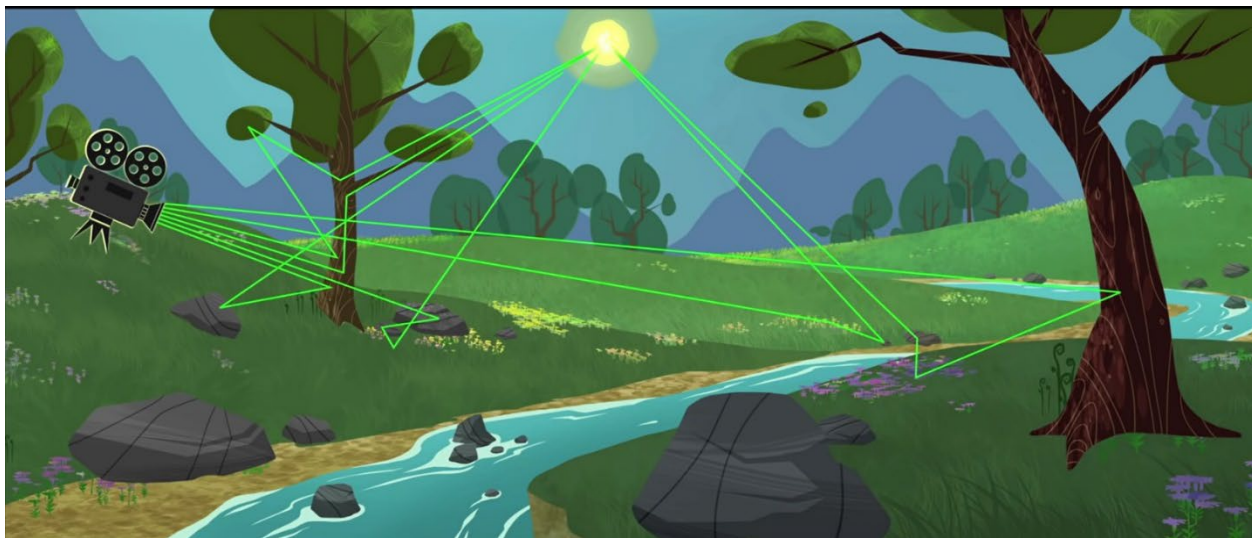


Professional Rendering Engines

Pixar Rendering Engine



Disney Hyperion



“Massive Raytracing Imaging” is daily business for Animation or Special Effects applications.

For efficient computing sophisticated methods have been developed, e.g.

- importance sampling
- differential rays

Rendering for Animation Movie



Introduction to
Rendering in Animation
Movies by Disney:

[https://www.youtube.com/
watch?v=4mvxkOr_UxA](https://www.youtube.com/watch?v=4mvxkOr_UxA)

Direct illumination only



With indirect illumination



For daily life sceneries we often have a huge dynamic range, e.g. 1:100000 which we are capable to detect with light coming from several light source and being reflected or scattered from different surfaces.

This requires:

- huge amount of rays together with efficient methods to avoid tracing ray which do not essentially contribute to the imaging
- several reflections, as the order of magnitude of reflected light mixes up again with less bright light sources e.g. in interior rooms and give a specific impression
- Complex models of reflection / scattering on surfaces, partially transmitting media with BDRF(4 variables) or even higher dimensional reflection functions taking subsurface scattering into account

Importance of indirect illumination



0 bounces (visible light sources)



1 bounce (direct illumination)



2 bounces



3 bounces



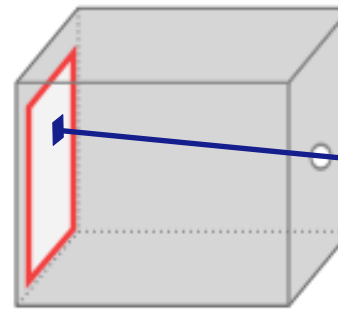
4 bounces



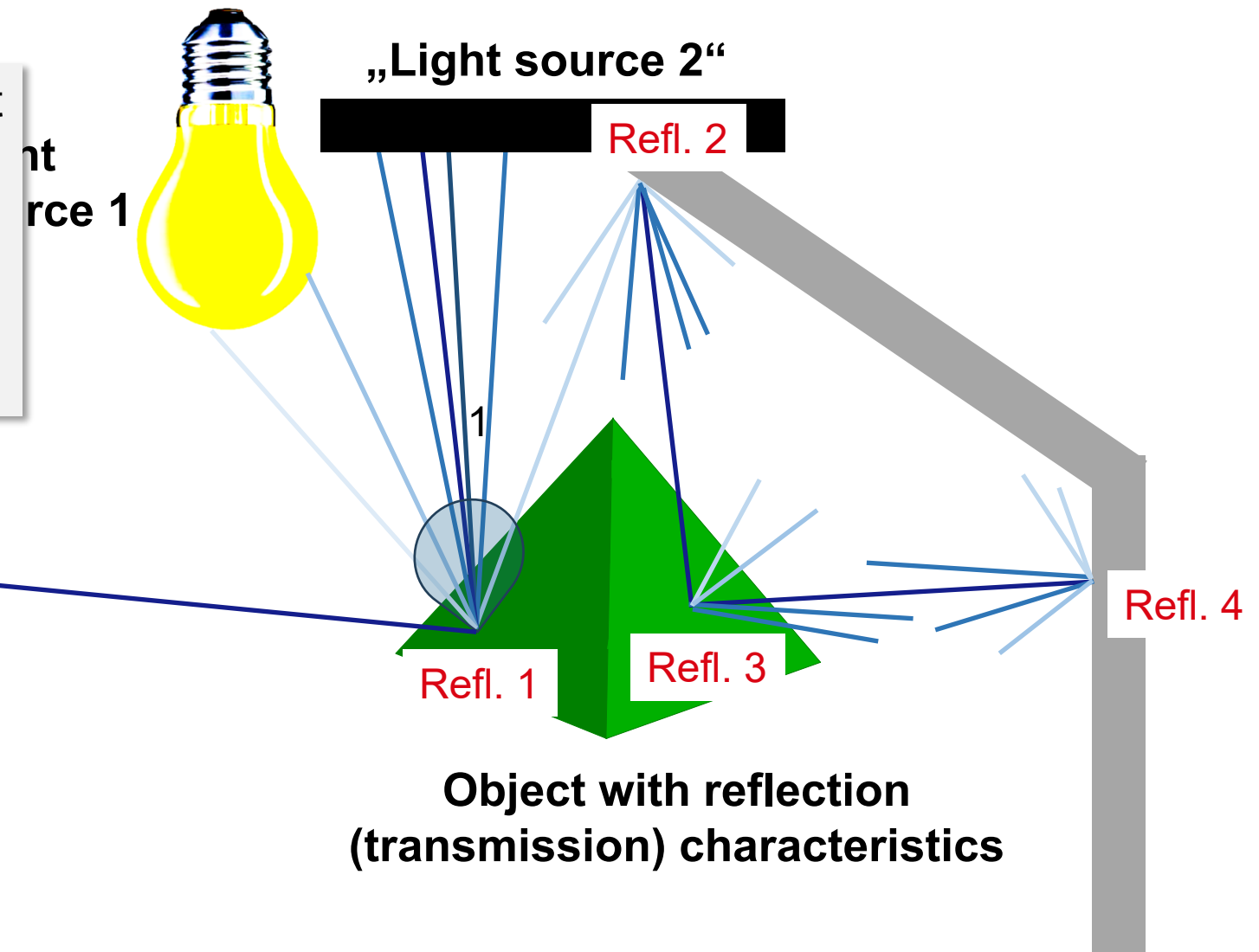
8 bounces



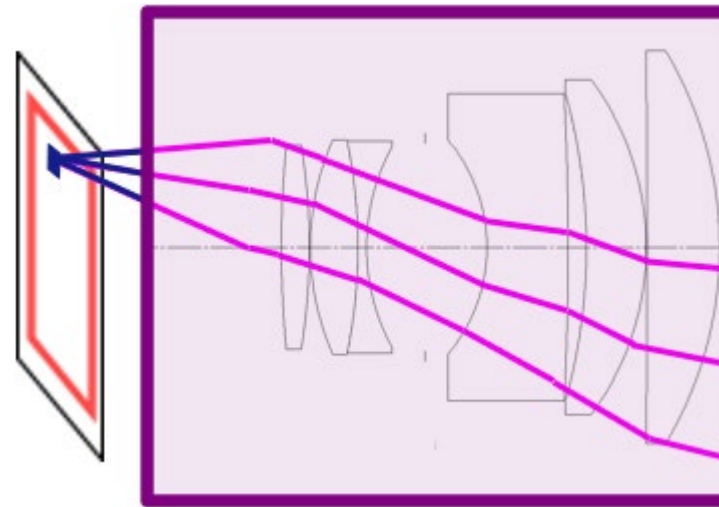
For complex scenes taking into account several reflections significantly increases the number of paths. For the realism of scene rendering it is required and crucial to model multi reflections.



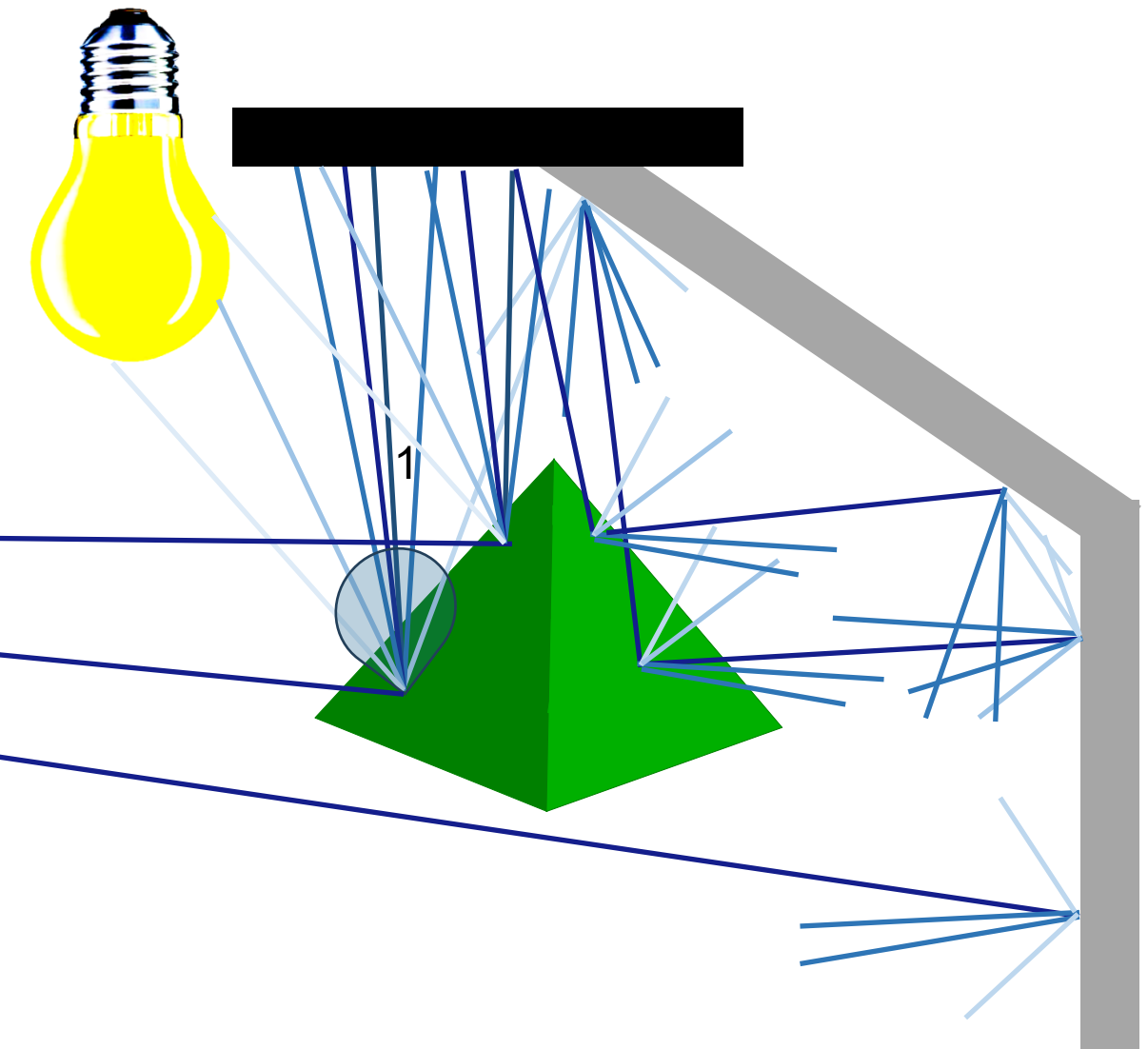
Camera



Replace pinhole with real lens!



Real Camera



3D-image simulation (view in Presentation mode)

ZEISS ZE/ZF Planar 1.4/85mm

3D-image simulation

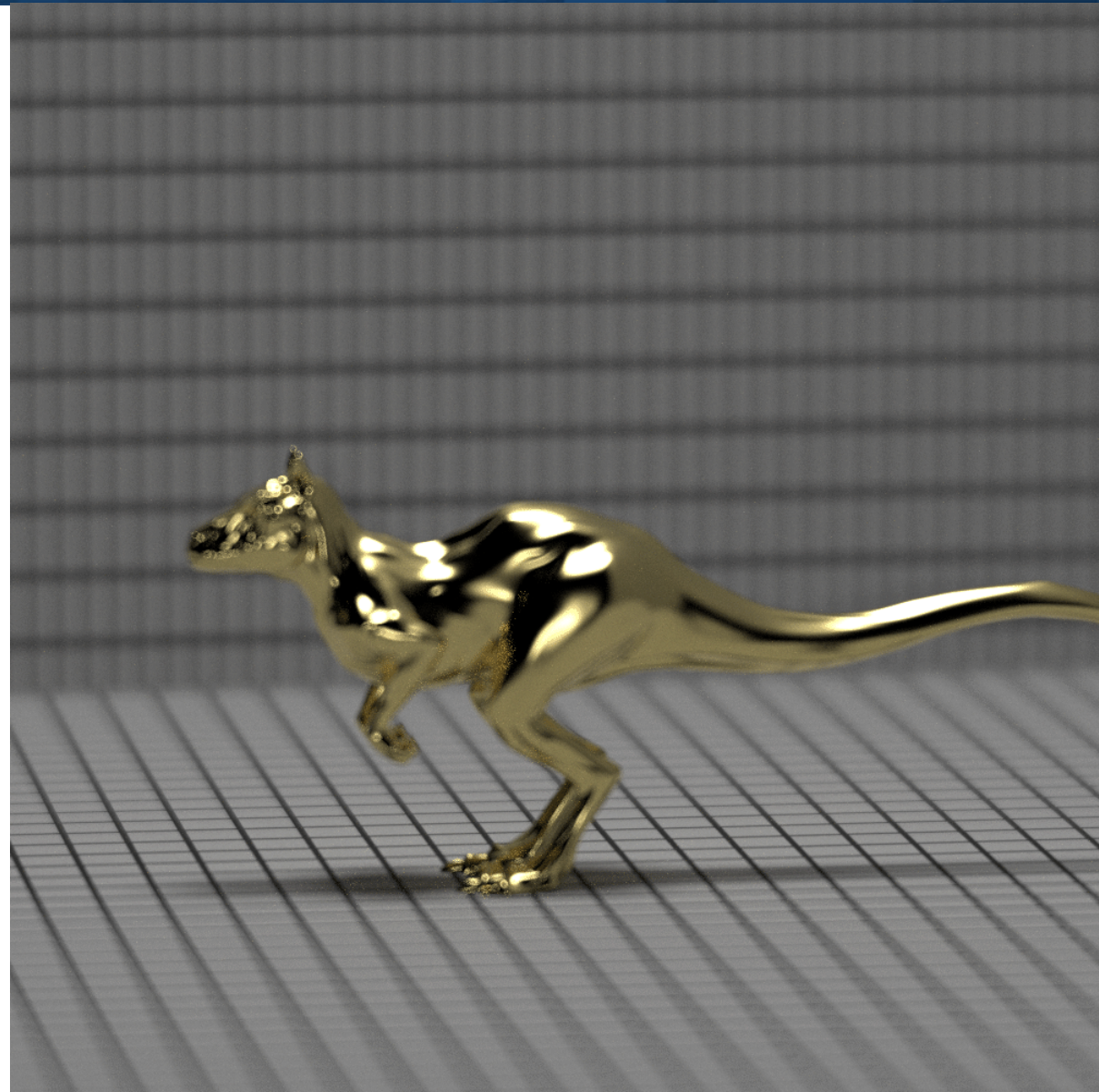
Object scene „killeroo“ courtesy of
[headus](#)/Rezard
(<http://www.pbrt.org/scenes.php>)

Sampling grid:

1000 x 1000 pixel

1024 rays/pixel

Input: design data of ZEISS ZE Planar T* 1.4/85

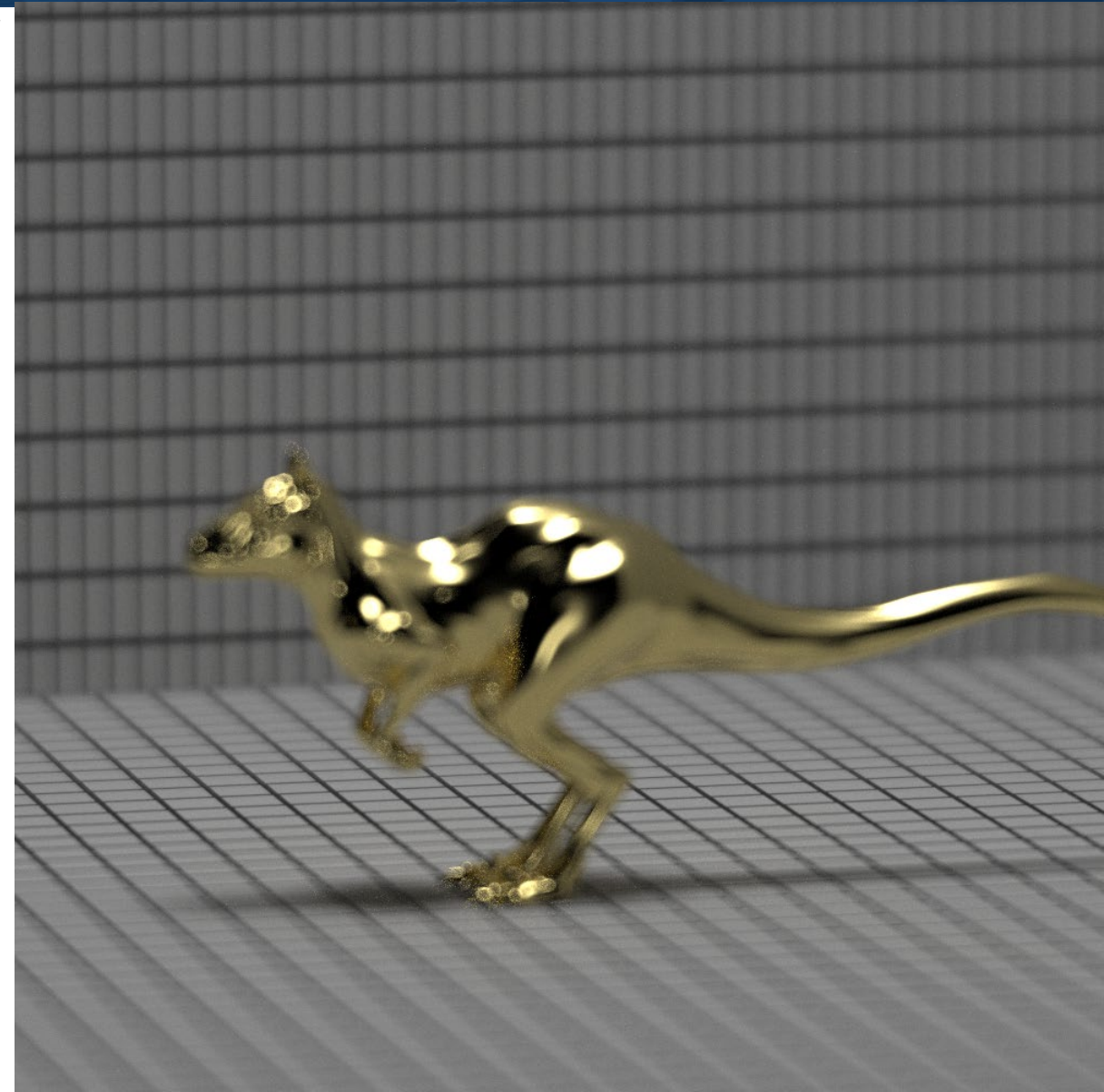
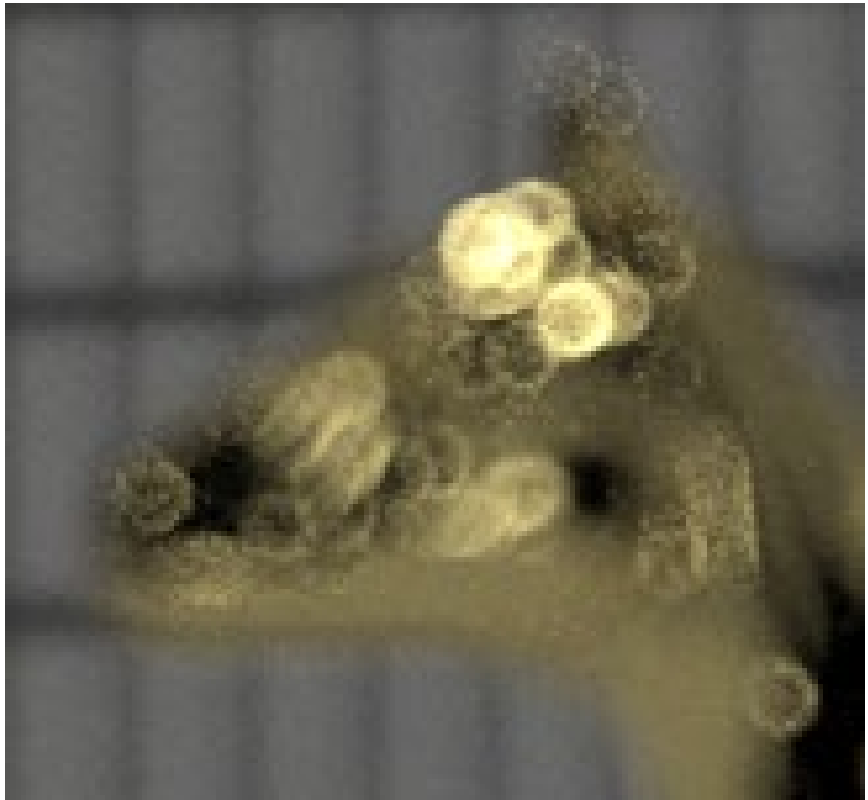


Variation of Aperture Shape

3D-image simulation

Object scene „killeroo“ courtesy of
[headus](#)/Rezard
(<http://www.pbrt.org/scenes.php>)

Sampling grid:
1500 x 1500 pixel
1024 rays/pixel



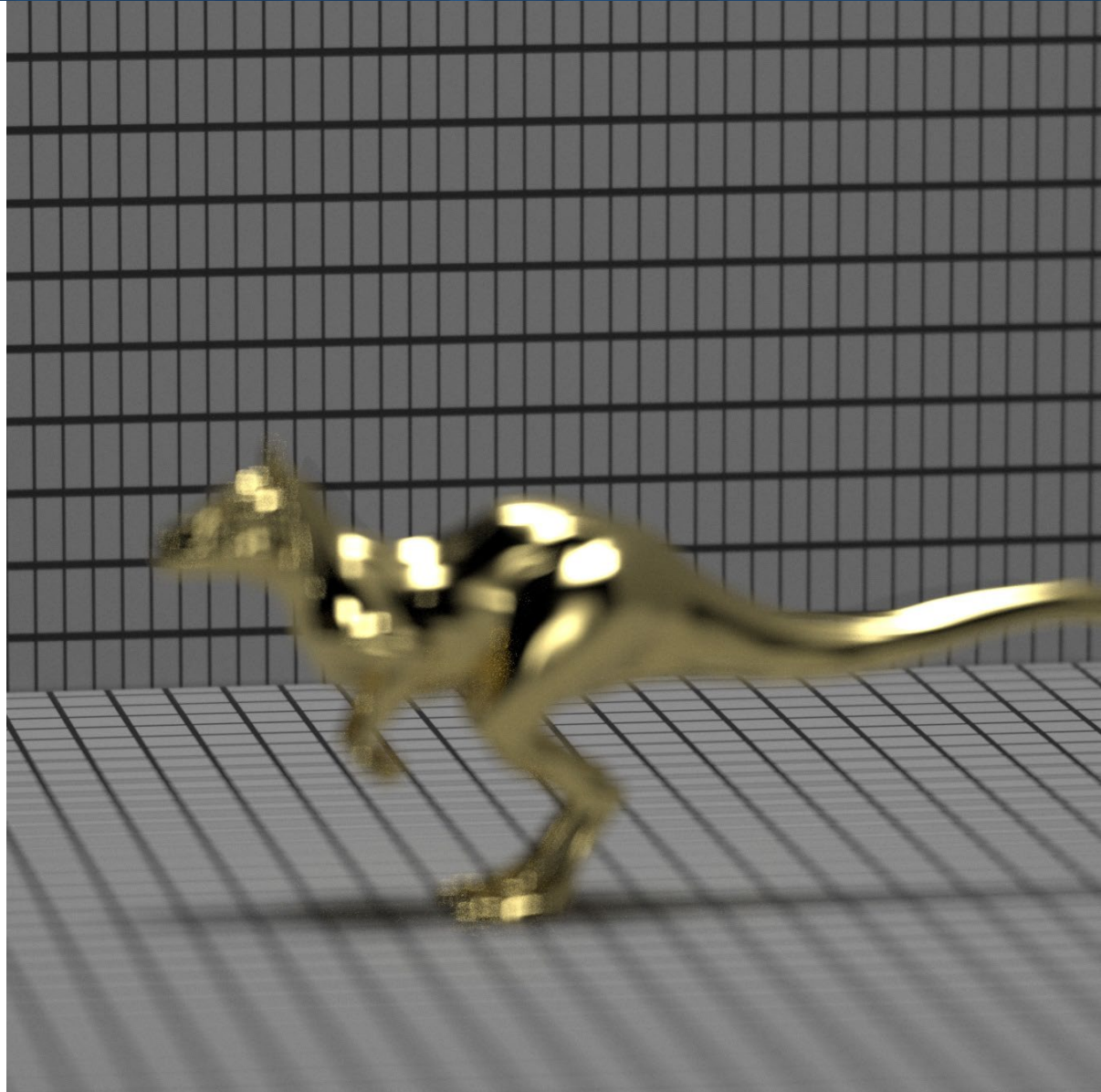
Variation of Aperture Shape

3D-image simulation

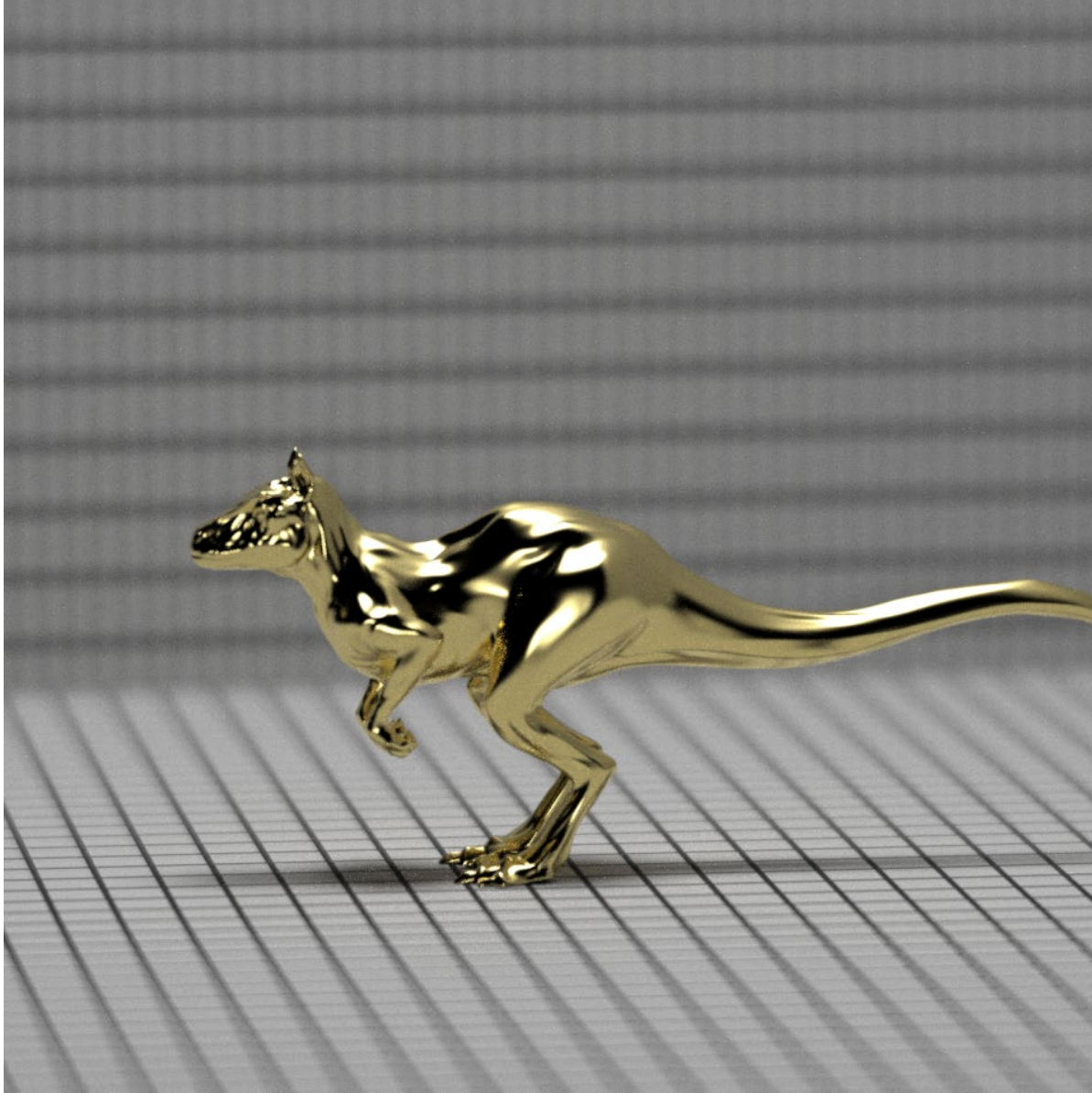
Sampling grid:
1500 x 1500 pixel
1024 rays/pixel



Object scene „killeroo“ courtesy of
[headus](#)/Rezard
(<http://www.pbrt.org/scenes.php>)



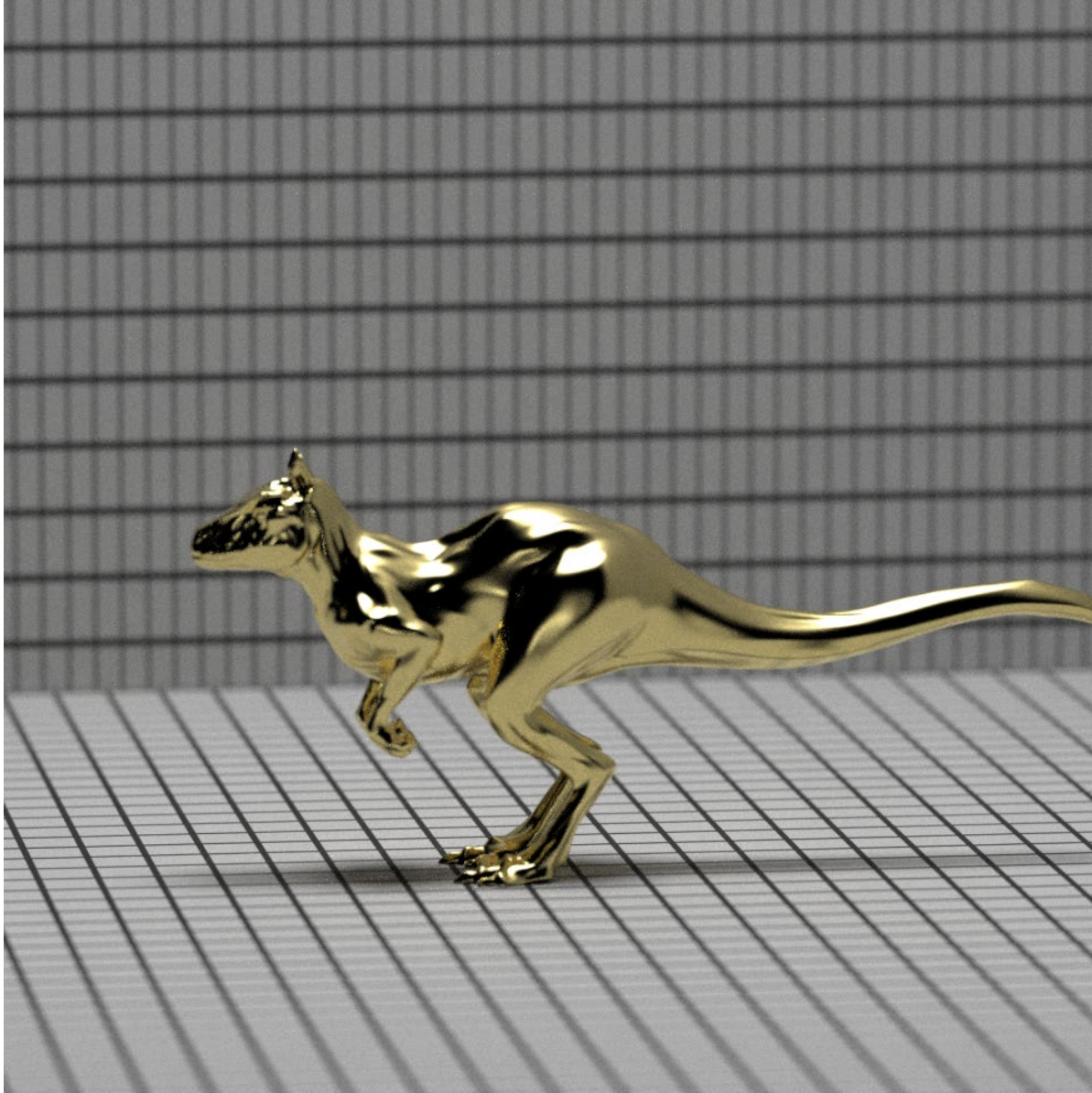
Variation of f-number



f/2.8

Object scene „killeroo“ courtesy of
[headus](#)/Rezard
(<http://www.pbrt.org/scenes.php>)

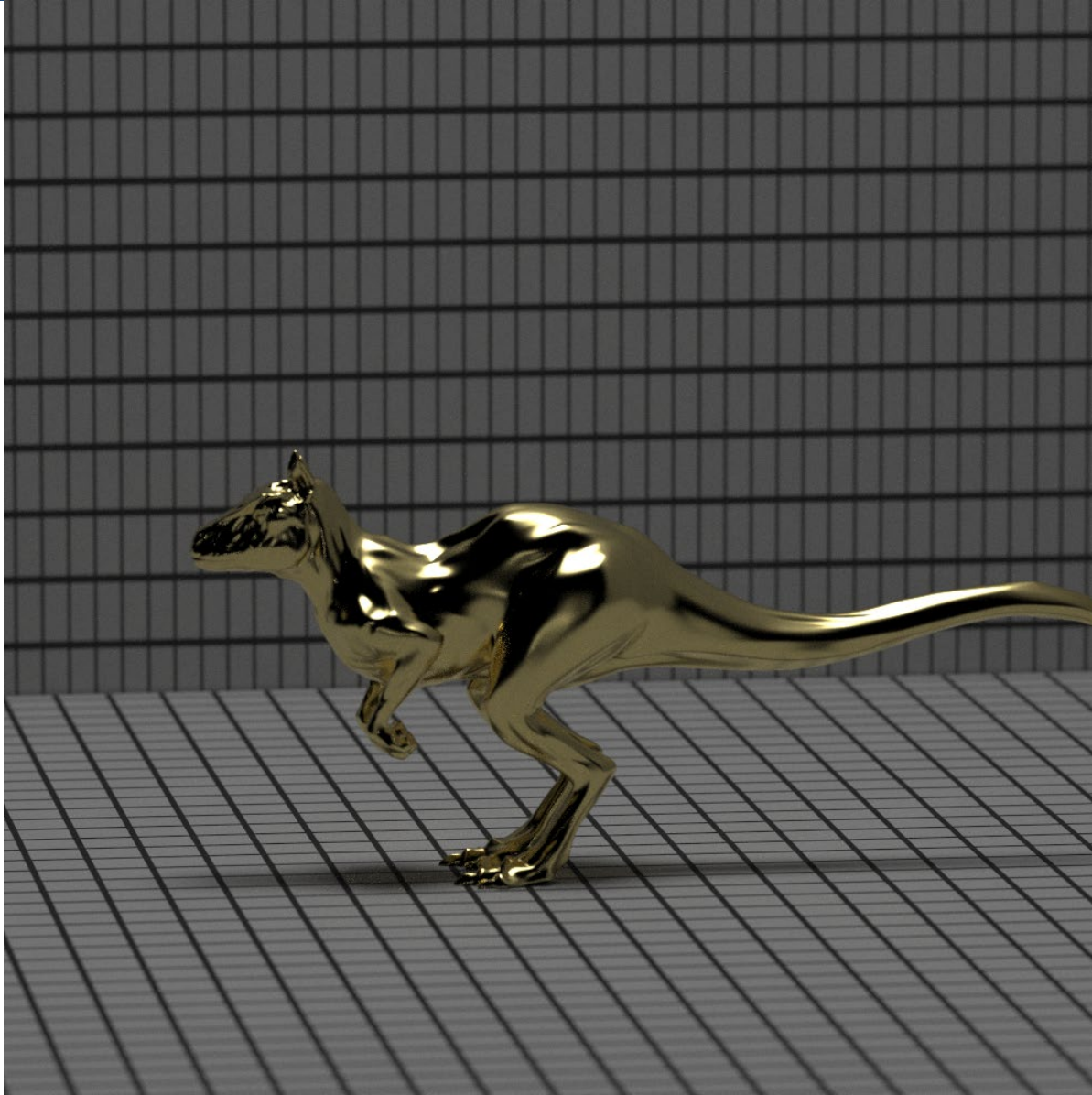
Variation of f-number



f/8

Object scene „killeroo“ courtesy of
[headus](#)/Rezard
(<http://www.pbrt.org/scenes.php>)

Variation of f-number



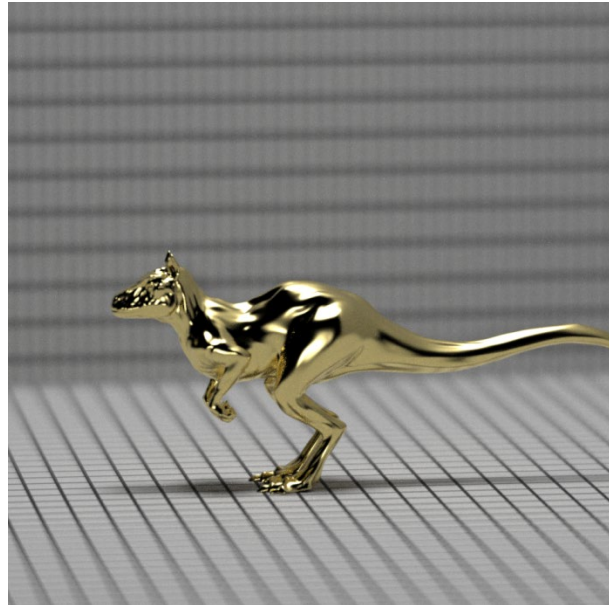
f/16

Object scene „killeroo“ courtesy of
[headus](#)/Rezard
(<http://www.pbrt.org/scenes.php>)

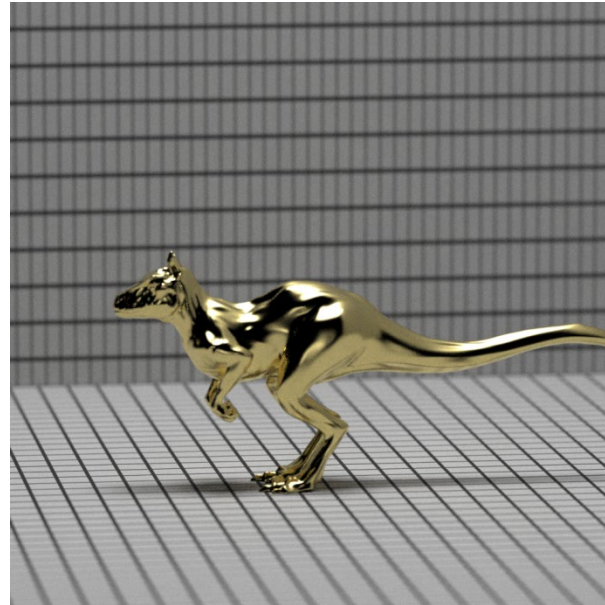
Variation of f-number: Effect on depth-of-field and irradiance

increased depth of field

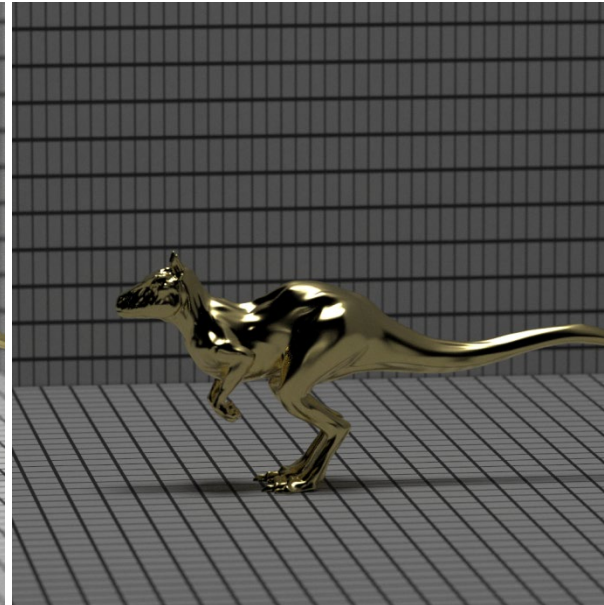
reduced brightness



f/2.8

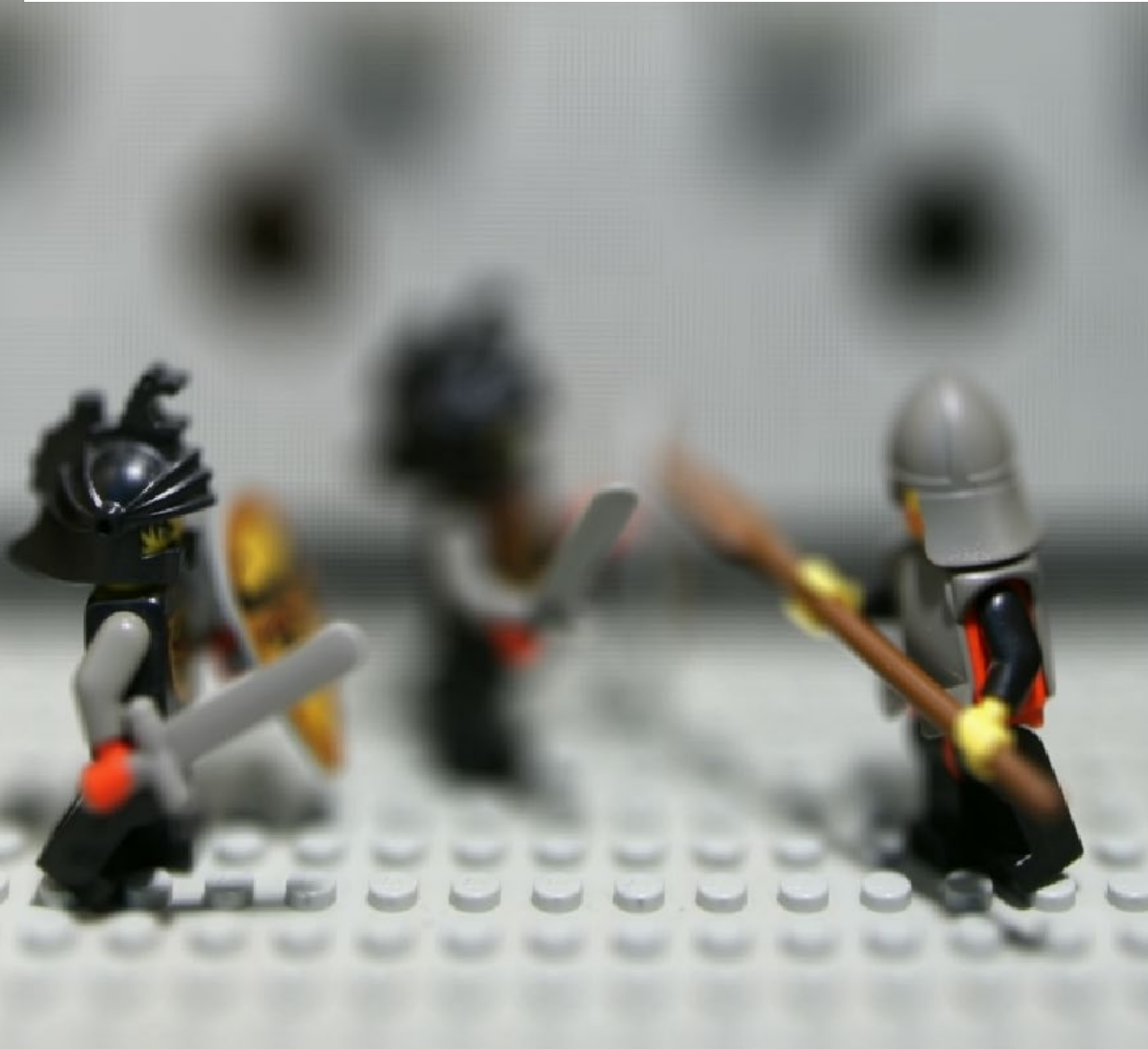


f/8

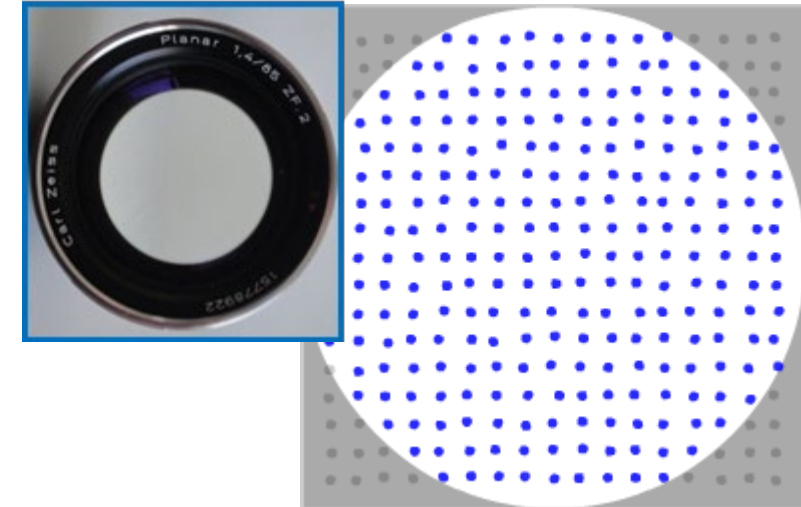


f/16

Depth of field is directly related to area of viewpoints = lens entrance pupil for single lens



lens entrance pupil



In standard photography lens entrance pupil defines the surface area of viewpoints on the captured 3D-scene.

This area is topologically continuous (usually approximately circular).

different
viewpoints
on scene



What is the relevant system parameter for background spot size?



Portrait diameter of object field*:

$$\phi_{ob,Portrait} = 700 \text{ mm} = \frac{\phi_{im}}{\beta}$$

Define parameter $c_{FOV} = \frac{1}{\tan w}$ and restrict for “portrait field-of-views”:

equivalent f	$\tan(w)$	$c_{FOV}=1/\tan(w)$
50	0,46	2,17
85	0,26	3,85
100	0,22	4,56
135	0,16	6,20

$$\phi_{rel.spot,\infty} = \frac{\phi_{EP}}{\phi_{im}} m = \frac{\phi_{EP}}{\phi_{ob,Portrait}} = \frac{\phi_{EP}}{700\text{mm}}$$

$$\tan w = \frac{\phi_{im}}{2f} \quad (\text{Half Field-of-view; object angle } w)$$

$$\phi_{EP} = \frac{f}{K} = \frac{\phi_{im}}{2K \tan w}$$

Define field-of-view coefficient:

Relation f-number F# and image-side numerical aperture NA':

$$\phi_{rel.spot,\infty} = \frac{c_{FOV}}{700\text{mm}} \phi_{im} NA'$$

constant for given field-of-view

$$c_{FOV} = \frac{1}{\tan w}$$

$$NA' = \frac{1}{2 F\#}$$

(square root of)
étendue

Relative background spot diameter scales directly with the product of field diameter and image-side NA.

*in case of shown proportion: 400mm in vertical direction corresponds to 700mm diagonal for 3:2 aspect ratio



Multi-camera system

replace large lens by many thin
small ones for smartphone...



Can you make natural bokeh just by
superposition of images from their different
perspectives? ... just like from a large
entrance pupil



Source: Stanford Imaging Lab





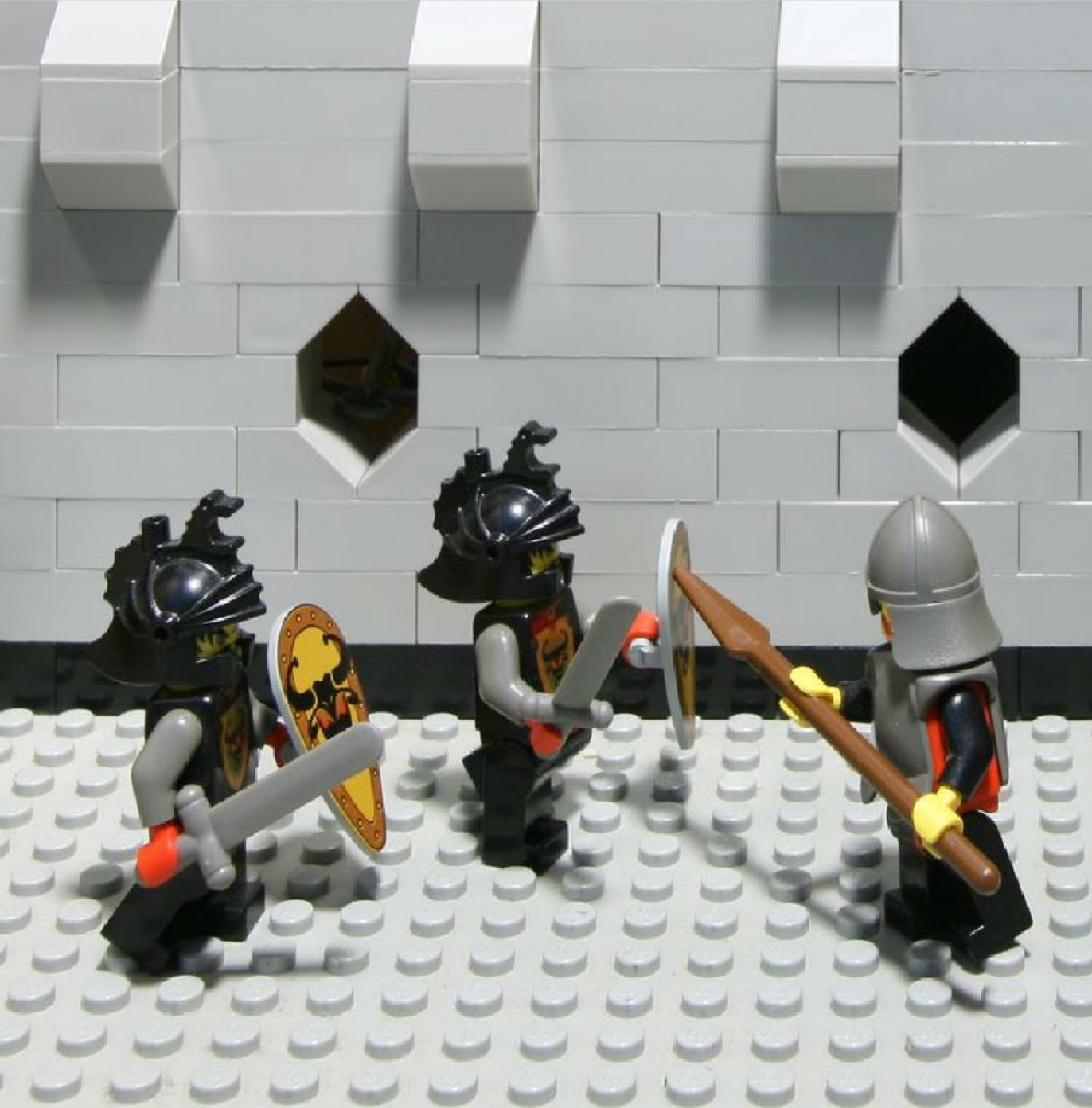
Source: Stanford Imaging Lab





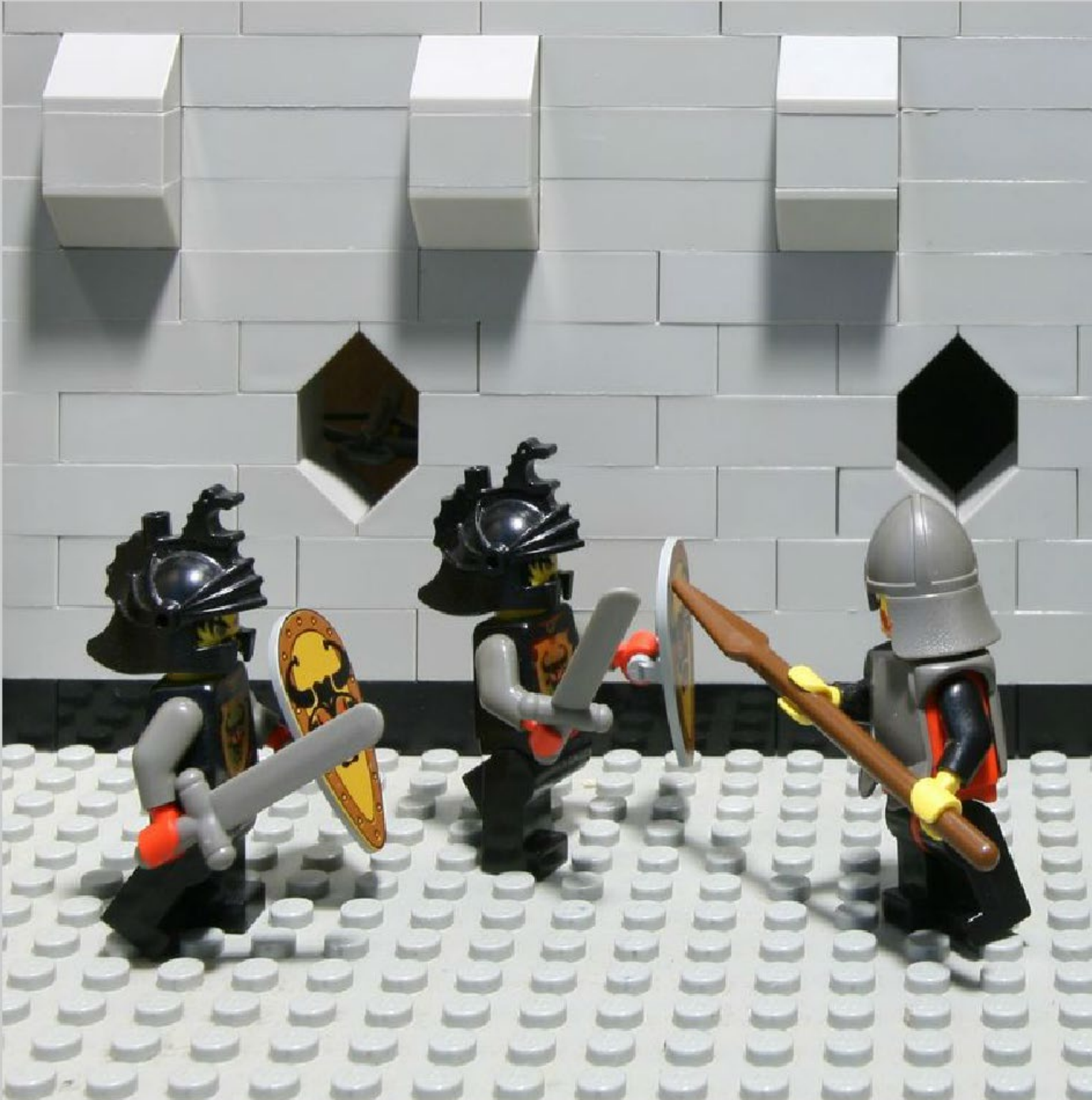
Source: Stanford Imaging Lab





Source: Stanford Imaging Lab





Source: Stanford Imaging Lab





Source: Stanford Imaging Lab





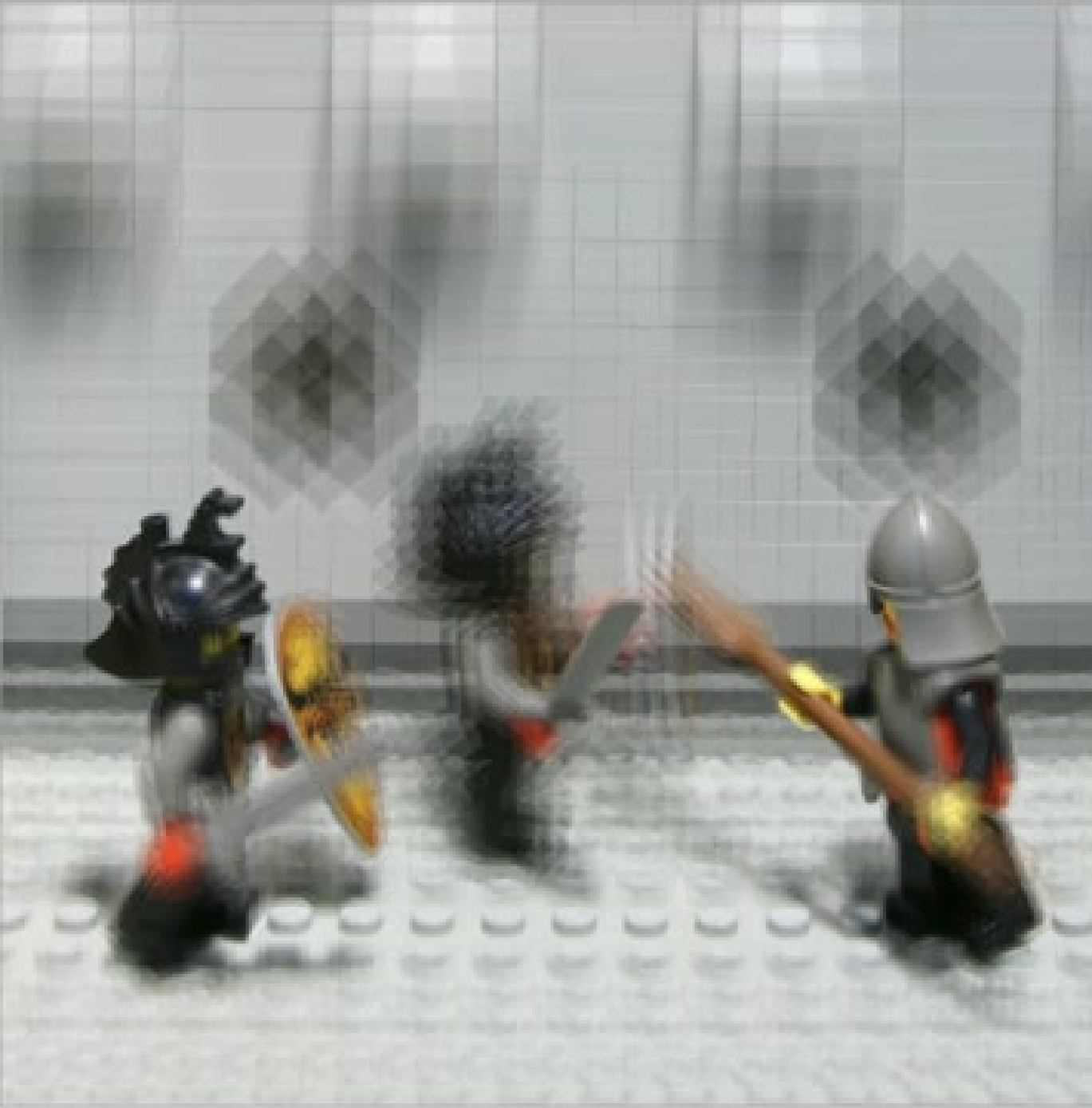
Source: Stanford Imaging Lab



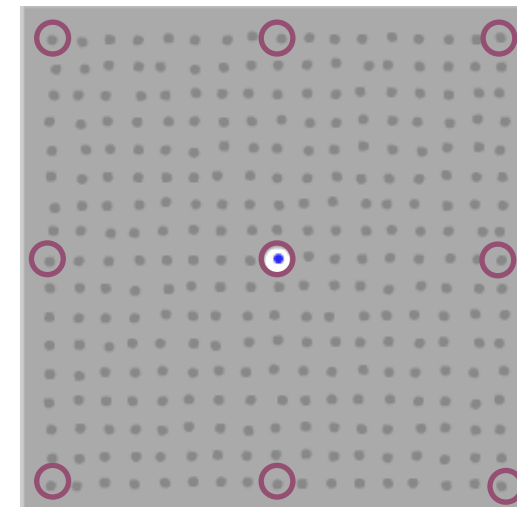


Source: Stanford Imaging Lab





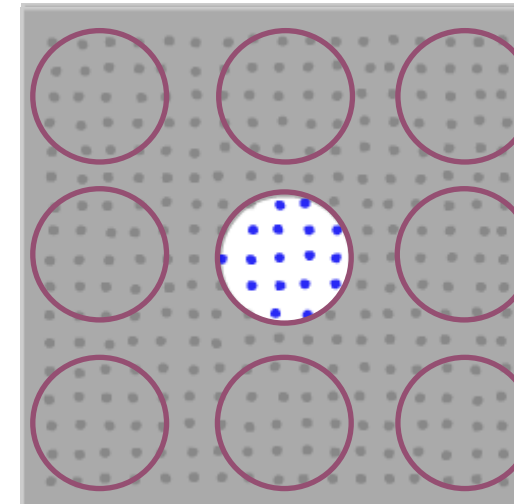
Superposition of image viewpoints



Superposition of images from separate viewpoints.
„Disrupted 3D-Look“ – not acceptable for photography*.



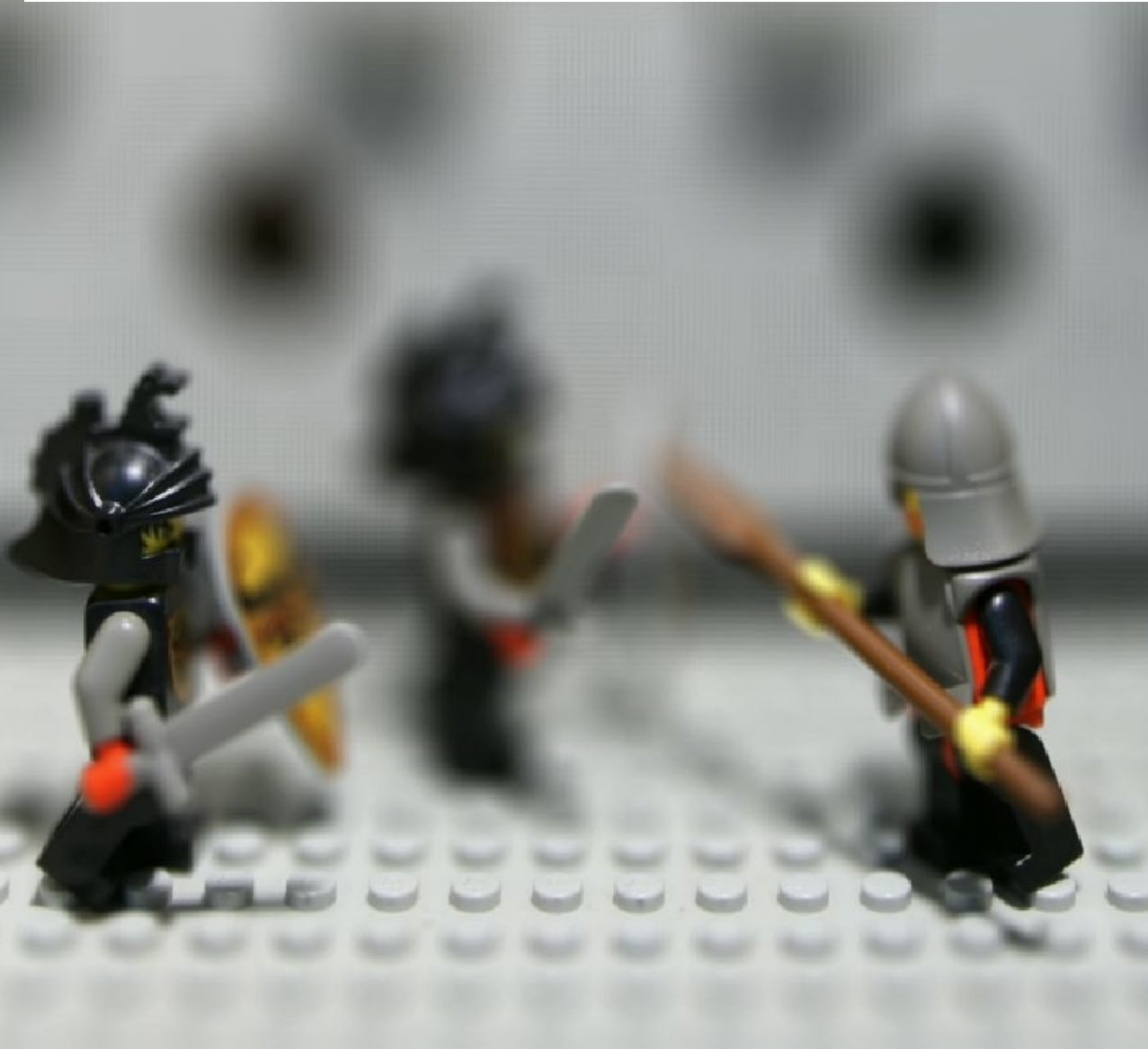
Combined Single Lens Perspectives



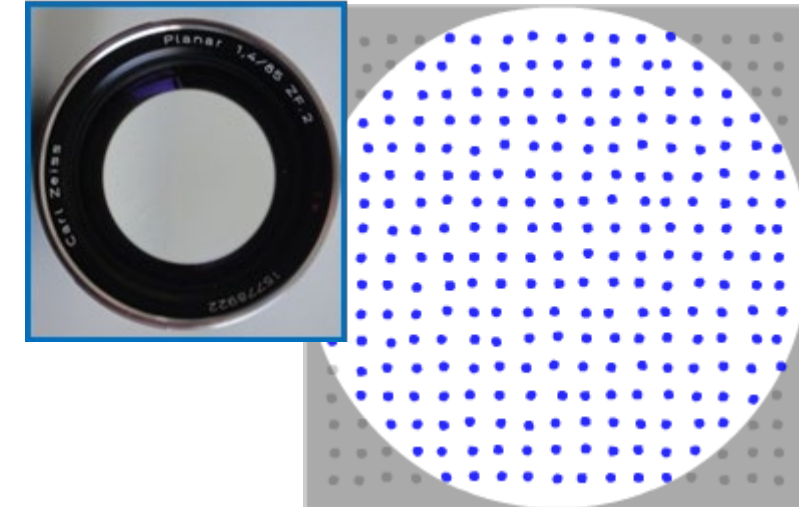
Smoothing the bokeh with higher aperture
multi-cameras...

Looks more appealing,
however still not nice near focus...

Depth of field is directly related to area of viewpoints = lens entrance pupil for single lens



lens entrance pupil



In standard photography lens entrance pupil defines the surface area of viewpoints on the captured 3D-scene.

This area is topologically continuous (usually approximately circular).

different
viewpoints
on scene

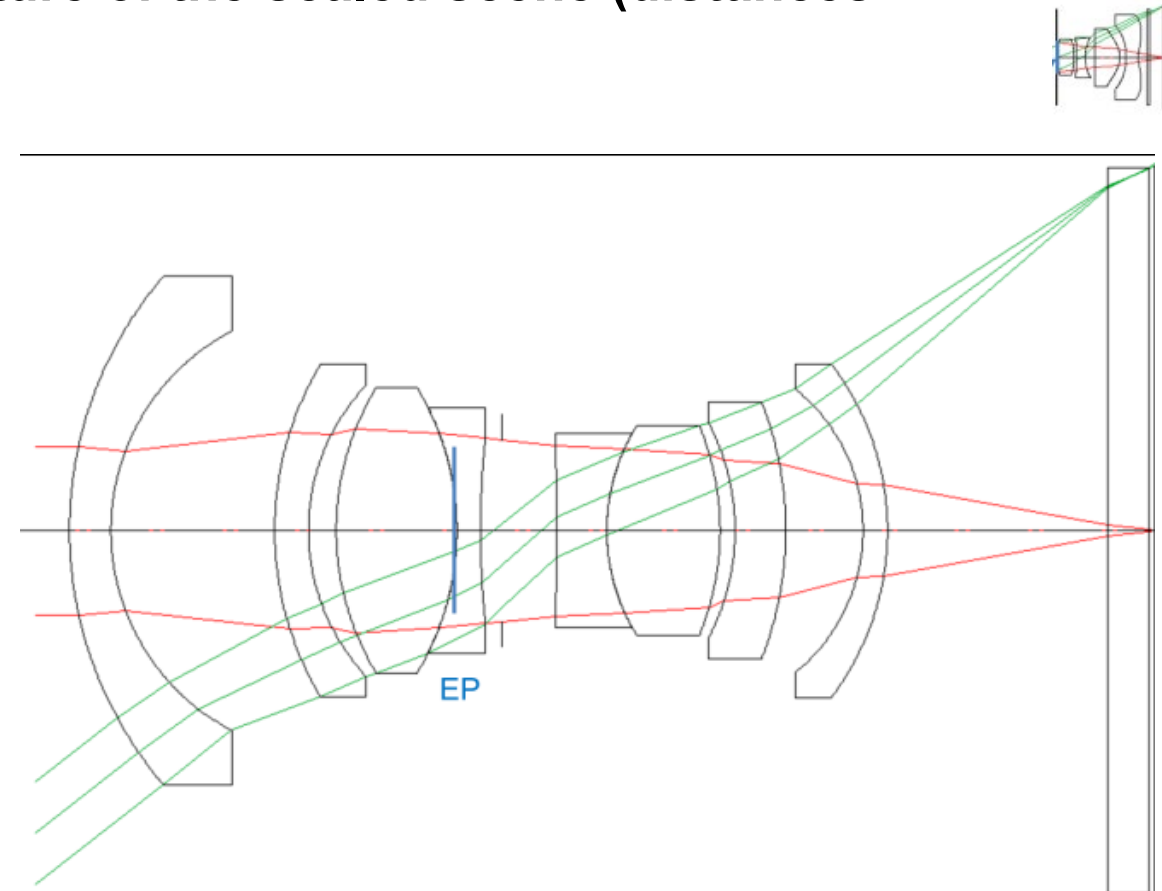


How to adapt depth of field of miniature models to real (large scale) scenes

Again consider two cameras with different sensor sizes and two lenses with same FOV.
Let c denote the crop factor, then **if we take the picture of the scaled scene (distances and object sizes!), then**

$$\frac{\varnothing_{spot,2}/h_2}{\varnothing_{spot,1}/h_1} = \frac{\frac{f_2^2}{F\#_2} \frac{(s_F - s)}{s_{FS}} h_1}{\frac{f_1^2}{F\#_1} \frac{(s_F - s)}{s_{FS}} h_2} = \frac{\frac{(cf_1)^2}{F\#_2} \frac{(cs_F - cs)}{cs_F cs} h_1}{\frac{f_1^2}{F\#_1} \frac{(s_F - s)}{s_{FS}} h_2}$$
$$= \frac{F\#_1}{F\#_2}$$

If we keep the aperture equal, the image appears same (also in terms of DoF)



Photography of Models and Depth of Field



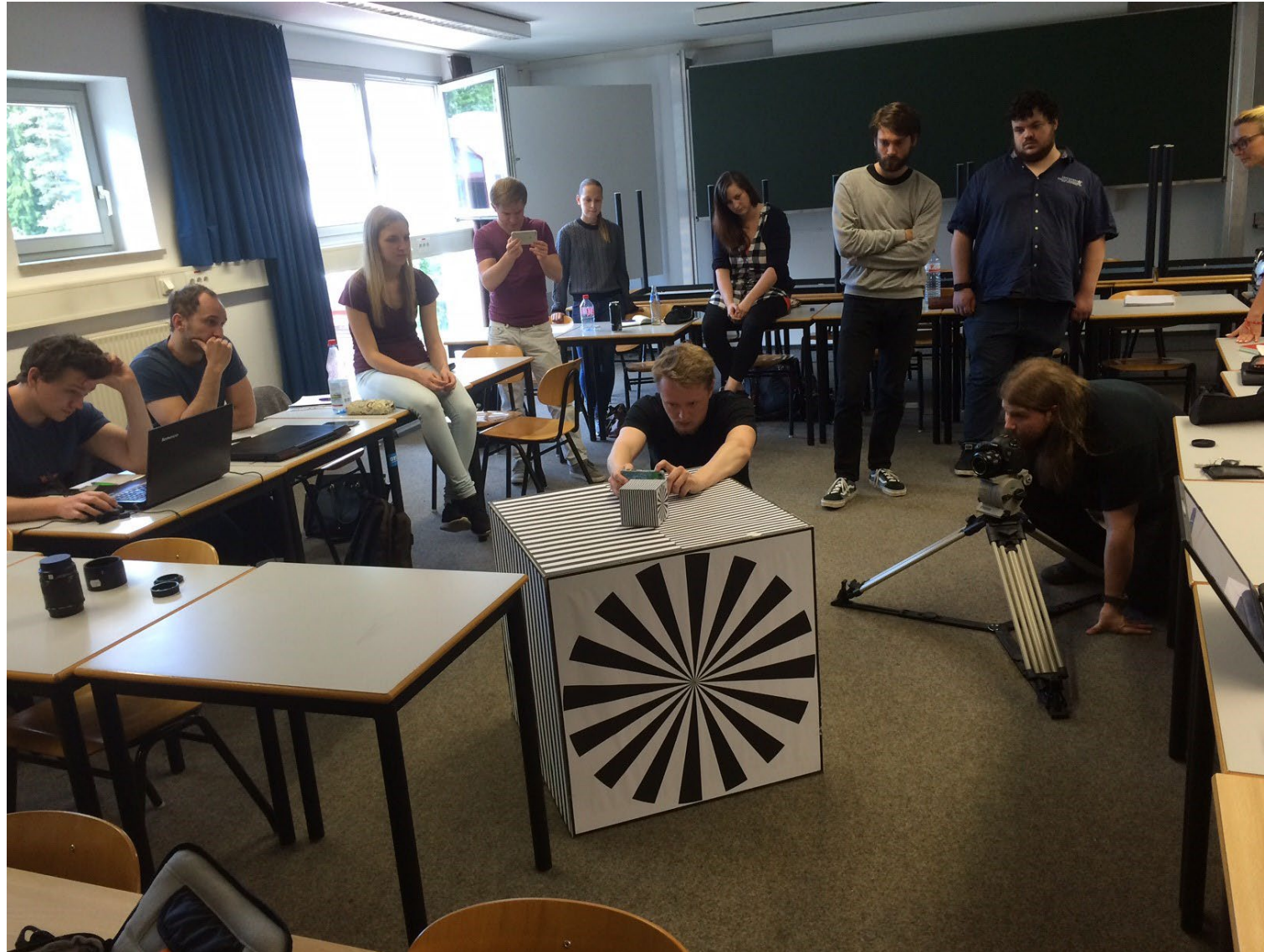
Photography of Models and Depth of Field



Photography of Models and Depth of Field



Scaling laws of optical imaging



Studies of depth-of-field
scaling laws

$$\frac{\varnothing_{spot,2}/h_2}{\varnothing_{spot,1}/h_1} = \frac{F\#_1}{F\#_2}$$

Two perspectives on 3D-imaging

Image = superposition of point spread functions

Principle of
ray path interpretation
duality: field
and pupil view!

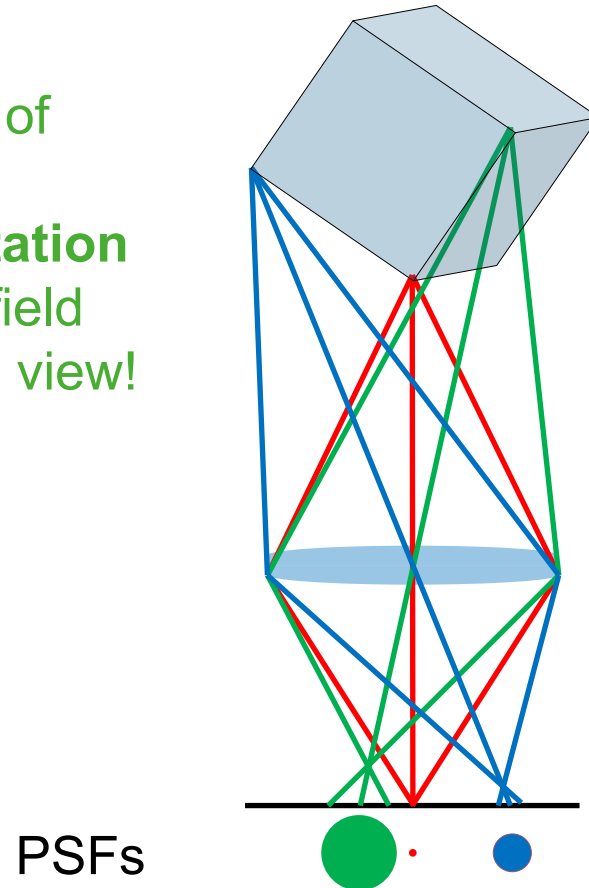
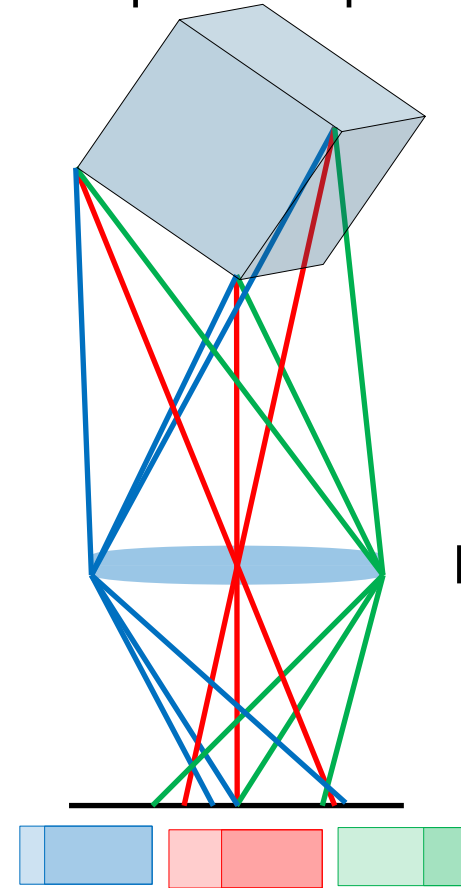


Image = superposition of all
viewpoints captured by lens aperture



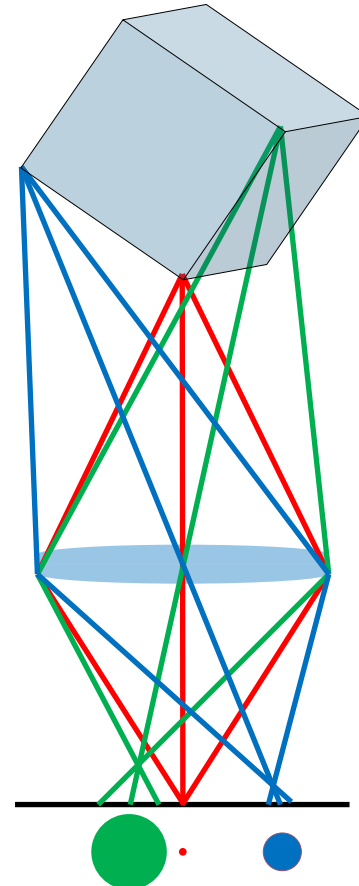
**Several
perspective
centers!**

Different viewpoints

Perspective projections
for viewpoints

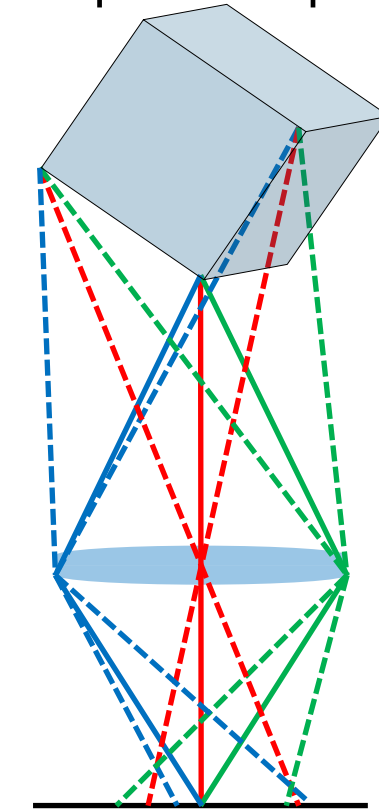
Two perspectives on 3D-imaging

Image = superposition of point spread functions

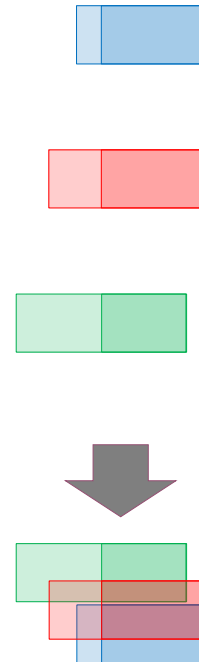


The object plane for which the rays through all „pupil pinholes“ hits one point in the image plane is focused.

Image = superposition of all viewpoints captured by lens aperture



focus on front edge:



Front edge sharp

Two perspectives on 3D-imaging: change of focus plane

Image = superposition of point spread functions

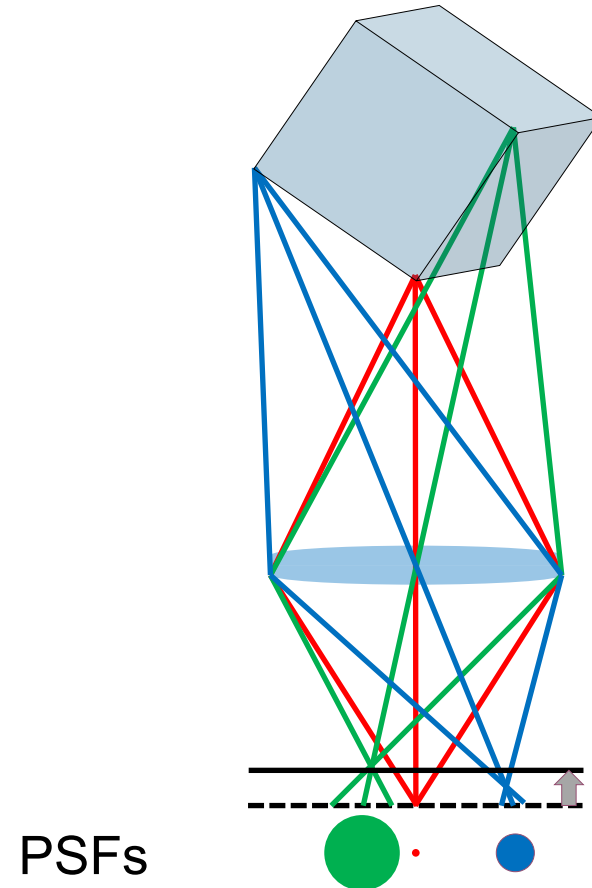
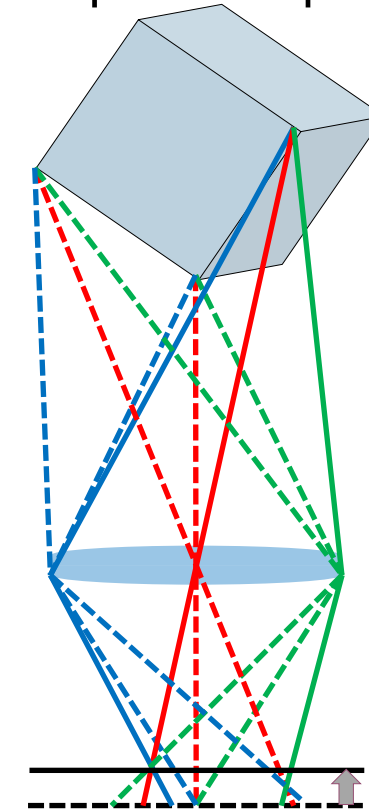
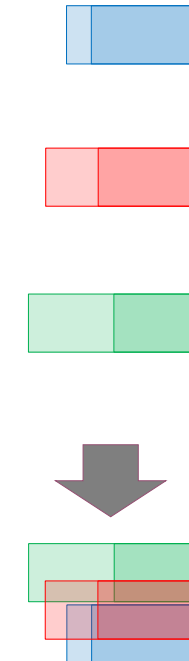


Image = superposition of all
viewpoints captured by lens aperture

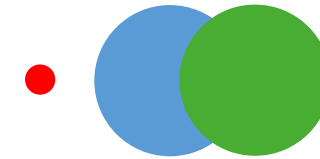
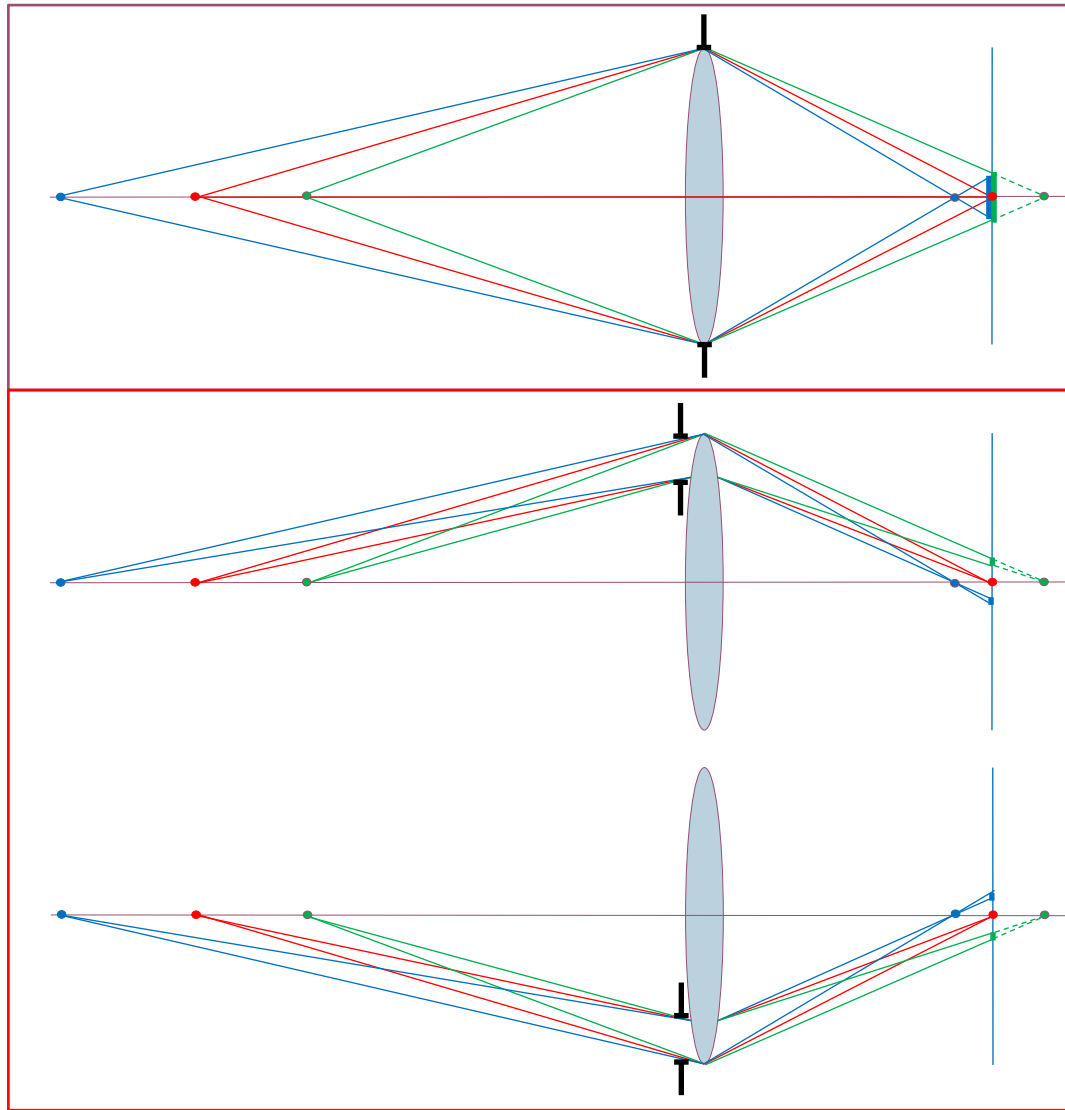


focus on front edge:

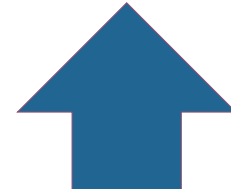


Right edge sharp

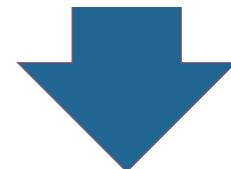
Capture of light on an image plane



Circle of confusion = out
of focus size of spot



Same calculation!



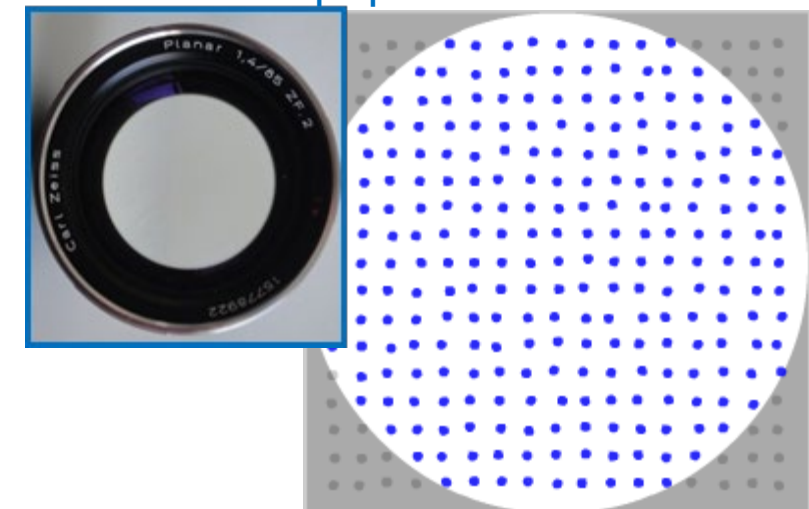
Perspective parallax for
single lens stereo



Source: Stanford Imaging Lab

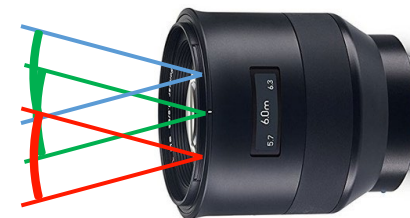
Depth of field is directly related to range of viewpoints

lens entrance pupil



The entrance pupil defines the surface of viewpoints on the captured 3D-scene. This area is topologically continuous (usually approximately circular).

**different
viewpoints
on scene**



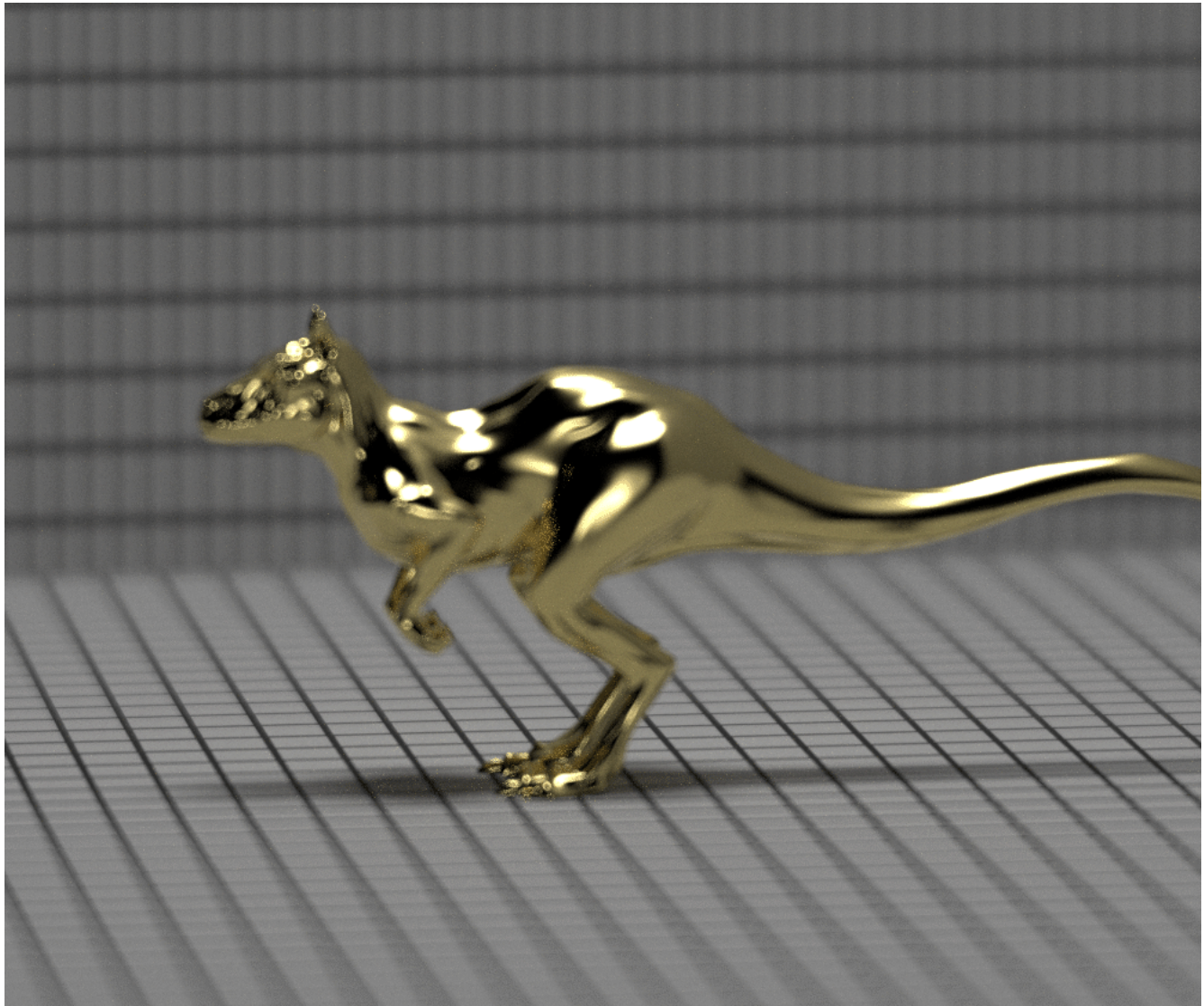
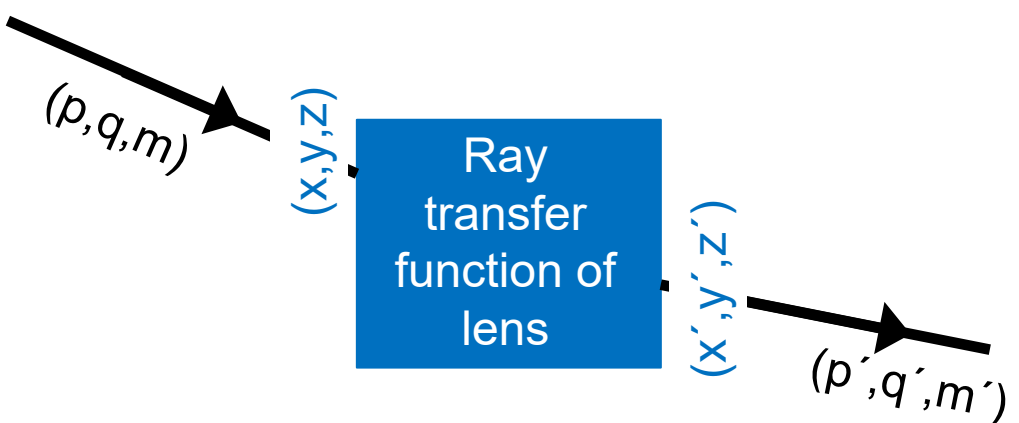
Ray tracing based 3D-image simulation

Lens transfer

„ray in“ → „ray out“

can be modeled via a parametrized model,
e.g. Hanika, Dachsbacher (2014).

Significantly **speeds up calculation**
compared to ray tracing through lens.



Optical System Design Software

Massive ray tracing and complex 3D objects (illumination, Straylight)

- Massive raytracing
- Illumination problems: High flexibility to model / optimize complex optical surfaces
- Complex objects, CAD import
 - diffraction or other physical-optical effects neglected

FRED
ASAP
RayJack ONE
LightTools
...

Optical Imaging System Design

- Geometrical and Diffraction-based analysis
- Optimization
- Systematic tolerancing
 - Partly: physical-optical propagation, quick ghost analysis, but limited use

Code-V
Zemax
OSLO
Quadoa
Synopsys

...

Wave-optical modeling (photonic devices, nano/micro-structured elements,...)

- Propagation of light in systems with elements / structures up to close to wavelength
- Masks / diffractive structures / metasurfaces
- Miniature photonics devices, e.g. integrated photonics
- polarization

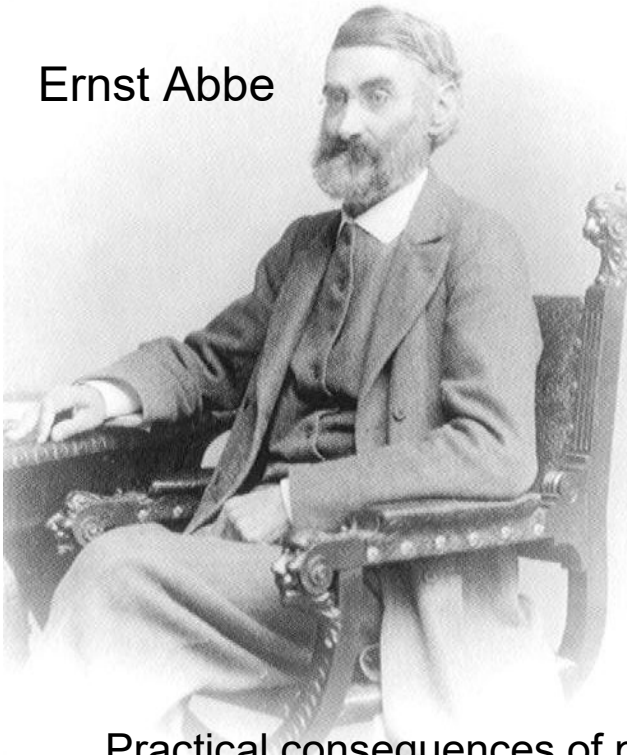
VirtualLab Fusion
Lumerical
RSoft
...

Tendency is to combine packages from both directions towards a more “holistic simulation”.

There are also application-specific simulation software packages, e.g. for optical lithography Solid-C or Prolith featuring partially coherent imaging together with modeling interaction with resist.

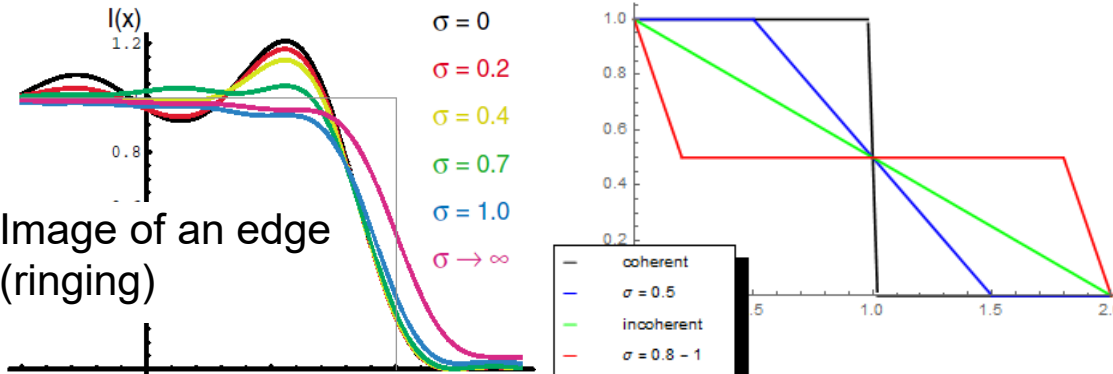
Extensions of Abbe's theory towards the description of modern microscopes or optical lithography system

Ernst Abbe



- **E. Abbe (1873).** Wave-optical imaging theory, optical resolution $\sim \lambda/NA$, optical information transfer and filtering, Fourier-Optics; Sine Condition, Achromatization, Computational and systematic approach for aberration correction
- **M. v. Laue (1907).** Propagation of partially coherent light
- **E. Schrödinger (1920).** Partial coherence in optical imaging
- **M. Berek (1926/27).** "coherence and consonance", Statistical optics, Coherence Function
- **F. Zernike (1934/38).** Propagation of coherence function, "effective source" for spatial illumination propagation; phase contrast microscopy; wavefront approximation with orthogonal functions
- **H.H. Hopkins (1951/53).** Imaging equations for partially coherent imaging (spatially coherent). Optical transfer function for partially coherent imaging ("transmission cross coefficients")
- **E. Wolf (1959).** Partially coherent imaging with polarized light, high NA imaging

Practical consequences of partial coherence:



Transferrable periodicities p to image space:

$$p \geq \frac{\lambda}{NA'} \quad \text{coherent}$$
$$p \geq \frac{\lambda}{2NA'} \quad \text{noncoherent, low contrast at high spatial frequencies}$$
$$p \geq \frac{\lambda}{2NA'} \quad \text{partially coherent, high contrast at high spatial freq.}$$

possible, high flexibility for image optimization

Homogeneous, non-conducting, linear media: Electrical field \vec{E} is a solution of wave equation

$$\left(\Delta - \frac{1}{c_M^2} \frac{\partial^2}{\partial t^2} \right) \vec{E} = 0$$

with $c_M = c/n$ the speed of light in a material of refractive index n. For a fixed frequency v the wave equation becomes the Helmholtz-equation

$$(\Delta + n^2 k^2) \vec{E} = 0, \text{ with } k = \frac{\omega}{c} = \frac{2\pi v}{c}.$$

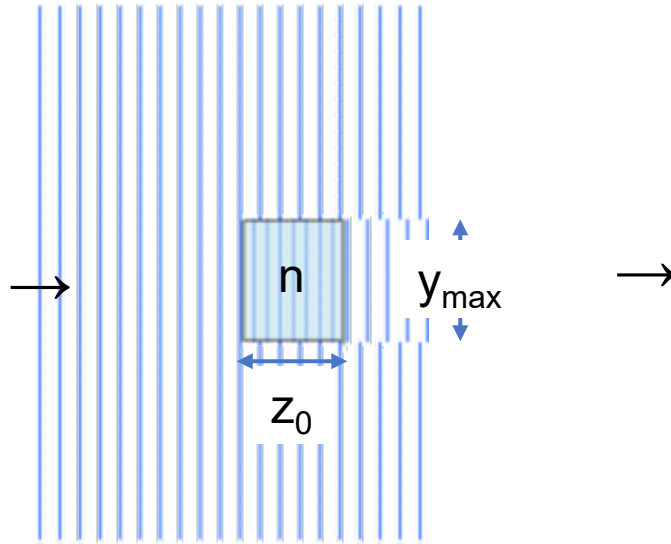
For a single component of the electrical field \vec{E} which we denote V an elementary solution of the Helmholtz-equation is a harmonic spherical wave:

$$V(\rho, t) = \frac{a}{\rho} \cos(\omega t - nk\rho + \varphi),$$

with $\rho = \sqrt{x^2 + y^2 + z^2}$, assuming the origin of the spherical wave at $(x_0, y_0, z_0) = (0, 0, 0)$, the amplitude a and the constant phase offset φ .

Linear System Transfer Model

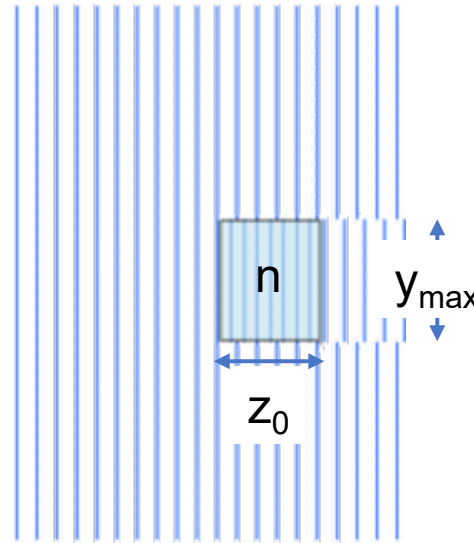
$$V_{in} = A \cos(\omega t - n k z + \varphi)$$



System Transfer

Linear System Transfer Model

$$V_{in} = A \cos(\omega t - n k z + \varphi)$$



$$V_{out} = A A_1 \cos(\omega t - n k z + \varphi + nkz_0)$$

Relative Amplitude:

A_1

Relative Phase shift:

$-nkz_0$

add in argument

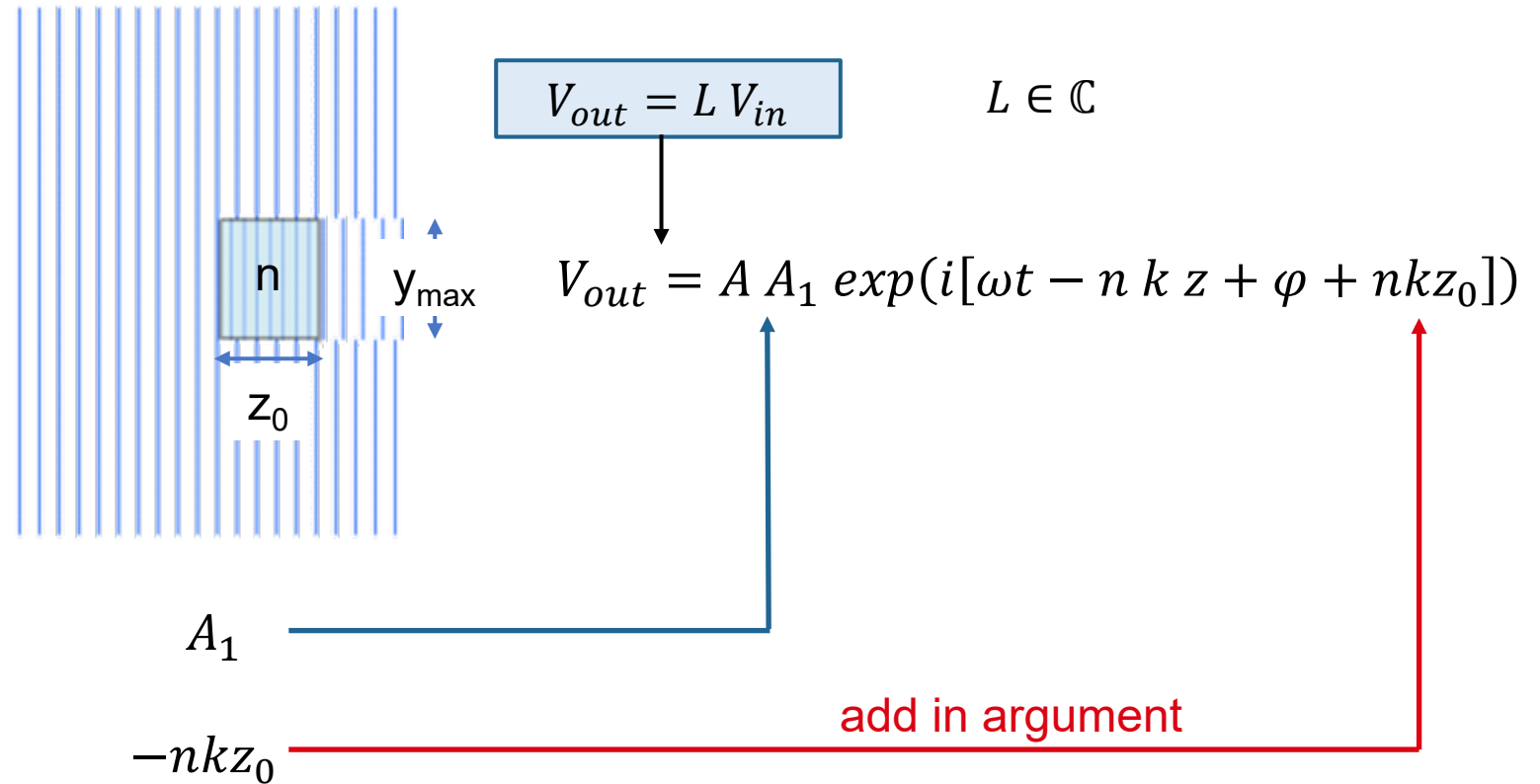
System Transfer

Linear System Transfer Model with complex numbers

$$V_{in} = A \exp(i[\omega t - n k z + \varphi])$$

Relative Amplitude:

Relative Phase shift:

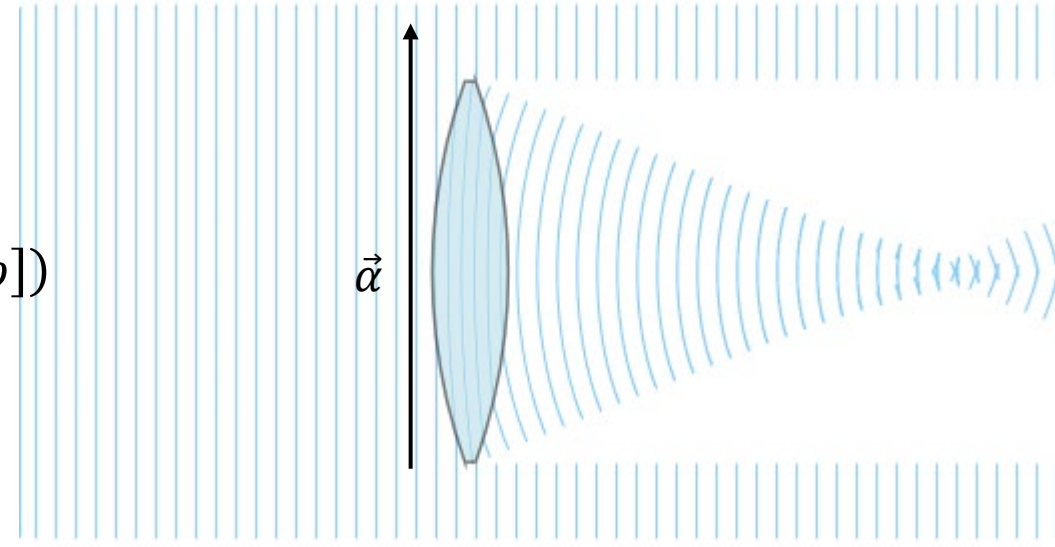


System Transfer

Linear operator for system transfer:
 $L = A_1 \exp(-i nkz_0)$

Lens wave transfer function

$$V_{in} = A \exp(i[\omega t - n k z + \varphi])$$



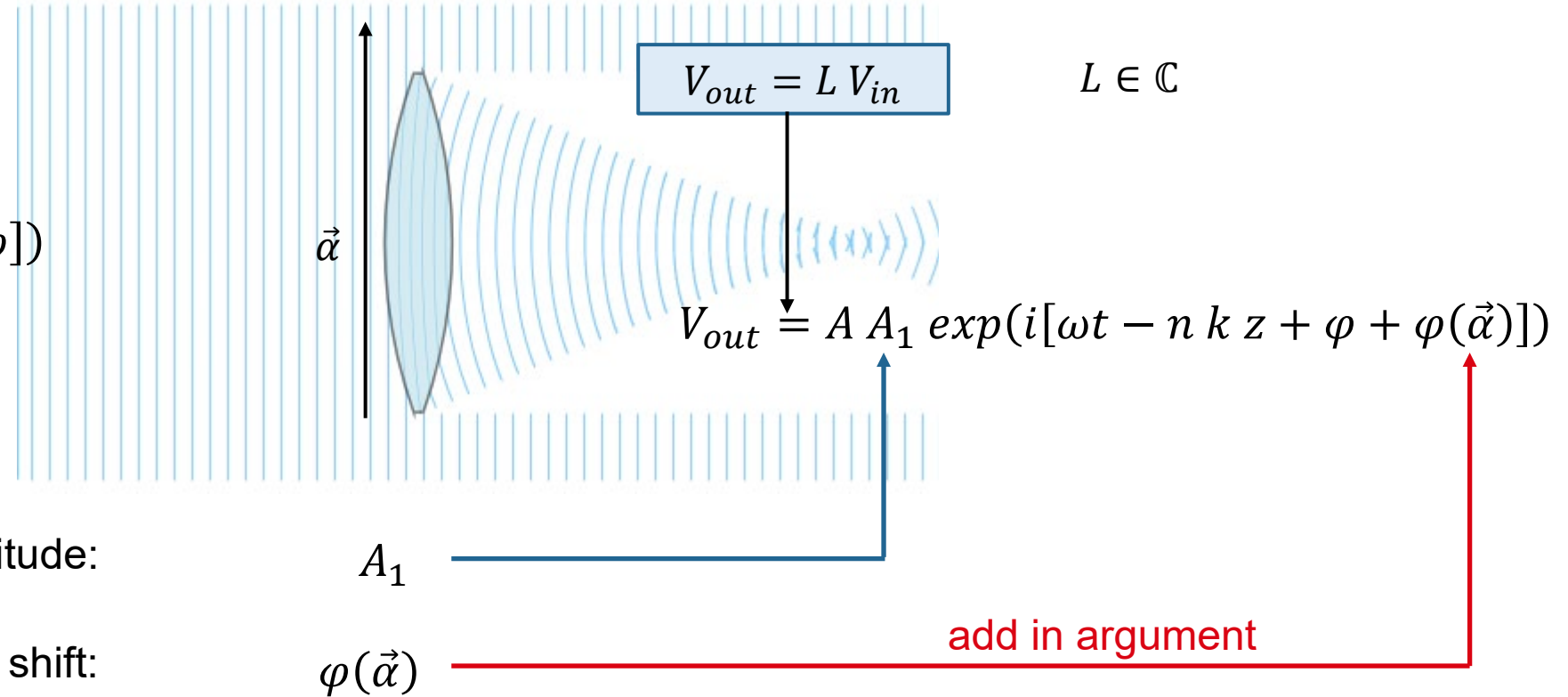
Relative Amplitude:

Relative Phase shift:

$$V_{in} = A \exp(i[\omega t - n k z + \varphi])$$

Relative Amplitude:

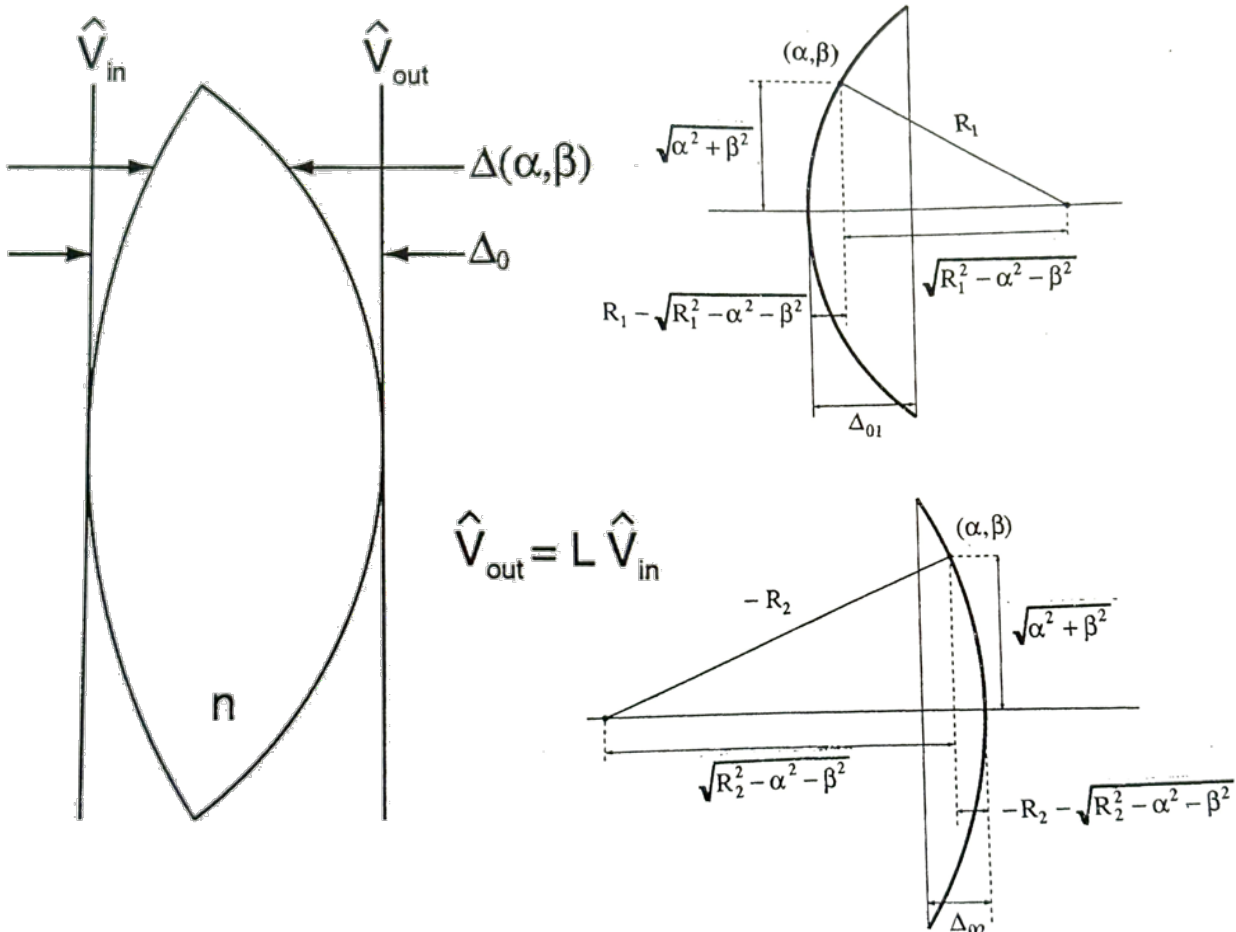
Relative Phase shift:



System Transfer

Linear operator for system transfer:
 $L = A_1 \exp(i\varphi(\vec{\alpha}))$

Simplified phase transfer of a lens



Simplified phase shift function of a lens
(measured along direction of axis only!):

$$\varphi(\vec{\alpha}) = kn\Delta(\vec{\alpha}) + k(\Delta_0 - \Delta(\vec{\alpha}))$$

with

$$\Delta(\vec{\alpha}) = \Delta_0 - R_1 \left(1 - \sqrt{1 - \frac{|\vec{\alpha}|^2}{R_1^2}} \right) - R_2 \left(1 - \sqrt{1 - \frac{|\vec{\alpha}|^2}{R_2^2}} \right)$$

Second order approximation: $\sqrt{1 - \frac{|\vec{\alpha}|^2}{R_1^2}} \approx 1 - \frac{|\vec{\alpha}|^2}{2R_1^2}$

yields $L(\vec{\alpha}) = L_0(\vec{\alpha}) \exp \left(-i \frac{k}{2} \Phi |\vec{\alpha}|^2 \right)$

Where L_0 describes the lens limit and eventual amplitude variation and

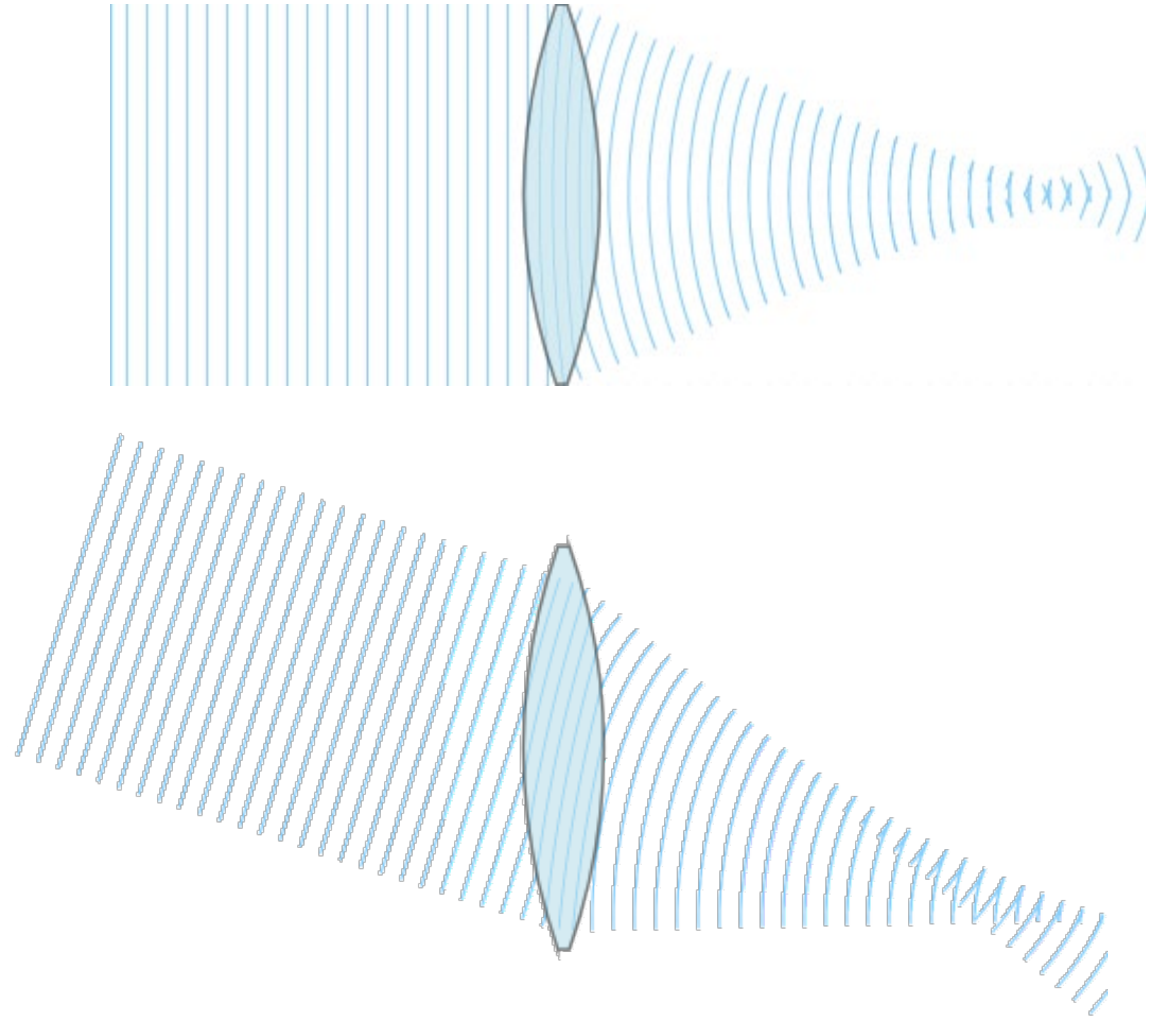
$$\Phi = (n - 1) \left(\frac{1}{R_1} - \frac{1}{R_2} \right)$$

„Goodmans'
thin lens“

Complex linear wave transfer function?

This propagation model $\varphi(\vec{\alpha})$ is limited, as

- due to the bending by Snell's law the assumption to measure OPL along axis is invalid
- the propagation depends also on the direction and origin of the incoming wave, $\varphi(\vec{\alpha})$ must be replaced by $\varphi(\vec{\alpha}, \vec{\xi})$



System transfer description in complex instead of real functions

$$V_{real}(t) = A \cos(\omega t - kz + \phi) \quad \text{real valued function for the scalar electro-magnetic field}$$

temporal angular frequency $\omega = 2\pi\nu$, the wave number $k = \frac{2\pi}{\lambda}$ and a phase offset ϕ

A phase shift cannot be expressed with a multiplication in the real. This is nothing other than the statement that the translation group in the real has two-dimensional irreducible representations, while the irreducible representations of abelian groups in complex vector spaces are always one-dimensional:

$$\begin{pmatrix} \cos m\phi & \sin m\phi \\ -\sin m\phi & \cos m\phi \end{pmatrix} \cong \begin{pmatrix} e^{im\phi} & 0 \\ 0 & e^{-im\phi} \end{pmatrix}.$$

Lenses and bodies with a different refractive index affect light waves in a first approximation in such a way that they cause phase shifts for the plane waves; it is therefore favorable to represent plane waves mathematically in such a way that this phase shift can be expressed mathematically simply. For this reason, it is convenient to replace the real-valued plane wave with a complex-valued one:

$$V(t) = \frac{1}{\sqrt{2}} A e^{-i(\omega t - kz + \phi)} = \frac{1}{\sqrt{2}} A (\cos(\omega t - kz + \phi) - i \sin(\omega t - kz + \phi)).$$

The imaginary part of this complex plane wave is created from the real part by a phase shift of $+\pi/2$. A phase shift of $-\pi/2$. would also be possible, you would only have to replace $-i$ with i . The factor $1/\sqrt{2}$ must also be taken into account here. It is introduced for the following reason: If you calculate the mean value of $V^2(t)$, you get

$$\langle V_{real}(t) V_{real}(t) \rangle = A^2 \langle \cos^2(\omega t - kz + \phi) \rangle = \frac{1}{2} A^2$$

System transfer description in complex instead of real functions

$$\langle V_{real}(t) V_{real}(t) \rangle = A^2 \langle \cos^2(\omega t - kz + \phi) \rangle = \frac{1}{2} A^2$$

This result can also be obtained by averaging $V(t)V^*(t)$:

$$\langle V(t)V^*(t) \rangle = \frac{1}{2} A^2 \langle 1 \rangle = \frac{1}{2} A^2,$$

if the factor $1/\sqrt{2}$ is used. In this description, the real process is therefore not given by the real part, but by $\sqrt{2}$ times the real part.

Mostly we are interested in stationary or temporally slowly varying quantity $\langle V(t)V^*(t) \rangle$. In case we are concerned with the field itself, V_{real} only is physically relevant.

$$V(t) = \frac{1}{\sqrt{2}} A e^{-i(\omega t - kz + \phi)} = \frac{1}{\sqrt{2}} A (\cos(\omega t - kz + \phi) - i \sin(\omega t - kz + \phi)).$$

real part physically relevant

“mathematical support construction”

The **analytical signal** for general wave fields introduced by Gabor (1946) is a natural generalization of this complex representation. Let $V^{(r)}(t)$ be a real physical field for which a Fourier representation exists:

$$V^{(r)}(t) = \int_{-\infty}^{\infty} \hat{V}^{(r)}(\nu) e^{-i2\pi\nu t} d\nu.$$

As $V^{(r)}$ is real, so the following applies

$\hat{V}^{(r)}(-\nu) = \hat{V}^{(r)*}(\nu)$, so in $\hat{V}^{(r)}(\nu) = A(\nu)e^{i\phi(\nu)}$, $A(\nu)$ is an even, $\phi(\nu)$ an odd function of ν , therefore

$$V^{(r)}(t) = 2 \int_0^{\infty} A(\nu) \cos(2\pi\nu t - \phi(\nu)) d\nu.$$

Shifting by $\pi/2$ yields

$$V^{(i)}(t) = -2 \int_0^{\infty} A(\nu) \sin(2\pi\nu t - \phi(\nu)) d\nu$$

and

$$V(t) = \frac{1}{\sqrt{2}} [V^{(r)}(t) + i V^{(i)}(t)] = \sqrt{2} \int_0^{\infty} A(\nu) e^{-i[2\pi\nu t - \phi(\nu)]} d\nu.$$

Thus we obtain the desired result, that the Fourier transform, the **amplitude spectrum, is a positive function**

$$\hat{V}(\nu) = \begin{cases} \sqrt{2}A(\nu)e^{i\phi(\nu)} = \sqrt{2} \hat{V}^{(r)}(\nu) & \text{für } \nu \geq 0 \\ 0, & \text{if } \nu < 0 \end{cases}$$

Alternative construction of the analytical signal

Given a real field $V^{(r)}(t)$. We are looking for a complex function $V(t)$ whose Fourier transform is half-sided, i.e. can only be non-zero for positive frequencies, and the spectrum should be exactly the same as that of the function $V^{(r)}(t)$:

$$\hat{V}(\nu) = \sqrt{2}\hat{V}^{(r)}(\nu) \hat{s}(\nu), \text{ where } \hat{s}(\nu) = \begin{cases} 1, & \text{if } \nu > 0 \\ 0, & \text{else} \end{cases} \text{ or } \hat{s}(\nu) = \text{sign}(\nu).$$

The Fourier transform of the Signum function is $s(t) = \frac{1}{2} \left[\delta(t) - \frac{i}{\pi t} \right]$;

Therefore, with the convolution theorem: $V(t) = \sqrt{2} \int_{-\infty}^{\infty} \hat{V}^{(r)}(t') s(t-t') dt'$

respectively, $V(t) = \frac{1}{\sqrt{2}} [V^{(r)}(t) + i V^{(i)}(t)]$

with $V^{(i)}(t) = H[V^{(r)}(t)] = \frac{1}{\pi} \int_{-\infty}^{\infty} \frac{\hat{V}^{(r)}(t')}{t'-t} dt'$.

Here $\int_{-\infty}^{\infty}$ means the Cauchy principal value of the integral: $\lim_{\varepsilon \rightarrow 0} \left\{ \int_{-\infty}^{t-\varepsilon} dt' + \int_{t+\varepsilon}^{\infty} dt' \right\}$. H is called the Hilbert transformation (symbol H); the integral is usually labelled with a slash.

Therefore applies:

The imaginary part of the analytical signal is obtained as the Hilbert transform of the real part.

Coherence function

$$\Gamma(P_1, P_2, t_1, t_2) = \left\langle \vec{E}(P_1, t_1) \cdot \overline{\vec{E}(P_2, t_2)} \right\rangle$$

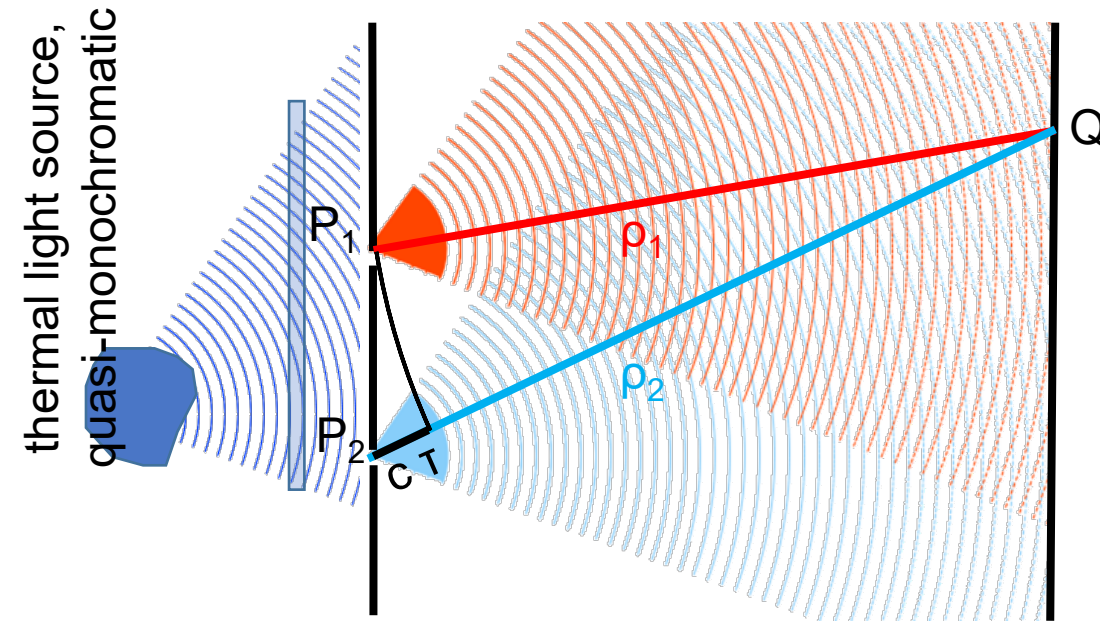
Intensity

$$I(P, t) = \Gamma(P, P, t, t) = \left\langle \vec{E}(P, t) \cdot \overline{\vec{E}(P, t)} \right\rangle$$

$$I = \lim_{T \rightarrow \infty} \frac{1}{T} \int_{-T}^T \vec{E} \cdot \vec{E} dt$$

Intensity distribution as time
average „with long exposure time“
of squared electrical field

Young's pinhole experiment and mutual coherence function



$$V(P_s, t) \quad s=1,2$$

$$V(Q, t) = K(Q, P_1) V\left(P_1, t - \frac{\rho_1}{c}\right) + K(Q, P_2) V\left(P_2, t - \frac{\rho_2}{c}\right)$$

(K = purely imaginary factor (in good approximation) for a quasi-monochromatic field)

Intensity at Q:

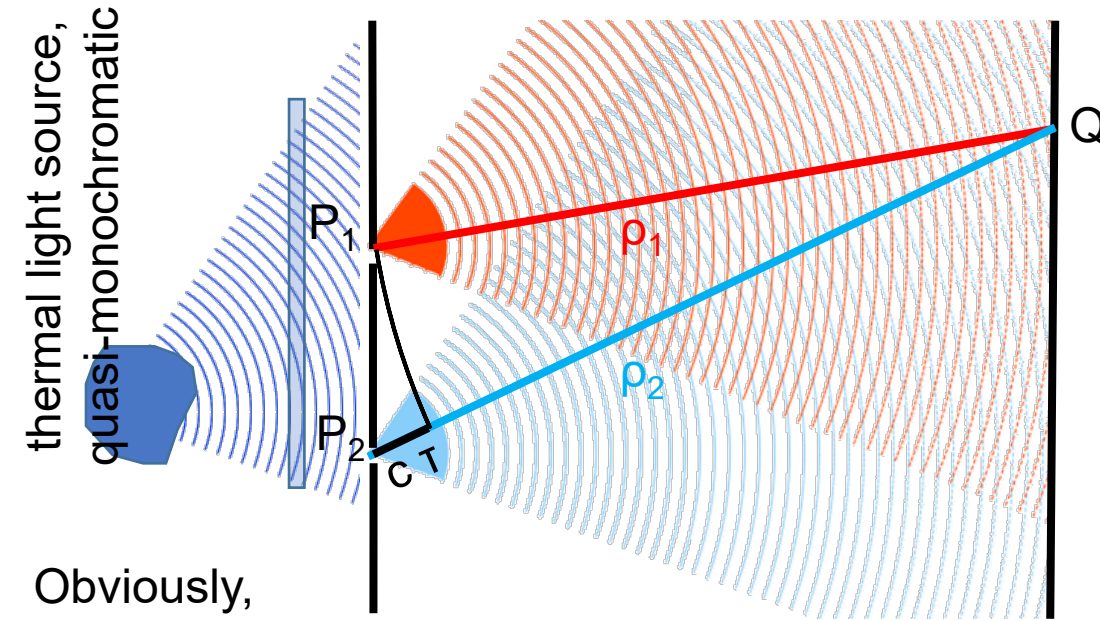
$$\begin{aligned} \langle V(Q, t) V^*(Q, t) \rangle &= I(Q) \\ &= |K(Q, P_1)|^2 \left\langle \left| V\left(P_1, t - \frac{\rho_1}{c}\right) \right|^2 \right\rangle + |K(Q, P_2)|^2 \left\langle \left| V\left(P_2, t - \frac{\rho_2}{c}\right) \right|^2 \right\rangle \\ &\quad + K(Q, P_1) \overline{K(Q, P_2)} \left\langle V\left(P_1, t - \frac{\rho_1}{c}\right) \overline{V\left(P_2, t - \frac{\rho_2}{c}\right)} \right\rangle \\ &\quad + \overline{K(Q, P_1)} K(Q, P_2) \left\langle \overline{V\left(P_1, t - \frac{\rho_1}{c}\right)} V\left(P_2, t - \frac{\rho_2}{c}\right) \right\rangle \end{aligned}$$

Ensemble average $\langle \quad \rangle = \int V_\omega \overline{V_\omega} W(d\omega)$ or time average

$$\Gamma(P_1, P_2, \tau) = \left\langle V\left(P_1, t - \frac{\rho_1}{c}\right) \overline{V\left(P_2, t - \frac{\rho_2}{c}\right)} \right\rangle \text{ which}$$

depends on time difference τ only.

Young's pinhole experiment and mutual coherence function



Obviously,

$$\Gamma(P_2, P_1, -\tau) = \left\langle \overline{V\left(P_1, t - \frac{\rho_1}{c}\right)} V\left(P_2, t - \frac{\rho_2}{c}\right) \right\rangle = \overline{\Gamma(P_1, P_2, \tau)}.$$

Closing one pinhole ($s=1,2$) gives the intensity:

$$\begin{aligned} I_s(Q) &= |K(Q, P_s)|^2 \left\langle \left| V\left(P_s, t - \frac{\rho_s}{c}\right) \right|^2 \right\rangle \\ &= |K(Q, P_s)|^2 \Gamma_s(P_s, P_s, 0) \end{aligned}$$

Shorthand: $\Gamma_{12}(\tau) \equiv \Gamma(P_1, P_2, \tau)$

With Schwarz inequality

$$\begin{aligned} &\left| \int V_\omega\left(P_1, t - \frac{\rho_1}{c}\right) \overline{V_\omega\left(P_2, t - \frac{\rho_2}{c}\right)} W(d\omega) \right| \\ &\leq \sqrt{\int \left| V_\omega\left(P_1, t - \frac{\rho_1}{c}\right) \right|^2 W(d\omega)} \sqrt{\int \left| V_\omega\left(P_2, t - \frac{\rho_1}{c}\right) \right|^2 W(d\omega)} \\ &= \sqrt{\Gamma_{11}(0)} \sqrt{\Gamma_{22}(0)} \end{aligned}$$

we get

$$|\Gamma_{12}(\tau)| \leq \sqrt{\Gamma_{11}(0)} \sqrt{\Gamma_{22}(0)}.$$

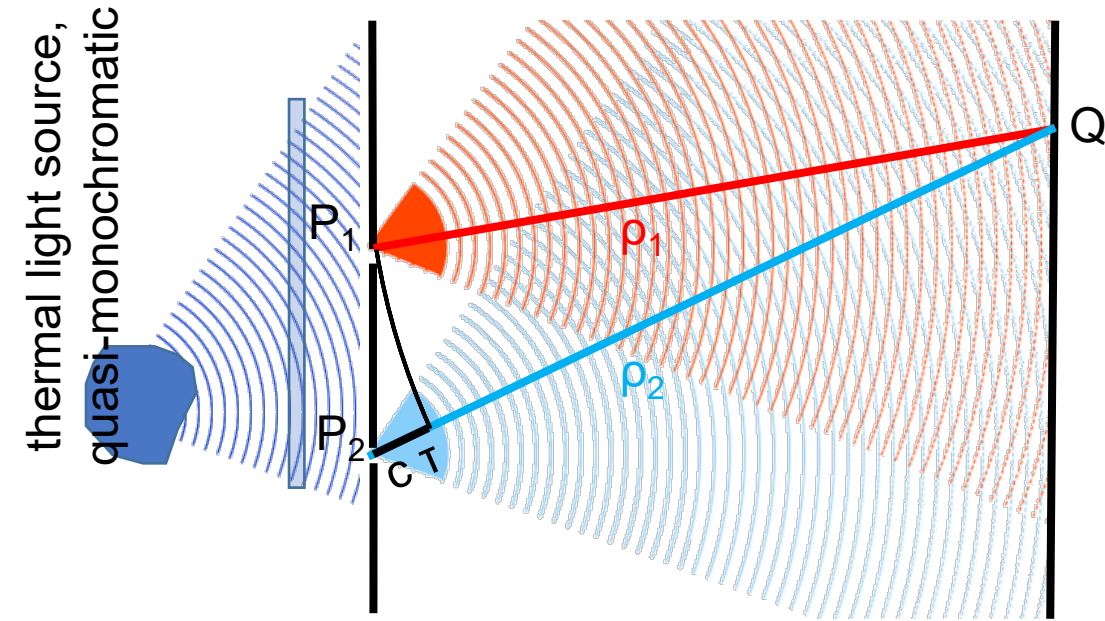
Therefore for the absolute value of

$$\gamma_{12}(\tau) = \frac{\Gamma_{12}(\tau)}{\sqrt{\Gamma_{11}(0) \Gamma_{22}(0)}} = |\gamma_{12}(\tau)| e^{i\Phi_{12}(\tau)}$$

we have:

$$0 \leq \gamma_{12}(\tau) = \frac{\Gamma_{12}(\tau)}{\sqrt{\Gamma_{11}(0) \Gamma_{22}(0)}} \leq 1.$$

Young's pinhole experiment and mutual coherence function



As $K(Q, P_s)$ is purely imaginary, $K(Q, P_1)\overline{K(Q, P_2)}$ is real.
 Therefore we get similarly as for coherent superposition:

$$\begin{aligned}
 I(Q) &= I_1(Q) + I_2(Q) + 2\text{Real} \left[K(Q, P_1) \overline{K(Q, P_2)} \Gamma_{12}(\tau) \right] \\
 &= I_1(Q) + I_2(Q) + 2K(Q, P_1) \overline{K(Q, P_2)} \text{Real}[\Gamma_{12}(\tau)] \\
 &= I_1(Q) + I_2(Q) + 2\sqrt{I_1(Q)}\sqrt{I_2(Q)} |\gamma_{12}(\tau)| \cos \Phi_{12}(\tau)
 \end{aligned}$$

$|\gamma_{12}(\tau)|$ determines the quality of the interference pattern.
 Visibility function according to Michelson:

$$V = \frac{I_{max} - I_{min}}{I_{max} + I_{min}}$$

$\gamma_{12}(0)$ complex degree of partial coherence

$|\gamma_{12}(0)|$ degree of partial coherence

$\Gamma(P_1, P_2, \tau)$ mutual coherence function (MCF)

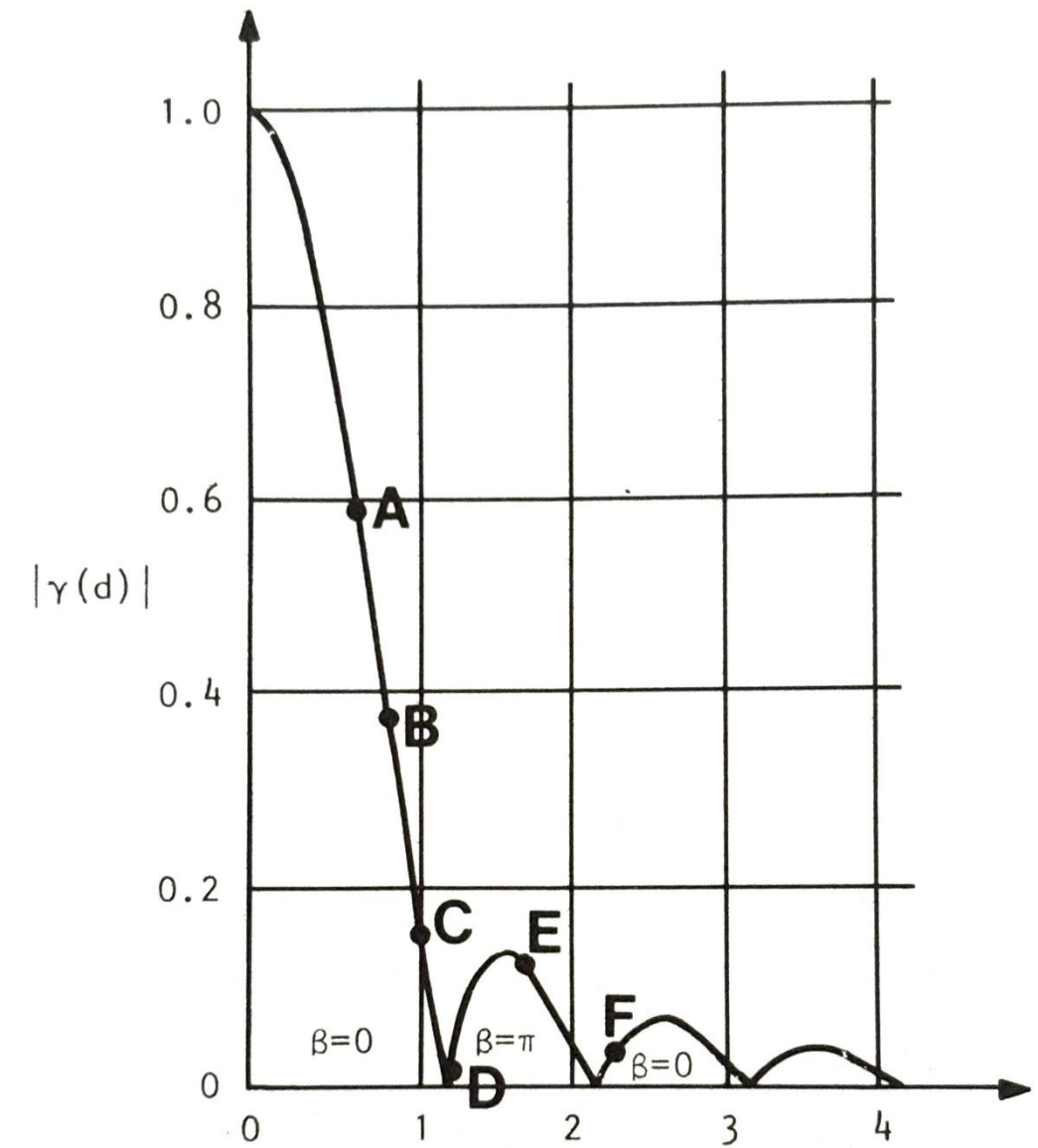
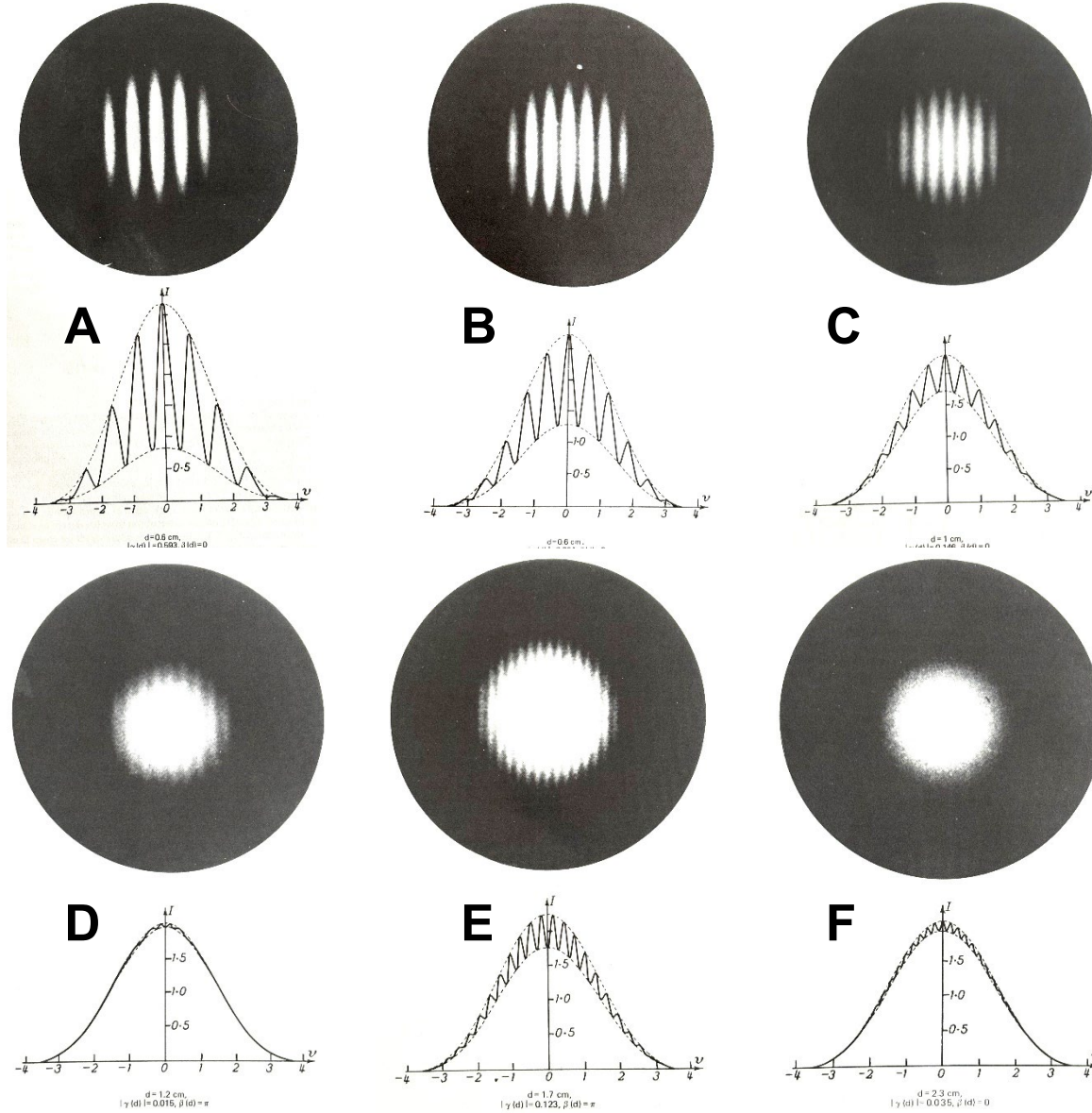
$|\gamma_{12}(0)| \approx 1$ mutually coherent

$|\gamma_{12}(0)| \approx 0$ mutually noncoherent

One can show, that:

- a) $\Gamma_{12}(\tau) = \Gamma_{12}^{rr}(\tau) - i\Gamma_{12}^{ri}(\tau)$
- b) $\Gamma_{11}^{ri}(0) = 0 = \Gamma_{11}^{ir}(0)$
- c) $\Gamma_{11}(0) = \Gamma_{11}^{rr}(0)$
- d) $\Gamma_{12}(\tau)$ is an analytical signal

Coherence function from double slit experiment



Propagation of the coherence function

The real part of the field amplitude $V^{(r)}(\underline{r}_1, t_1)$ shall fulfill the wave equation: $\left(\Delta_1 - \frac{1}{c^2} \frac{\partial^2}{\partial t_1^2}\right) V^{(r)}(\underline{r}_1, t_1) = 0$

$V^{(i)}(\underline{r}_1, t_1)$ also fulfills the wave equation, therefore also the linear combination: $\left(\Delta_1 - \frac{1}{c^2} \frac{\partial^2}{\partial t_1^2}\right) V(\underline{r}_1, t_1) = 0$

Multiplication with $\overline{V(\underline{r}_2, t_2)}$ yields: $\left(\Delta_1 - \frac{1}{c^2} \frac{\partial^2}{\partial t_1^2}\right) V(\underline{r}_1, t_1) \overline{V(\underline{r}_2, t_2)} = 0$

Indexing ω and $W(d\omega)$ yields $\left(\Delta_1 - \frac{1}{c^2} \frac{\partial^2}{\partial t_1^2}\right) \Gamma(\underline{r}_1, t_1; \underline{r}_2, t_2) = 0$ and $\left(\Delta_2 - \frac{1}{c^2} \frac{\partial^2}{\partial t_2^2}\right) \Gamma(\underline{r}_1, t_1; \underline{r}_2, t_2) = 0$.

If Γ depends only on $t_2 - t_1 = \tau$, we obtain $\left(\Delta_s - \frac{1}{c^2} \frac{\partial^2}{\partial t_s^2}\right) \Gamma(\underline{r}_1, \underline{r}_2, \tau) = 0$ für $s = 1, 2$.

If we calculate with the temporal Fourier transforms (the truncated functions), only the components for $\nu_1 = \nu_2$ remain after the time integration (before the limit $T \rightarrow \infty$). Thus, the **coherence function also fulfills the Helmholtz-equation**

$$(\Delta_s + k^2) \hat{\Gamma}(\underline{r}_1, \underline{r}_2, \nu) = 0, \quad s = 1, 2,$$

with $k = \frac{2\pi\nu}{c} = \frac{\omega}{c}$. This would also have been obtained if $\Gamma_{12}(\tau) = \int_0^\infty \hat{\Gamma}_{12}(\nu) e^{-i2\pi\nu\tau} d\nu$ had been used in the above wave equations.

Field amplitude $V(\underline{r}, t)$ with spectrum $\hat{V}(\underline{r}, \nu)$. Light source left-hand of half-space, $z < 0$, to illuminate aperture O. x_s, y_s coordinates in plane $z = 0$. Let $\hat{V}(x_s, y_s, 0, \nu)$ be known, to be determined: $\hat{V}(x, y, z, \nu)$ for $z > 0$.

$$\Delta_1 \hat{V}(\underline{r}_1, \nu) = -k^2 V(\underline{r}_1, \nu)$$

$$\Delta_1 \hat{G}_0(\underline{r}, \underline{r}_1, \nu) = -k^2 \hat{G}_0(\underline{r}, \underline{r}_1, \nu) - \delta(\underline{r} - \underline{r}_1) \quad (\underline{r} \text{ is the parameter})$$

with $\hat{G}_0(\underline{r}, \underline{r}_1, \nu) = \frac{e^{ik\rho}}{4\pi\rho}$, $\rho = |\underline{r} - \underline{r}_1|$. We obtain

$$\hat{V}(\underline{r}, \nu) = \iint_O \left[\hat{G}_0(\underline{r}, \underline{s}, \nu) \frac{\partial \hat{V}(\underline{s}, \nu)}{\partial n(\underline{s})} - \hat{V}(\underline{s}, \nu) \frac{\partial \hat{G}_0(\underline{r}, \underline{s}, \nu)}{\partial n(\underline{s})} \right] d\mu_F(\underline{s})$$

$V(\underline{r}, \nu)$ is the field amplitude in the volume V , bordered by S .

We are looking for \hat{G}^\wedge , which disappears on the plane $z = 0$. This is done by finding a suitable solution to the homogeneous equation

$$(\Delta_1 + k^2) \hat{G}_0(\underline{r}_m, \underline{r}_1, \nu) = 0$$

Rayleigh-Sommerfeld diffraction theory

Add \hat{G}_0 , and \underline{r}_m is a point on the left side of the half-plane ($z < 0$).

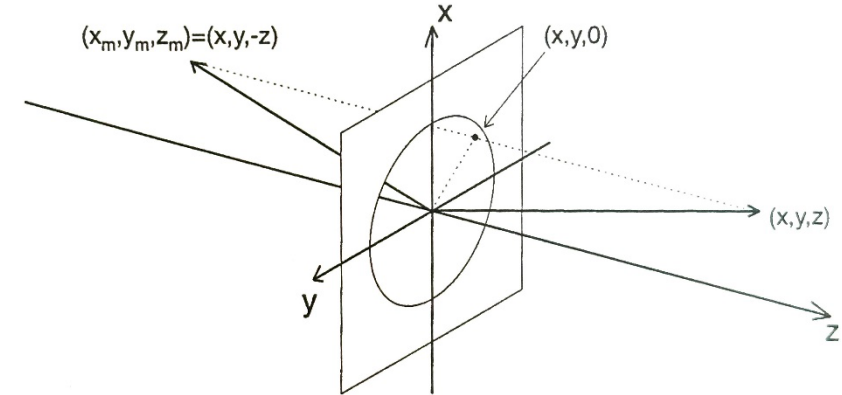
Let \underline{r}_m be the mirrored point to \underline{r} , with respect to the plane

$$z = 0: x_m = x, y_m = y, z_m = -z: \quad \hat{G}(\underline{r}, \underline{r}_1, v) = \hat{G}_0(\underline{r}, \underline{r}_1, v) - \hat{G}_0(\underline{r}_m, \underline{r}_1, v)$$

Using Sommerfeld's radiation condition, the part of the surface

integral of the sphere for $r \rightarrow \infty$ disappears: $\hat{V}(\underline{r}, v) \cong f(\vartheta, \phi) \frac{e^{ikr}}{r}$, thus

$$\hat{V}(\underline{r}, v) = - \iint_{R+B} \hat{V}(\underline{s}, v) \frac{\partial \hat{G}(\underline{r}, \underline{s}, v)}{\partial n(\underline{s})} dx_s dy_s$$



- Assumptions:
- 1) $\hat{V}(\underline{s}, v)$ is the same within the opening as if the screen were not there. stop size $\gg \lambda$
 - 2) On stop: $\hat{V}(\underline{s}, v) = 0$

$$\begin{aligned}
 \hat{G}(\underline{r}, \underline{r}_1, v) &= \hat{G}_0(\underline{r}, \underline{r}_1, v) - \hat{G}_0(\underline{r}_m, \underline{r}_1, v) = \frac{e^{ik|\underline{r}-\underline{r}_1|}}{4\pi|\underline{r}-\underline{r}_1|} - \frac{e^{ik|\underline{r}_m-\underline{r}_1|}}{4\pi|\underline{r}_m-\underline{r}_1|} \\
 &= \frac{e^{ik\sqrt{(x-x_1)^2 + (y-y_1)^2 + (z-z_1)^2}}}{4\pi\sqrt{(x-x_1)^2 + (y-y_1)^2 + (z-z_1)^2}} - \frac{e^{ik\sqrt{(x_m-x_1)^2 + (y_m-y_1)^2 + (z_m-z_1)^2}}}{4\pi\sqrt{(x-x_1)^2 + (y-y_1)^2 + (z-z_1)^2}}
 \end{aligned}$$

Rayleigh-Sommerfeld diffraction theory

$-\frac{\partial}{\partial n(\underline{s})}$ is the partial derivative of z at $x_s, y_s, z=0$

$$\frac{\partial \hat{G}(\underline{r}, \underline{s}, \nu)}{\partial n(\underline{s})} = \left[-\frac{1}{\rho^2} \frac{\partial \rho}{\partial z_1} e^{ik\rho} + \frac{1}{\rho} e^{ik\rho} ik \frac{\partial \rho}{\partial z_1} + \frac{1}{\rho_m^2} \frac{\partial \rho_m}{\partial z_1} e^{ik\rho_m} - \frac{ik}{\rho_m} e^{ik\rho_m} \frac{\partial \rho_m}{\partial z_1} \right]_{z_1=0}$$

$$\frac{\partial \rho}{\partial z_1} \Big|_{z_1=0} = \frac{-z}{\rho}, \quad \frac{\partial \rho_m}{\partial z_1} = \frac{-z}{\rho}, \quad \rho = |\underline{r} - \underline{s}| = \sqrt{(x - x_s)^2 + (y - y_s)^2 + z^2}$$

$$-\frac{\partial \hat{G}(\underline{r}, \underline{s}, \nu)}{\partial n(\underline{s})} = \frac{1}{2\pi} \frac{z}{\rho^3} e^{ik\rho} - \frac{ik}{2\pi} \frac{z}{\rho^2} e^{ik\rho} = \frac{z}{2\pi\rho} (1 - ik\rho) \frac{e^{ik\rho}}{\rho^2}$$

$$\rho = \sqrt{(x - x_s)^2 + (y - y_s)^2 + z^2}$$

Thus we obtain:

$$\hat{V}(x, y, z, \nu) = \iint_P \hat{V}(x_s, y_s, 0, \nu) \left[\frac{1}{2\pi} \frac{z}{\rho} (1 - ik\rho) \frac{e^{ik\rho}}{\rho^2} \right] dx_s dy_s$$

The approximation is valid for dimensions of aperture large against the wavelength. If one approaches this expression, one obtains the Fresnel diffraction formula in quadratic order and the Fraunhofer diffraction formula in linear order.

General model of optical system intensity computation (hypothetical!)

$$\hat{I}(x_1, y_1, x_2, y_2, z, \nu) = \iint \iint_{S_1, S_2} \hat{I}(x_{s1}, y_{s1}, x_{s2}, y_{s2}, 0, \nu) \left[\frac{1}{2\pi} \cos \vartheta_1 (1 - ik\rho_1) \frac{e^{ik\rho_1}}{\rho_1^2} \right] \left[\frac{1}{2\pi} \cos \vartheta_1 (1 + ik\rho_2) \frac{e^{-ik\rho_2}}{\rho_2^2} \right] dx_{s1} dy_{s1} dx_{s2} dy_{s2}$$

boundary
surface 1 boundary
surface 2



Geometrical boundaries
(absorbing, transmitting areas)

to be applied at object and k system boundary surfaces
+ geometrical boundaries of stops, field stops etc
even for systems with just a few optical surfaces not feasible computation task without further approximations

$$\hat{I}_{im}(x_1, y_1, z_{im}, \nu) = \hat{I}_{im}(x_1, y_1, x_1, y_2, z_{im}, \nu) = \\ 4(k+1) \text{ integrals!}$$

$$= \iint_{S_{k,1}} \iint_{S_{k,1}} \dots \iint_{S_{k,1}} \iint_{S_{2,2}} \iint_{S_{1,1}} \iint_{S_{1,2}} \dots \iint \iint_{S_{ob,1}, S_{ob,2}} \hat{I}_{im}(x_{s1}, y_{s1}, x_{s2}, y_{s2}, 0, \nu) \\ \times \left[\frac{1}{2\pi} \cos \vartheta_1 (1 - ik\rho_1) \frac{e^{ik\rho_1}}{\rho_1^2} \right] \left[\frac{1}{2\pi} \cos \vartheta_1 (1 + ik\rho_2) \frac{e^{-ik\rho_2}}{\rho_2^2} \right] \\ \times dx_{sob1} dy_{sob1} dx_{sob2} dy_{sob2} dx_{s1} dy_{s1} dx_{s2} dy_{s2} \dots dx_{sk1} dy_{sk1} dx_{sk2} dy_{sk2}$$

Fresnel- and Fraunhofer approximation

If you approximate this expression, you get the Fresnel formula in quadratic order and the Fraunhofer diffraction formula in linear order:

Amplitude terms:

$$k\rho = \frac{2\pi\nu}{c} \rho = \frac{2\pi}{\lambda} \rho \gg 1$$

Visible light: $\lambda \approx 0.5 \cdot 10^{-6} m$
 $\rightarrow \rho \gg 10^{-7} m \approx 0.1 \mu m$

$$\begin{aligned} \hat{V}(x, y, z, \nu) &= \iint_P \hat{V}(x_s, y_s, 0, \nu) \left[\frac{1}{2\pi\rho} \frac{z}{\rho} (1 - ik\rho) \frac{e^{ik\rho}}{\rho^2} \right] dx_s dy_s \\ &\approx -\frac{i}{\lambda} \iint \hat{V}(x_s, y_s, 0) \cos \vartheta \frac{e^{ik\rho}}{\rho} dx_s dy_s \\ \frac{1}{\rho} &= z \sqrt{1 - \frac{2(xx_s + yy_s)}{z^2} + \frac{x_s^2 + y_s^2}{z^2}} \approx \frac{1}{z} \end{aligned}$$

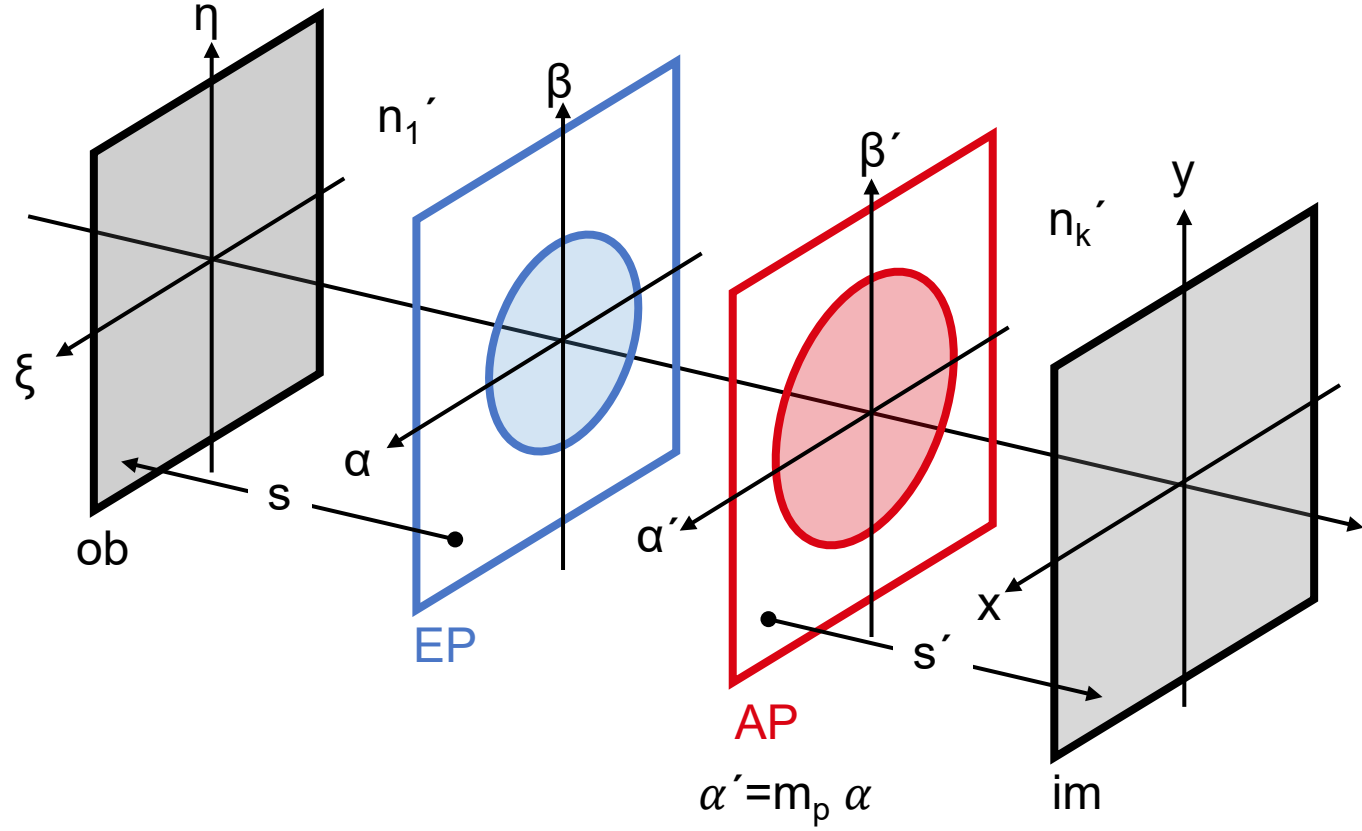
Phase terms with series expansion up to second order:

$$\begin{aligned} \rho &= \sqrt{(x - x_s)^2 + (y - y_s)^2 + z^2} = z \sqrt{1 + \left(\frac{x - x_s}{z}\right)^2 + \left(\frac{y - y_s}{z}\right)^2} \\ &= z \left(1 + \frac{1}{2} \left(\frac{x - x_s}{z}\right)^2 + \frac{1}{2} \left(\frac{y - y_s}{z}\right)^2 + \dots \right) \\ &= z \left(1 + \frac{1}{2} \frac{x^2 - 2xx_s + x_s^2}{z^2} + \frac{1}{2} \frac{y^2 - 2yy_s + y_s^2}{z^2} + \dots \right) \end{aligned}$$

$$\rho \approx z + \underbrace{\frac{xx_s + yy_s}{z}}_{\text{Fraunhofer}} + \underbrace{\frac{x_s^2 + y_s^2}{2z}}_{\text{Fresnel}}$$

in phase function z is an irrelevant offset

Paraxial wave-optical imaging model



$\xi \in \mathbb{R}^2$ object coordinates (ob),
 $\alpha \in \mathbb{R}^2$ entrance pupil coordinates (EP)
 $\alpha' \in \mathbb{R}^2$ exit pupil coordinates (AP)
 $x \in \mathbb{R}^2$ image coordinates (im)

Here all coordinates are in units of length [mm]

Lens aperture $L_0(\alpha) = \Im_{\{|\alpha| \leq \alpha_0\}}(\alpha)$

circular pupil with radius α_0 :

$$\Im_{\{|\alpha| \leq \alpha_0\}}(\alpha) = \begin{cases} 1, & \text{für } |\alpha| \leq \alpha_0 \\ 0, & \text{sonst} \end{cases}$$

Lens focusing (quadratic term)

$$\exp\left(-i\frac{\pi}{\lambda}m_p\Phi|\alpha|^2\right).$$

$\Phi = -n_1/f = n'_k/f'$ refractive power with respect to principal planes. With respect to EP the refractive power is $m_p\Phi$, and regarding AP respectively Φ/m_p .

Paraxial imaging model: Transfer of coherence function from object to image plane via entrance and exit pupil

object → EP:

$$\Gamma_{EP}(\alpha_1, \alpha_2) = \left(\frac{n_1}{\lambda s} \right)^2 \exp \left(-i \frac{\pi n_1}{\lambda s} (|\alpha_1|^2 - |\alpha_2|^2) \right)$$

$$\times \iint d\xi_1 d\xi_2 \Gamma_{ob}(\xi_1, \xi_2) \exp \left(i \frac{2\pi n_1}{\lambda s} (\alpha_1 \cdot \xi_1 - \alpha_2 \cdot \xi_2) \right) \exp \left(-i \frac{\pi n_1}{\lambda s} (|\xi_1|^2 - |\xi_2|^2) \right)$$

EP → AP:

Scaling to AP magnified by m_p :

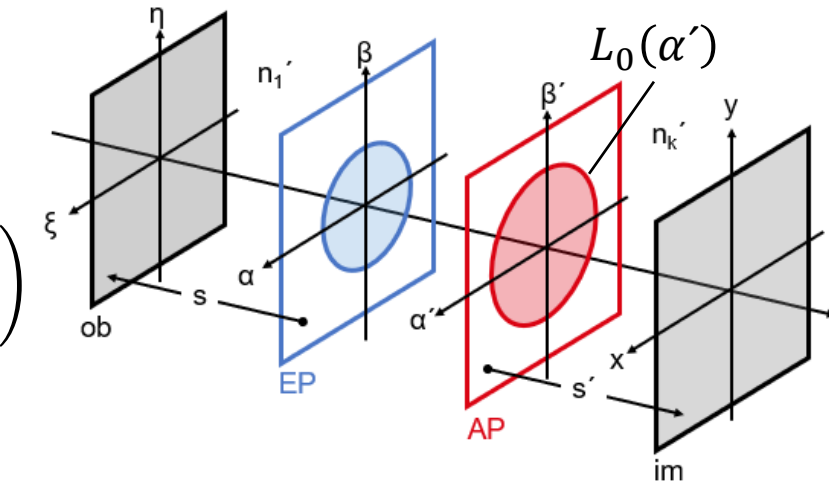
$$\Gamma_{AP}(\alpha_1', \alpha_2') = \frac{1}{m_p^2} \Gamma_{EP} \left(\frac{\alpha_1}{m_p}, \frac{\alpha_2}{m_p} \right)$$

Stop (diffraction) and focusing phase fct: $\Gamma_{AP}'(\alpha_1', \alpha_2') = \Gamma_{AP}(\alpha_1', \alpha_2') L_0(\alpha_1') L_0(\alpha_2') \exp \left(-i \frac{\pi \Phi}{\lambda m_p} (|\alpha_1'|^2 - |\alpha_2'|^2) \right)$

AP → image:

$$\Gamma_{im}(x_1, x_2)$$

$$= \left(\frac{n'_k}{\lambda s'} \right)^2 \exp \left(i \frac{\pi n'_k}{\lambda s'} (|x_1|^2 - |x_2|^2) \right) \iint d\alpha_1' d\alpha_2' m_p^2 \Gamma_{AP}(\alpha_1', \alpha_2') \exp \left(-i \frac{2\pi n'_k}{\lambda s'} (\alpha_1' \cdot \xi_1 - \alpha_2' \cdot \xi_2) \right) \exp \left(i \frac{\pi n'_k}{\lambda s'} (|\alpha_1'|^2 - |\alpha_2'|^2) \right)$$



Same expressed in entrance pupil coordinates

object → EP:

$$\Gamma_{EP}(\alpha_1, \alpha_2) = \left(\frac{n_1}{\lambda s}\right)^2 \exp\left(-i \frac{\pi n_1}{\lambda s} (|\alpha_1|^2 - |\alpha_2|^2)\right)$$

$$\times \iint d\xi_1 d\xi_2 \Gamma_{ob}(\xi_1, \xi_2) \exp\left(i \frac{2\pi n_1}{\lambda s} (\alpha_1 \cdot \xi_1 - \alpha_2 \cdot \xi_2)\right) \exp\left(-i \frac{\pi n_1}{\lambda s} (|\xi_1|^2 - |\xi_2|^2)\right)$$

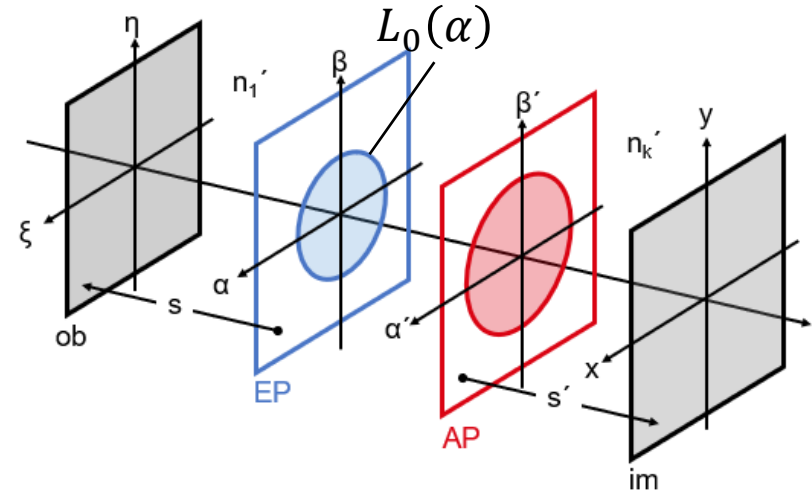
EP → AP:

$$m_p^2 \Gamma_{AP}(\alpha_1, \alpha_2) = \Gamma_{EP}(\alpha_1, \alpha_2) L_0(\alpha_1) L_0(\alpha_2) \exp\left(-i \frac{\pi}{\lambda} m_p \Phi (|\alpha_1|^2 - |\alpha_2|^2)\right)$$

AP → image:

$$\Gamma_{im}(x_1, x_2) = \left(\frac{n'_k}{\lambda s'}\right)^2 \exp\left(i \frac{\pi n'_k}{\lambda s'} (|x_1|^2 - |x_2|^2)\right)$$

$$\times \iint d\alpha_1 d\alpha_2 m_p^2 \Gamma_{AP}(m_p \alpha_1, m_p \alpha_2) \exp\left(-i \frac{2\pi n'_k}{\lambda s'} (\alpha_1 \cdot \xi_1 - \alpha_2 \cdot \xi_2)\right) \exp\left(i \frac{\pi n'_k}{\lambda s'} (|\alpha_1|^2 - |\alpha_2|^2)\right)$$



Paraxial imaging model: Transfer of coherence function from object to image plane via entrance and exit pupil

Combining all steps yields following coherence function in the image plane:

$$\Gamma_{im}(x_1, x_2) = m_p^2 \left(\frac{n_1}{\lambda s} \right)^2 \left(\frac{n'_k}{\lambda s'} \right)^2 \exp \left(i \frac{\pi}{\lambda} \frac{n'_k}{s'} (|x_1|^2 - |x_2|^2) \right)$$

$$\times \iint d\xi_1 d\xi_2 \Gamma_{ob}(\xi_1, \xi_2) \exp \left(-i \frac{\pi}{\lambda} \frac{n_1}{s} (|\xi_1|^2 - |\xi_2|^2) \right)$$

$$\times \iint d\alpha_1 d\alpha_2 L_0(\alpha) L_0(\alpha) \exp \left(i \frac{\pi}{\lambda} \left(-\frac{n_1}{s} + m_p^2 \frac{n'_k}{s'} - m_p \Phi \right) (|\alpha_1|^2 - |\alpha_2|^2) \right)$$

$$\times \exp \left(i \frac{2\pi}{\lambda} \left(\alpha_1 \cdot \left(\frac{n_1}{s} \xi_1 - m_p \frac{n'_k}{s'} x_1 \right) - \alpha_2 \cdot \left(\frac{n_1}{s} \xi_2 - m_p \frac{n'_k}{s'} x_2 \right) \right) \right).$$

Paraxial imaging model: Transfer of coherence function from object to image plane via entrance and exit pupil

Combining all steps yields following coherence function in the image plane:

$$\Gamma_{im}(x_1, x_2) = m_p^2 \left(\frac{n_1}{\lambda s} \right)^2 \left(\frac{n'_k}{\lambda s'} \right)^2 \exp \left(i \frac{\pi n'_k}{\lambda s'} (|x_1|^2 - |x_2|^2) \right)$$

quadratic phase term **image**
(irrelevant for intensity)

$$\times \iint d\xi_1 d\xi_2 \Gamma_{ob}(\xi_1, \xi_2) \exp \left(-i \frac{\pi n_1}{\lambda s} (|\xi_1|^2 - |\xi_2|^2) \right)$$

quadratic phase term **object**

$$\times \iint d\alpha_1 d\alpha_2 L_0(\alpha) L_0(\alpha) \exp \left(i \frac{\pi}{\lambda} \left(-\frac{n_1}{s} + m_p^2 \frac{n'_k}{s'} - m_p \Phi \right) (|\alpha_1|^2 - |\alpha_2|^2) \right)$$

quadratic phase term **pupil**

$$\times \exp \left(i \frac{2\pi}{\lambda} \left(\alpha_1 \cdot \left(\frac{n_1}{s} \xi_1 - m_p \frac{n'_k}{s'} x_1 \right) - \alpha_2 \cdot \left(\frac{n_1}{s} \xi_2 - m_p \frac{n'_k}{s'} x_2 \right) \right) \right).$$

**linear phase terms:
combining pupil and field**

Paraxial imaging model: Intensity distribution

With $I_{im}(x) = \Gamma_{im}(x, x)$ we obtain the intensity distribution in the image plane:

$$I_{im}(x) = m_p^2 \left(\frac{n_1}{\lambda s} \right)^2 \left(\frac{n'_k}{\lambda s'} \right)^2$$

$$\times \iint d\xi_1 d\xi_2 \Gamma_{ob}(\xi_1, \xi_2) \exp \left(-i \frac{\pi n_1}{\lambda s} (|\xi_1|^2 - |\xi_2|^2) \right)$$

quadratic phase term **object**

$$\times \iint d\alpha_1 d\alpha_2 L_0(\alpha) L_0(\alpha) \exp \left(i \frac{\pi}{\lambda} \left(-\frac{n_1}{s} + m_p^2 \frac{n'_k}{s'} - m_p \Phi \right) (|\alpha_1|^2 - |\alpha_2|^2) \right)$$

quadratic phase term **pupil**

$$\times \exp \left(i \frac{2\pi}{\lambda} \left(\alpha_1 \cdot \left(\frac{n_1}{s} \xi_1 - m_p \frac{n'_k}{s'} x \right) - \alpha_2 \cdot \left(\frac{n_1}{s} \xi_2 - m_p \frac{n'_k}{s'} x \right) \right) \right).$$

**linear phase terms:
combining pupil and field**

Paraxial imaging model: Intensity distribution

With $I_{im}(x) = \Gamma_{im}(x, x)$ we obtain the intensity distribution in the image plane:

$$I_{im}(x) = m_p^2 \left(\frac{n_1}{\lambda s} \right)^2 \left(\frac{n'_k}{\lambda s'} \right)^2$$

$$\times \iint d\xi_1 d\xi_2 \Gamma_{ob}(\xi_1, \xi_2) \exp \left(-i \frac{\pi n_1}{\lambda s} (|\xi_1|^2 - |\xi_2|^2) \right)$$

quadratic phase term **object**

$$\times \iint d\alpha_1 d\alpha_2 L_0(\alpha) L_0(\alpha) \exp \left(i \frac{\pi}{\lambda} \left(-\frac{n_1}{s} + m_p^2 \frac{n'_k}{s'} - m_p \Phi \right) (|\alpha_1|^2 - |\alpha_2|^2) \right)$$

quadratic phase term **pupil**

$$\times \exp \left(i \frac{2\pi}{\lambda} \left(\alpha_1 \cdot \left(\frac{n_1}{s} \xi_1 - m_p \frac{n'_k}{s'} x \right) - \alpha_2 \cdot \left(\frac{n_1}{s} \xi_2 - m_p \frac{n'_k}{s'} x \right) \right) \right).$$

**linear phase terms:
combining pupil and field**

Paraxial imaging model: Intensity distribution

With $I_{im}(x) = I_{im}(x, x)$ we obtain the intensity distribution in the image plane:

$$I_{im}(x) = m_p^2 \left(\frac{n_1}{\lambda s} \right)^2 \left(\frac{n'_k}{\lambda s'} \right)^2$$

$$\times \iint d\xi_1 d\xi_2 \Gamma_{ob}(\xi_1, \xi_2) \exp \left(-i \frac{\pi n_1}{\lambda s} (|\xi_1|^2 - |\xi_2|^2) \right)$$

$$\times \iint d\alpha_1 d\alpha_2 L_0(\alpha) L_0(\alpha) \exp \left(i \frac{\pi}{\lambda} \left(-\frac{n_1}{s} + m_p^2 \frac{n'_k}{s'} - m_p \Phi \right) (|\alpha_1|^2 - |\alpha_2|^2) \right)$$

$$\times \exp \left(i \frac{2\pi}{\lambda} \left(\alpha_1 \cdot \left(\frac{n_1}{s} \xi_1 - m_p \frac{n'_k}{s'} x \right) - \alpha_2 \cdot \left(\frac{n_1}{s} \xi_2 - m_p \frac{n'_k}{s'} x \right) \right) \right).$$

quadratic phase term **object**

quadratic phase term **pupil**

**linear phase terms:
combining pupil and field**

$$-\frac{n_1}{s} + m_p^2 \frac{n'_k}{s'} = m_p \Phi = \frac{n'_k}{n_1} \frac{m_p}{f'}$$

$$\frac{n_1}{n'_k} \frac{s'}{s} = m_p m$$

For conjugate object and image plane

$$I_{im}(x) = \left(\frac{n_1}{\lambda m s}\right)^4 \iint d\xi_1 d\xi_2 \Gamma_{ob}(\xi_1, \xi_2) \exp\left(-i \frac{\pi n_1}{\lambda s} (|\xi_1|^2 - |\xi_2|^2)\right)$$
$$\times \iint d\alpha_1 d\alpha_2 L_0(\alpha_1) L_0(\alpha_2) \exp\left(-i \frac{2\pi}{\lambda s} \left(\alpha_1 \cdot \left(\frac{x}{m} - \xi_1\right) - \alpha_2 \cdot \left(\frac{x}{m} - \xi_2\right)\right)\right)$$

The α^2 -Term disappears with the focus condition $-\frac{n_1}{s} + m_p^2 \frac{n'_k}{s'} = m_p \Phi$.

The linear phase term $\exp\left(-i \frac{2\pi}{\lambda s} \alpha \cdot \left(\frac{x}{m} - \xi\right)\right)$ couples the image coordinate x with the magnification m to the object coordinates ξ .

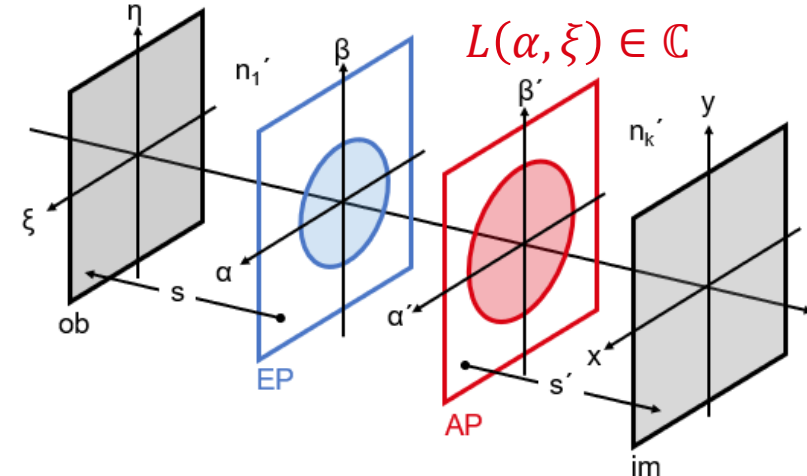
The terms squared in ξ superimpose the coherence functions in the object and image plane.

Generalization of the paraxial system transfer and incorporating the object function

For conjugate object and image plane

$$I(x) = \left(\frac{n_1}{\lambda m s} \right)^4 \iint d\xi_1 d\xi_2 \Gamma_{ob}'(\xi_1, \xi_2) A_{ob}(\xi_1) A_{ob}^*(\xi_1)$$

$$\times \iint d\alpha_1 d\alpha_2 \underline{L(\alpha_1, \xi_1)} L^*(\alpha_2, \xi_2) \exp \left(-i \frac{2\pi}{\lambda s} \left(\alpha_1 \cdot \left(\frac{x}{m} - \xi_1 \right) - \alpha_2 \cdot \left(\frac{x}{m} - \xi_2 \right) \right) \right)$$



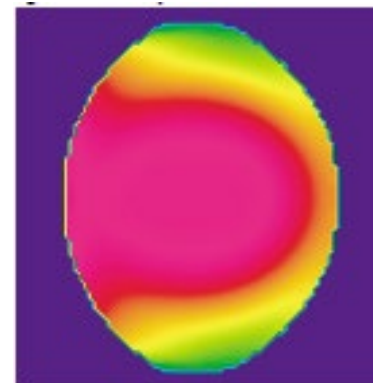
Generalization of **pupil function** to complex valued function $L_0(\alpha) \rightarrow L_0(\alpha, \xi) \exp(i2\pi W(\alpha, \xi)) = L(\alpha, \xi)$ including

- **aberrations** $W(\alpha, \xi)$
- variable pupil transmission („**apodization**“) $L_0(\alpha, \cdot)$
- variable pupil shape over object field („**vignetting**“) $L_0(\cdot, \xi)$

Rewrite object coherence function $\Gamma_{ob}'(\xi_1, \xi_2) = \Gamma_{ob}(\xi_1, \xi_2) \exp \left(-i \frac{\pi n_1}{\lambda s} (|\xi_1|^2 - |\xi_2|^2) \right)$ including

- **object function** $A_{ob}(\xi)$

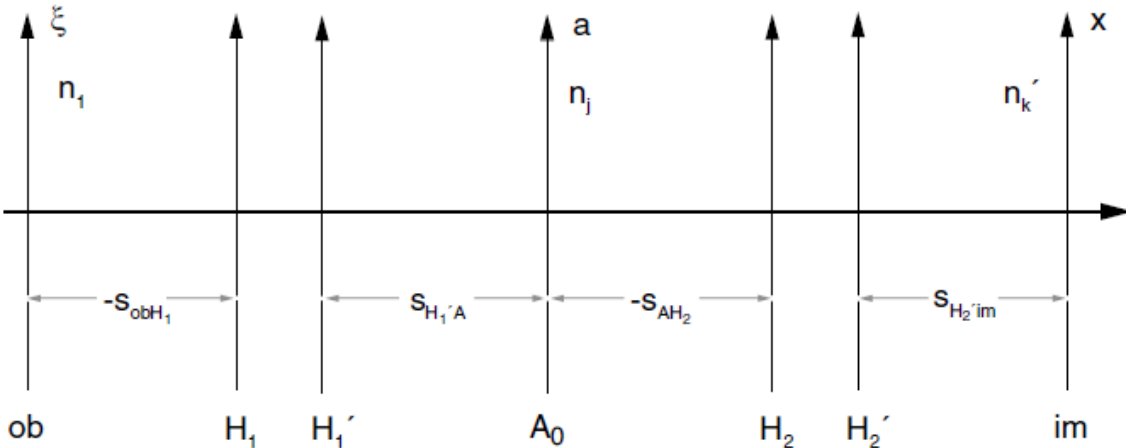
The object function may be a (combined) amplitude and phase object either in transmission or reflection



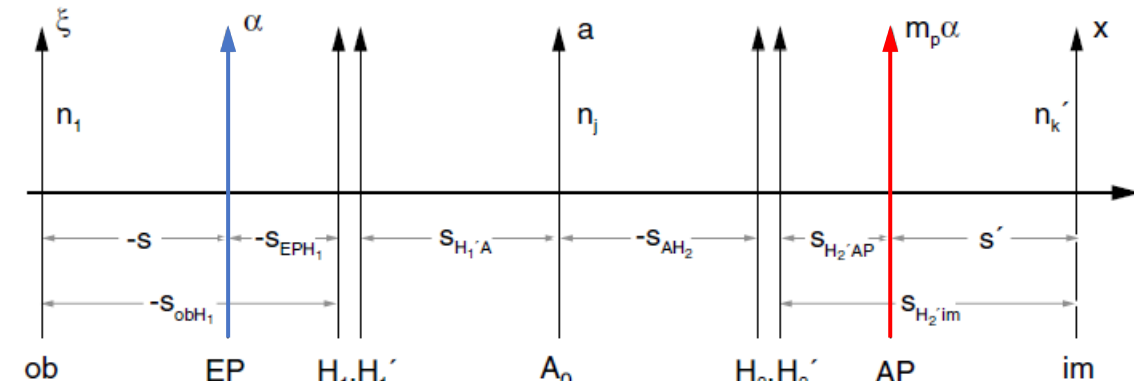
microscopy, lithography combined amplitude/phase transmittance, photography reflectance/emittance

Paraxial structure of wave-optical model

a) System represented by front system / stop / rear system:



b) Transformation to system represented by EP / AP:



The coherence function may be computed in an analogous way from

- object plane via the system in front of the stop described by a pair of principal planes, to stop
- diffraction at stop, $\Gamma'_A(a_1, a_2) = A_0(a_1)A_0(a_2)\Gamma_A(a_1, a_2)$
- stop via back part of systems principal planes to image plane

The resulting coherence function can be shown to be completely equal to the one obtained via entrance and exit pupil with

- the proper magnification factors between stop and EP-, AP-planes, $a = m_{A,EP}\alpha$, $m_p = m_{AP,A} m_{A,EP}$ and $A(a/m_{A,EP}) = L_0(\alpha)$
- straightforward summation of the distances s , s' as in figure b)
- paraxial refractive power addition law

$$\Phi = \Phi_1 + \Phi_2 - d\Phi_1\Phi_2$$

Paraxial structure is incorporated in wave-optical model

Rayleigh-Sommerfeld diffraction spherical surface

Transfer to aplanatic case

The Rayleigh-Sommerfeld formula for diffraction can be written as

$$\hat{V}(x, y, z, \nu) = \iint \hat{V}(x_s, y_s, 0, \nu) R(x - x_s, y - y_s, z, \nu) dx_s dy_s$$

with $R(x - x_s, y - y_s, z, \nu) = \frac{1}{2\pi} \cos \vartheta (1 - ik\rho) \frac{e^{ik\rho}}{\rho^2}$

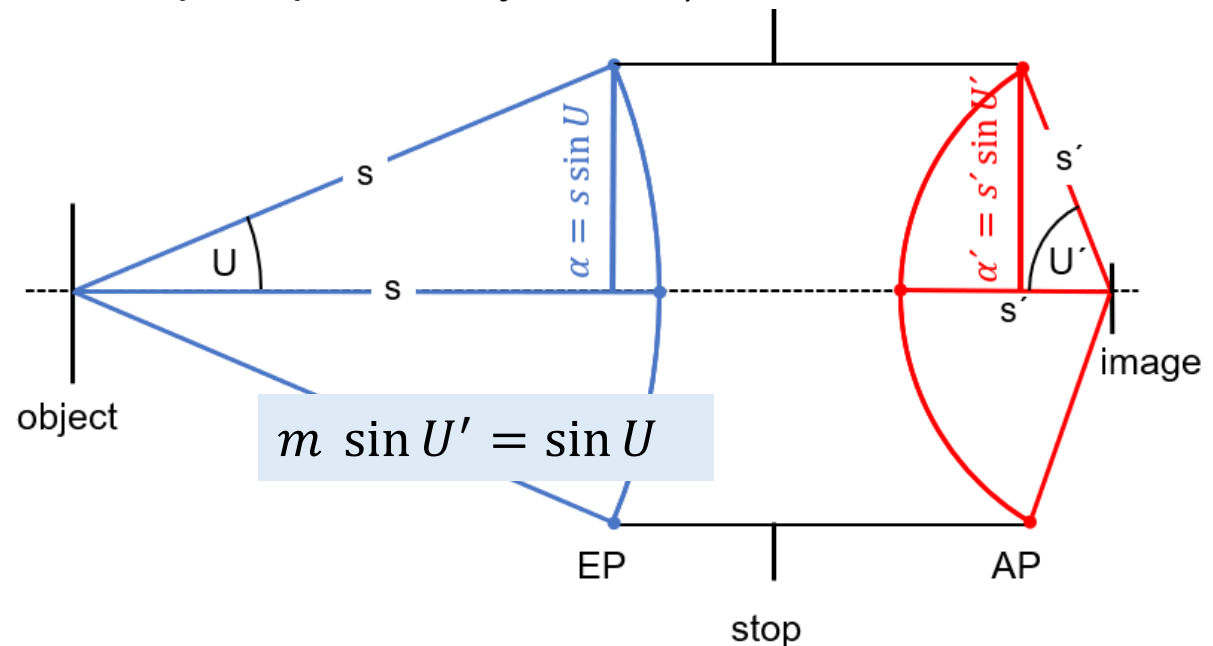
In the spatial frequency range, you have the product relationship (with $\kappa=1/\lambda$):

$$\tilde{V}(\kappa p, \kappa q, z, \nu) = \tilde{V}(\kappa p, \kappa q, 0, \nu) e^{ikmz} \quad (\text{for } p^2 + q^2 > 1 \text{ this drops exponentially for } z>0) \text{ with}$$

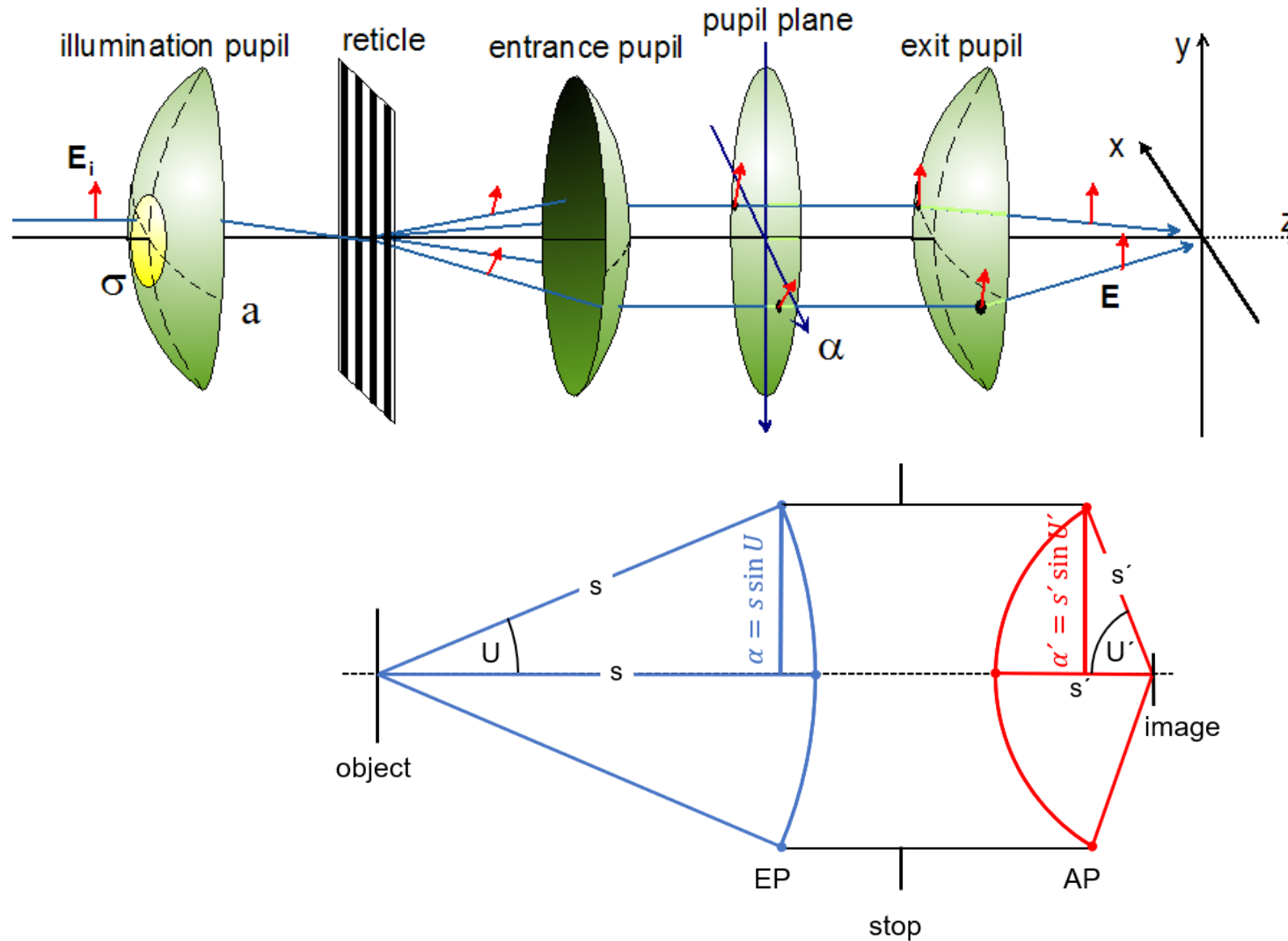
$$\tilde{V}(\kappa p, \kappa q, z, \nu) = \int \hat{V}(x, y, z, \nu) e^{-i2\pi\kappa(px+qy)} dx dy$$

$$m = \begin{cases} \sqrt{1 - p^2 - q^2} & p^2 + q^2 \leq 1 \\ i\sqrt{p^2 + q^2 - 1} & p^2 + q^2 > 1 \end{cases}$$

$$\frac{e^{ikr}}{r} = \int \frac{1}{m} e^{ikmz} e^{ik(px+qy)} dp dq$$



High-NA imaging with aplanatic system

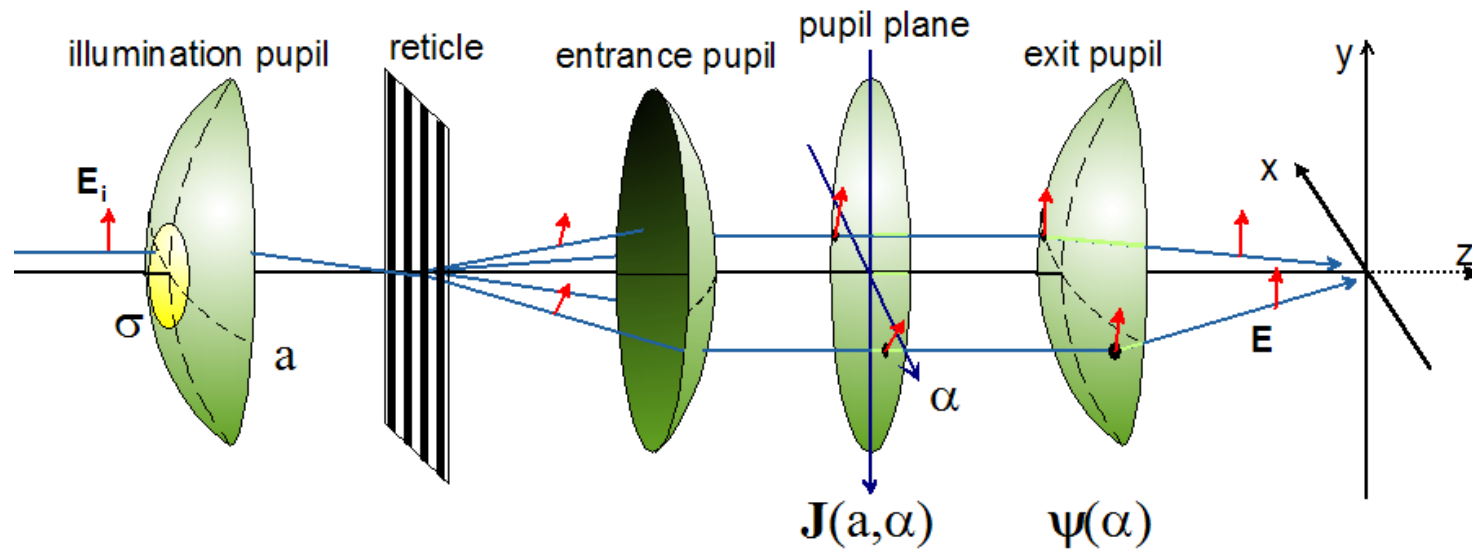


Transfer from pupil to image with sine-scaled pupil coordinates α' with Fourier Transform Integral:

$$\iint d\alpha' L(\alpha', \cdot) \exp\left(-i \frac{2\pi}{\lambda} w \alpha' \cdot x\right)$$

Aberration function in pupil function $L_0(\alpha', \xi) \exp(i 2\pi W(\alpha', \xi))$ is computed by ray-tracing.

Imaging model for high-NA imaging including polarization: scalar pupil (phase, apodization) must be generalized

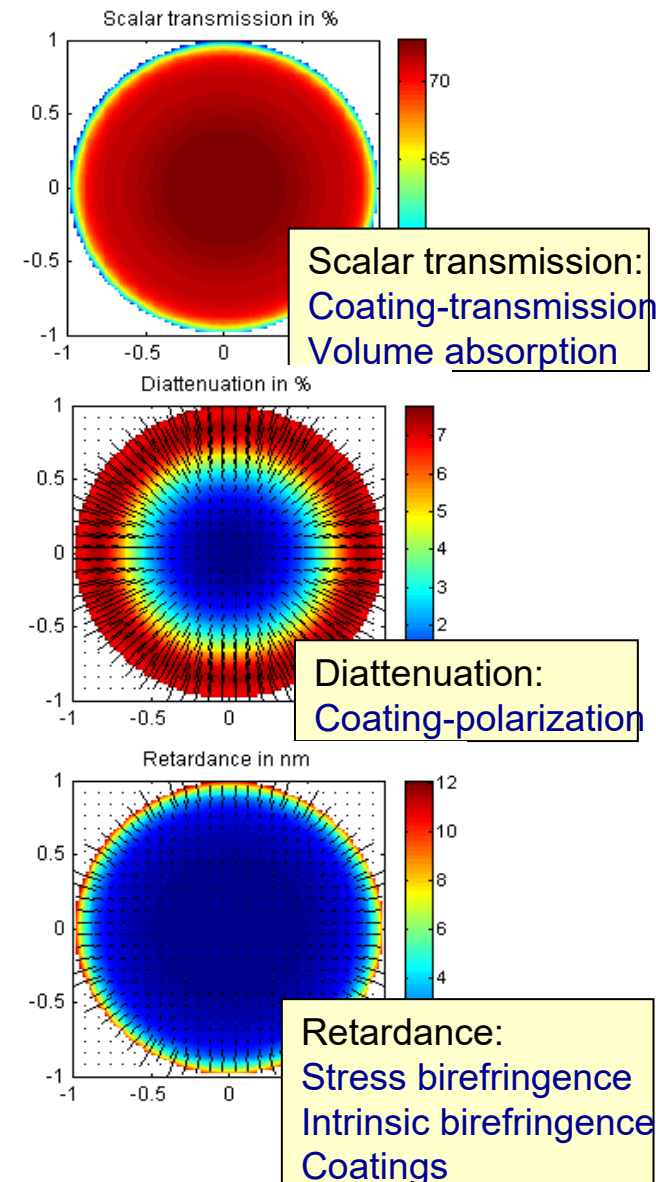


$$I_{coh}(x, a) = \left| \int d\alpha \begin{pmatrix} \Psi_{xx} & \Psi_{yx} \\ \Psi_{xy} & \Psi_{yy} \\ \Psi_{xz} & \Psi_{yz} \end{pmatrix} \cdot \begin{pmatrix} J_{xx} & J_{yx} \\ J_{xy} & J_{yy} \end{pmatrix}(\alpha) \begin{bmatrix} T_{ob}(e_x) \\ e_y \end{bmatrix} (\alpha - \sigma a) \exp(-i2\pi w\alpha \cdot x) \right|^2$$

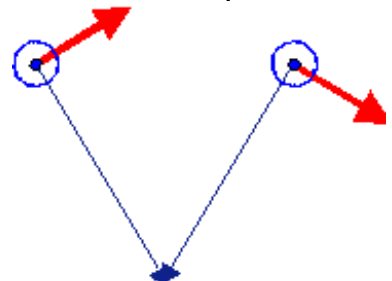
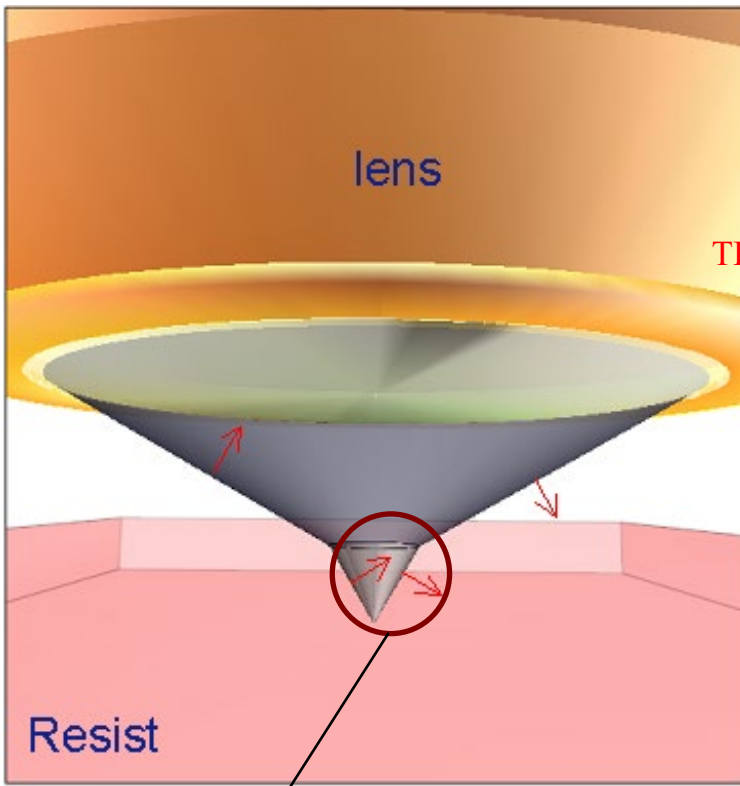
Transform of E-field to angular directions in image space

Jones-Pupil includes retardation and diattenuation of lens

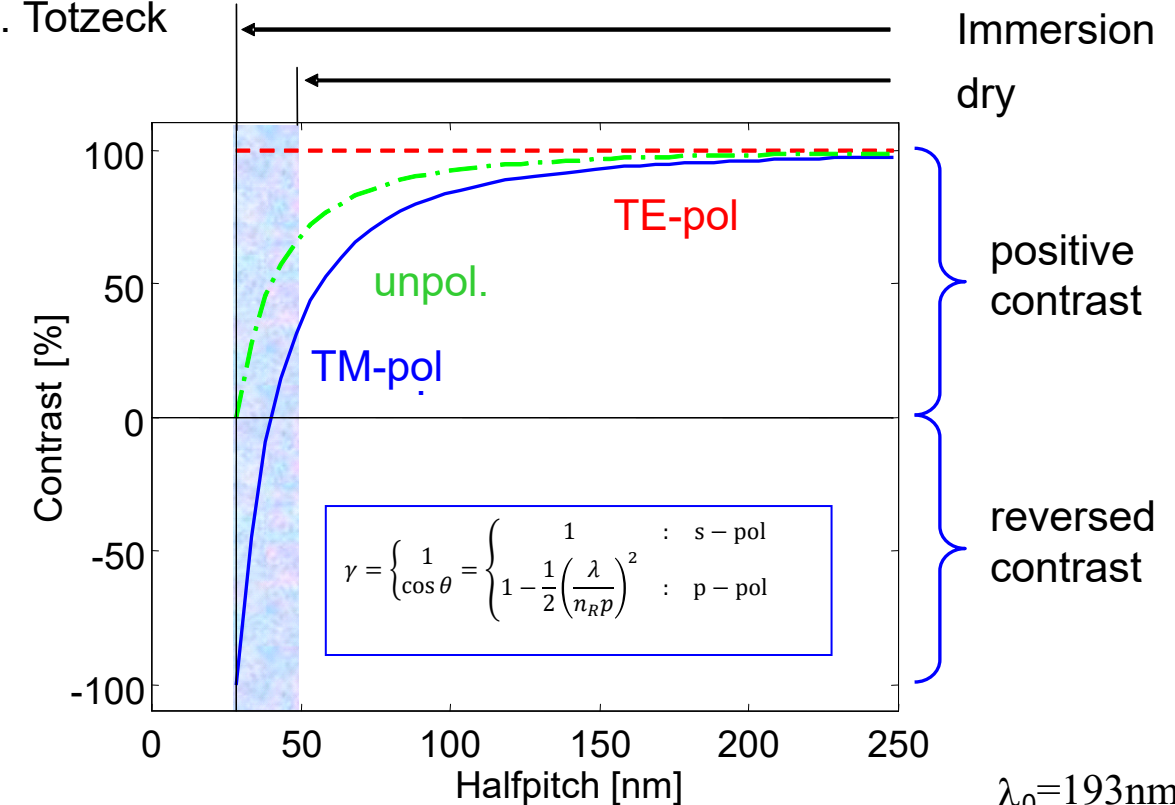
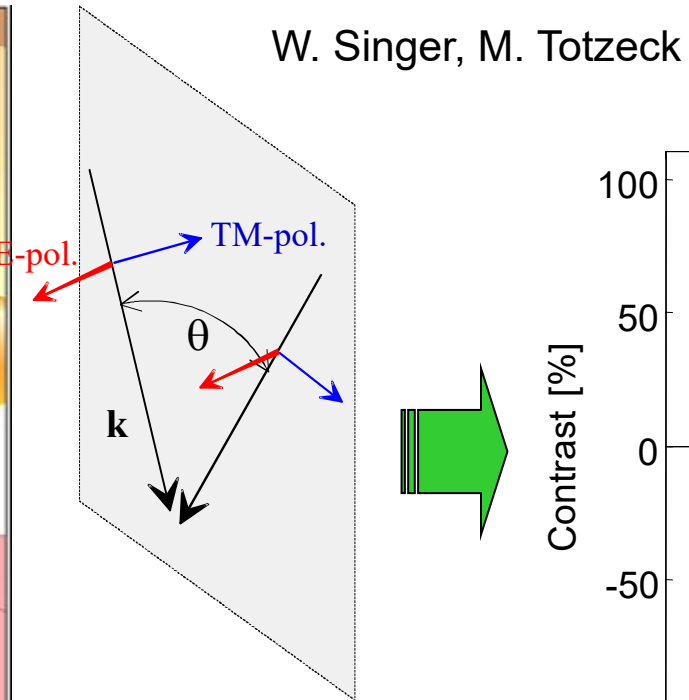
Illumination polarization state



Vector effect high NA



High propagation
angles in resist:
TM components
are **not** parallel



**Illumination with
tangential
polarization (TE only)**



$$\lambda_0 = 193 \text{ nm}$$

$$n_R = 1.7$$

Non-coherent case, van Cittert-Zernike-Theorem:

$$\Gamma(\underline{s}_1, \underline{s}_2, 0) = \frac{\bar{\lambda}^2}{\pi} I(\underline{s}_1) \delta^{(2)}(\underline{s}_1 - \underline{s}_2) \quad \text{non-coherent coherence function with } I(\underline{s}_1) = \Gamma(\underline{s}_1, \underline{s}_1)$$

$$\Gamma(\underline{r}_1, \underline{r}_2, 0) = \frac{\bar{\lambda}^2}{\pi} \iint_P I(\underline{s}_1) \left[\frac{\partial \hat{G}(\underline{r}_1, \underline{s}, \nu)}{\partial n(\underline{s})} \frac{\partial \hat{G}^*(\underline{r}_2, \underline{s}, \nu)}{\partial n(\underline{s})} \right] dx_s dy_s$$

$I(\underline{s}_1)$ is real and positive. Light becomes more coherent through propagation.

Diameter of the aperture small against z: $\frac{d}{z} \ll 1$ and $k\rho \gg 1$: $\frac{\partial \hat{G}(\underline{r}_1, \underline{s}, \nu)}{\partial n(\underline{s})} = \frac{1}{2\pi} \cos \vartheta_1 (1 - i\bar{k}\rho_1) \frac{e^{i\bar{k}\rho_1}}{\rho_1^2} \approx \frac{-i}{\bar{\lambda}z} e^{i\bar{k}\rho_1}$

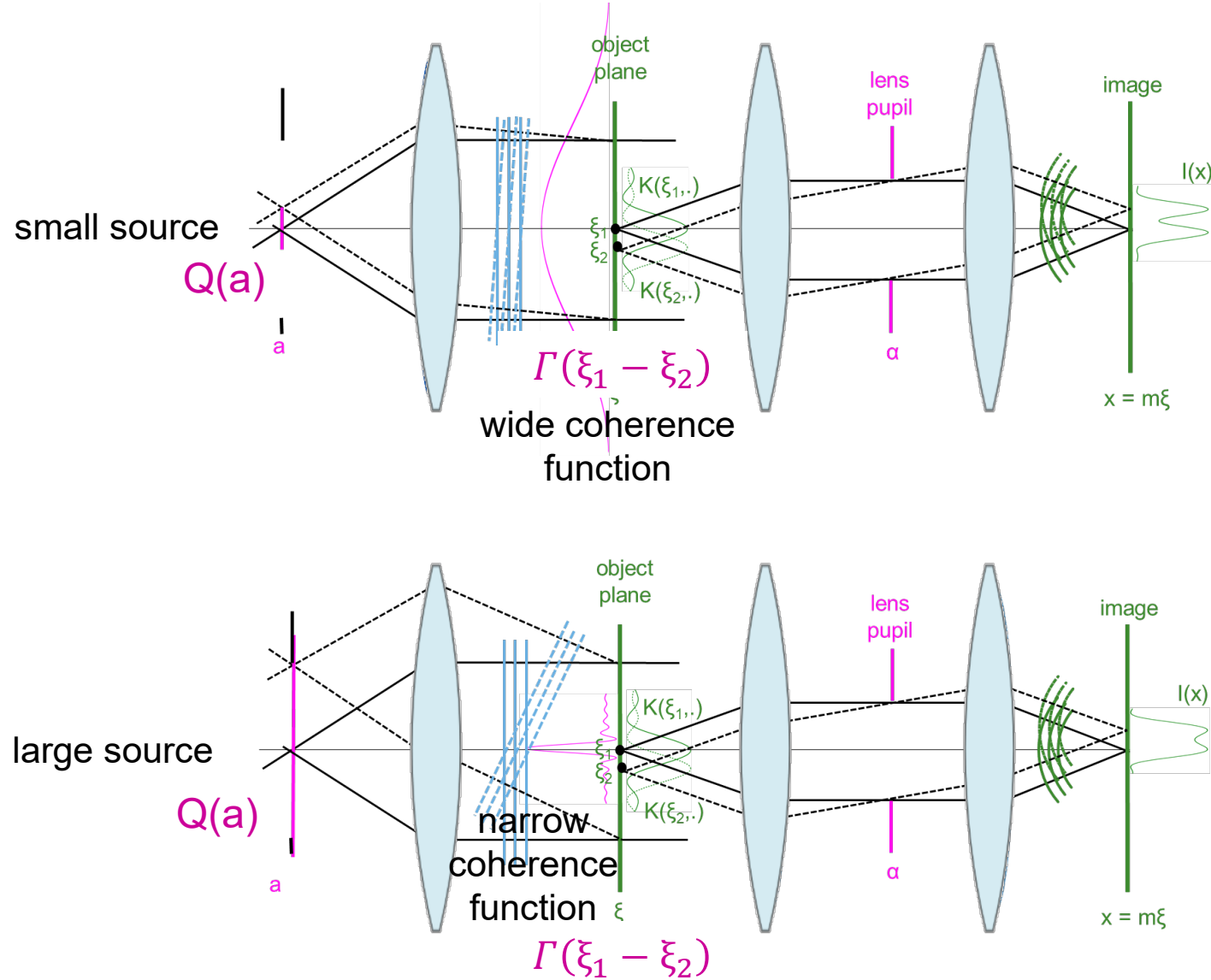
This yields: $\Gamma(\underline{r}_1, \underline{r}_2) = \frac{1}{\pi z^2} \iint_P I(\underline{s}_1) e^{i\bar{k}(\rho_1 - \rho_2)} dx_s dy_s$

$$\rho_1 - \rho_2 \approx \left(\underline{r}_1 - \frac{x_1 x_s + y_1 y_s}{z} + \frac{x_s^2 + y_s^2}{2z} \right) - \left(\underline{r}_2 - \frac{x_2 x_s + y_2 y_s}{z} + \frac{x_s^2 + y_s^2}{2z} \right)$$

You get: $\Gamma(\underline{r}_1, \underline{r}_2) = \frac{e^{i\bar{k}(\underline{r}_1 - \underline{r}_2)}}{\pi z^2} \iint_P I(\underline{s}_1) e^{-i2\pi \frac{x_{12}x_s + y_{12}y_s}{\bar{\lambda}z}} dx_s dy_s$

Van Cittert-Zernike Theorem: The Spatial Coherence Function $\Gamma(\underline{r}_1, \underline{r}_2)$ in the plane of observation is the two-dimensional Fourier transform of the optical intensity distribution in the incoherent source aperture. $\Gamma(\underline{r}_1, \underline{r}_2)$ depends on difference variables. The intensity is constant.

Van Cittert-Zernike theorem

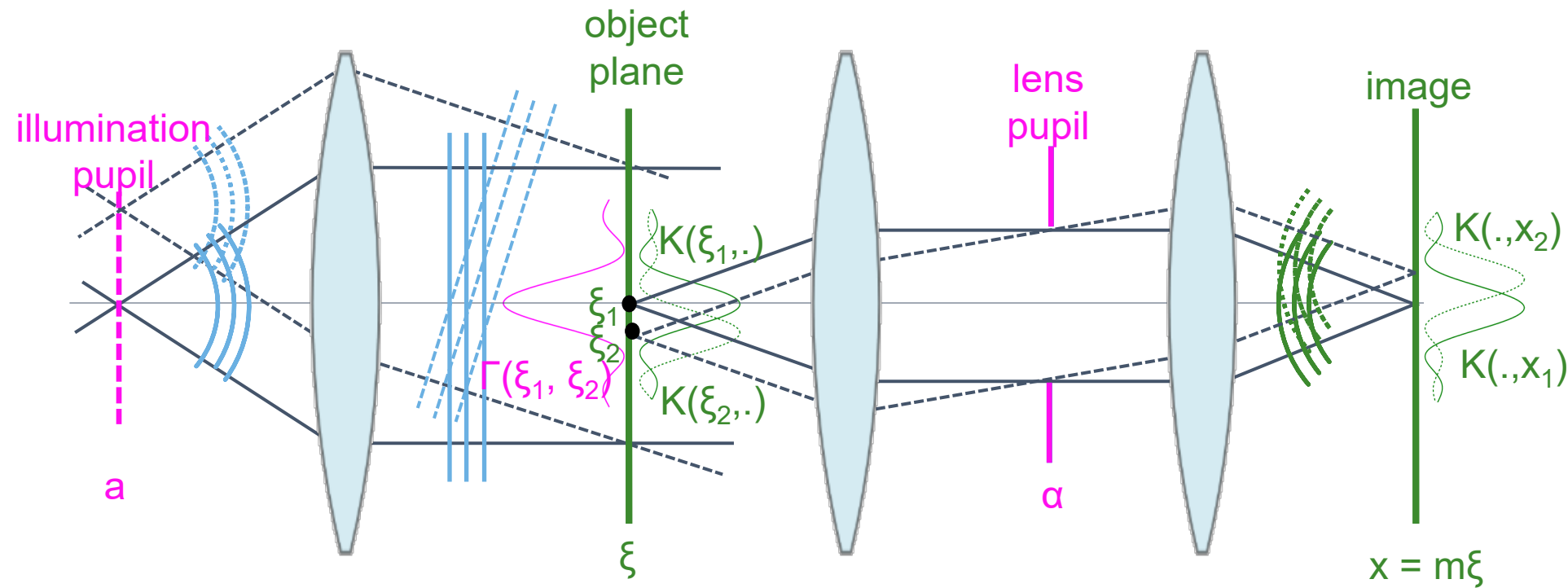


Van Cittert-Zernike theorem: model effective light source in illumination system

$$\Gamma(\xi_1 - \xi_2) = \iint Q(a) e^{-i2\pi\sigma w_a \cdot (\xi_1 - \xi_2)} dx_s dy_s$$

\uparrow
 coherence function in object plane \uparrow
 effective light source Q

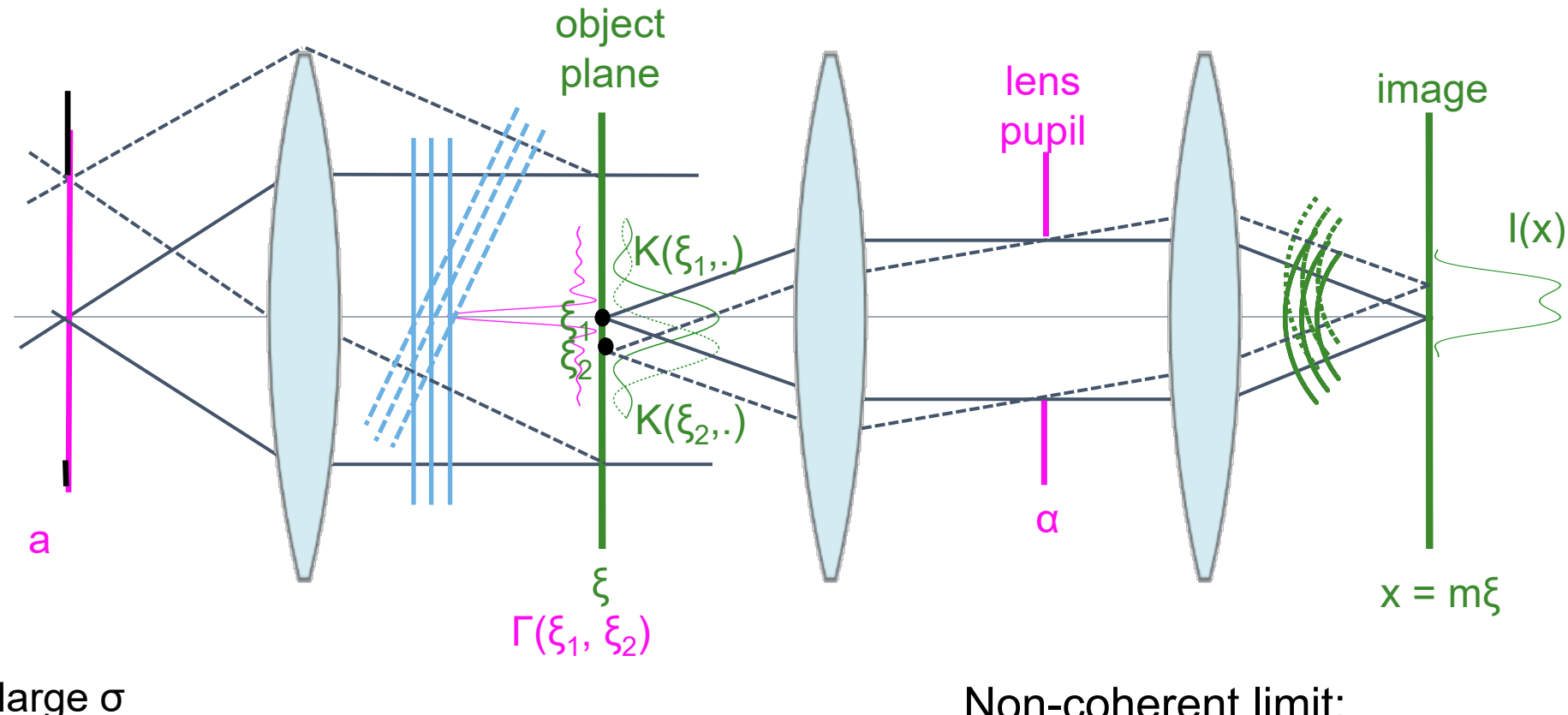
Partially coherent imaging



Partially coherent Intensity Distribution of two pinholes in image plane

$$I(x) = |K(x, \xi_1)|^2 + |K(x, \xi_2)|^2 + 2 \Gamma(\xi_1, \xi_2) \operatorname{Re}(K(x, \xi_1) K^*(x, \xi_2))$$

Partially coherent imaging



large σ

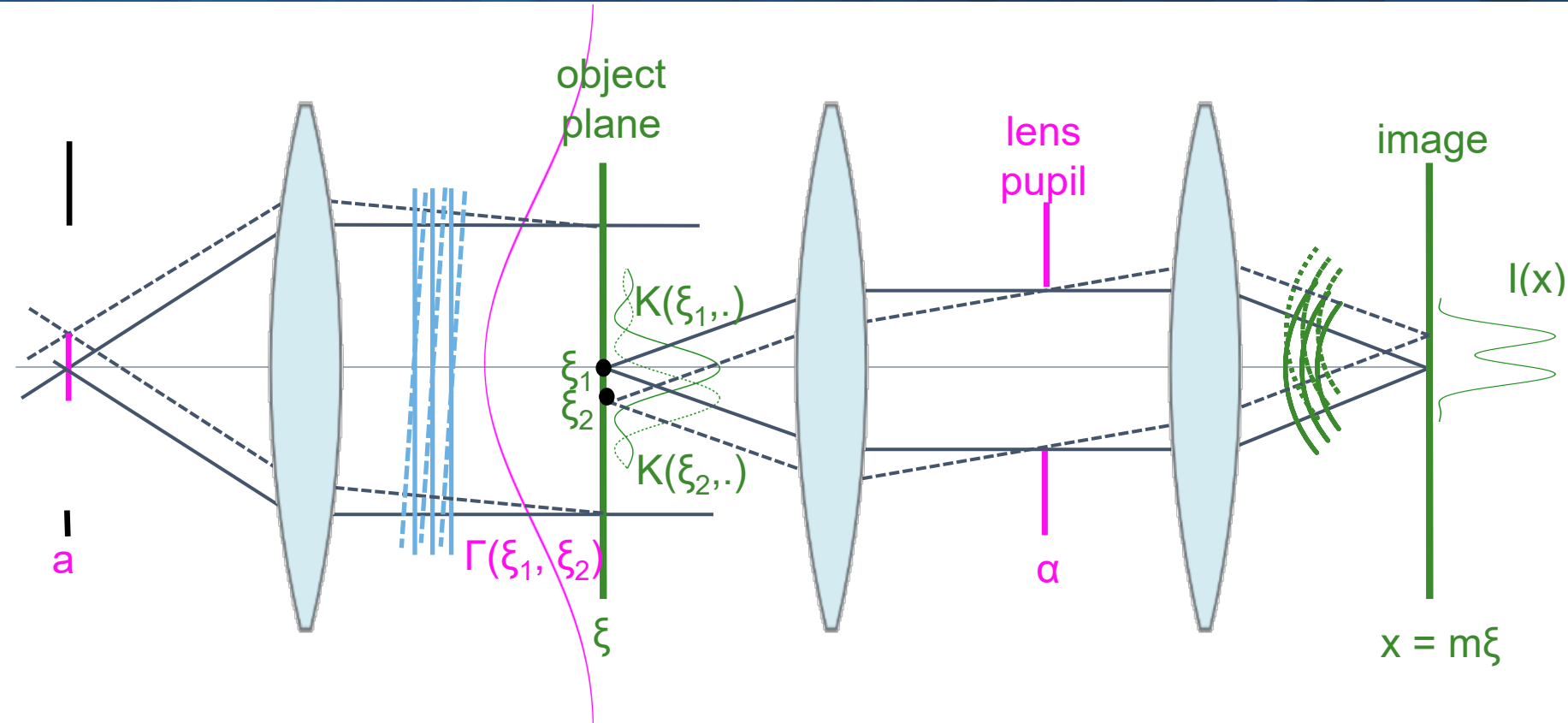
correlation over small object area

incoherent imaging

Non-coherent limit:

$$I(x) = |K(x, \xi_1)|^2 + |K(x, \xi_2)|^2$$

Partially coherent imaging



small σ

correlation over large object area

coherent imaging

Coherent limit:

$$I(x) = |K(x, \xi_1)|^2 + |K(x, \xi_2)|^2 + 2 \cos \varphi \operatorname{Re}(K(x, \xi_1) K^*(x, \xi_2))$$

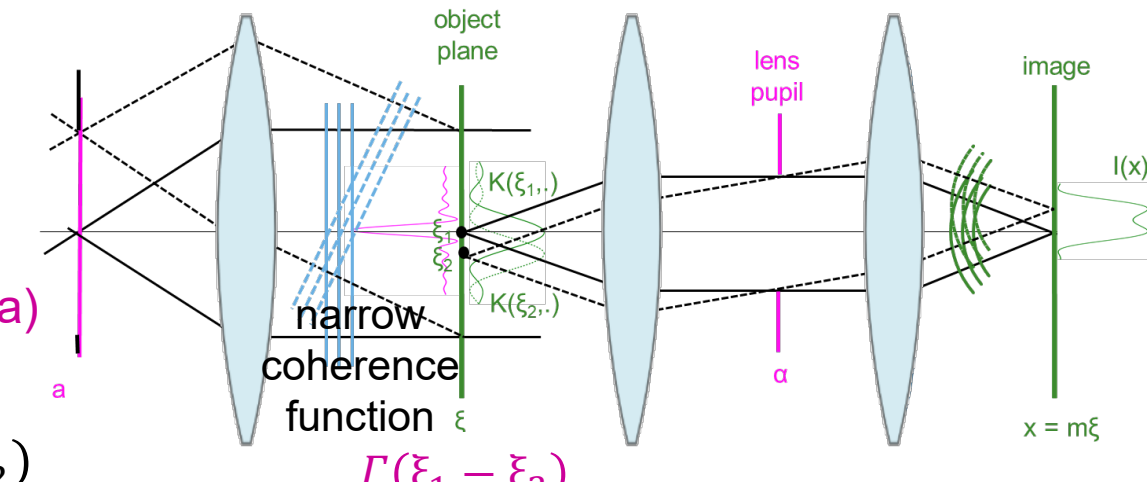
Interpretation of imaging equation with amplitude point spread function

Inserting the coherence function in the object plane

$$\Gamma_{ob}(\xi_1 - \xi_2) = \iint da Q(a) \exp(-i2\pi\sigma_w a \cdot (\xi_1 - \xi_2)).$$

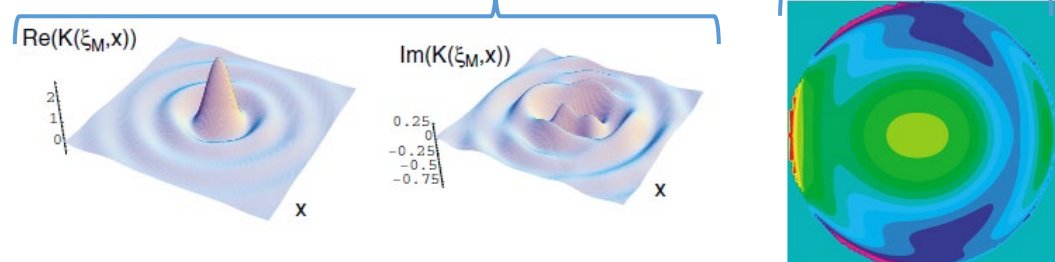
in the general form of the partially coherent imaging equation

$$I(x) = \iint d\xi_1 d\xi_2 \Gamma_{ob}(\xi_1, \xi_2) A_{ob}(\xi_1) A_{ob}^*(\xi_2) K(x, \xi_1) K^*(x, \xi_2)$$



Complex valued amplitude point spread function:

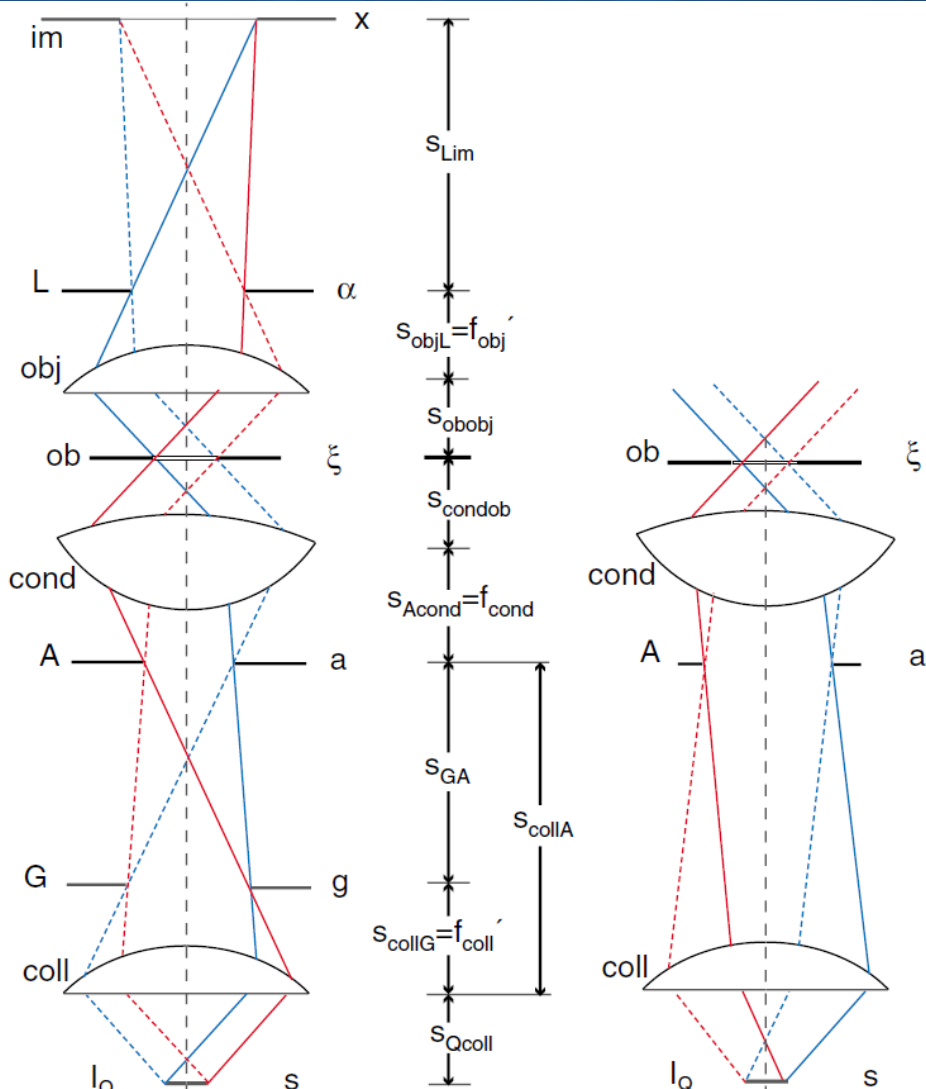
$$K(x, \xi) = \iint d\alpha L(\alpha, \xi) \exp(-i2\pi w \alpha \cdot (x/m - \xi))$$



$$L_0(\alpha, \xi) \exp(i2\pi W(\alpha, \xi)) = L(\alpha, \xi)$$

Complex valued pupil function containing aberrations, pupil shape, apodization

Critical and Köhler Illumination



Köhler illumination

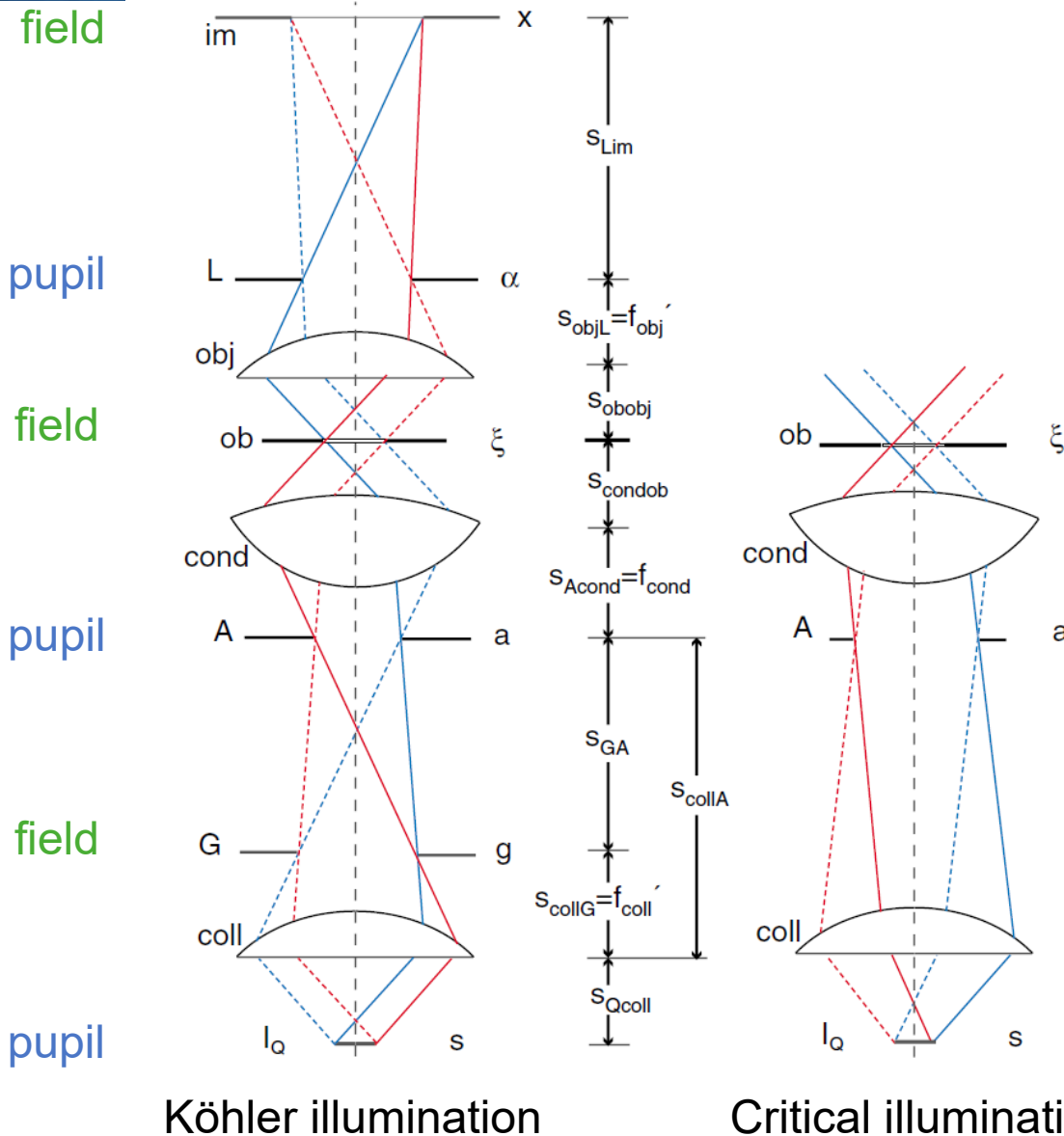
Critical illumination

Köhler's and critical illumination

“object –image light path”: Along the dashed or solid line pairs

“pupil light path”: along the **red** and **blue** pairs of lines, respectively

Critical and Köhler Illumination

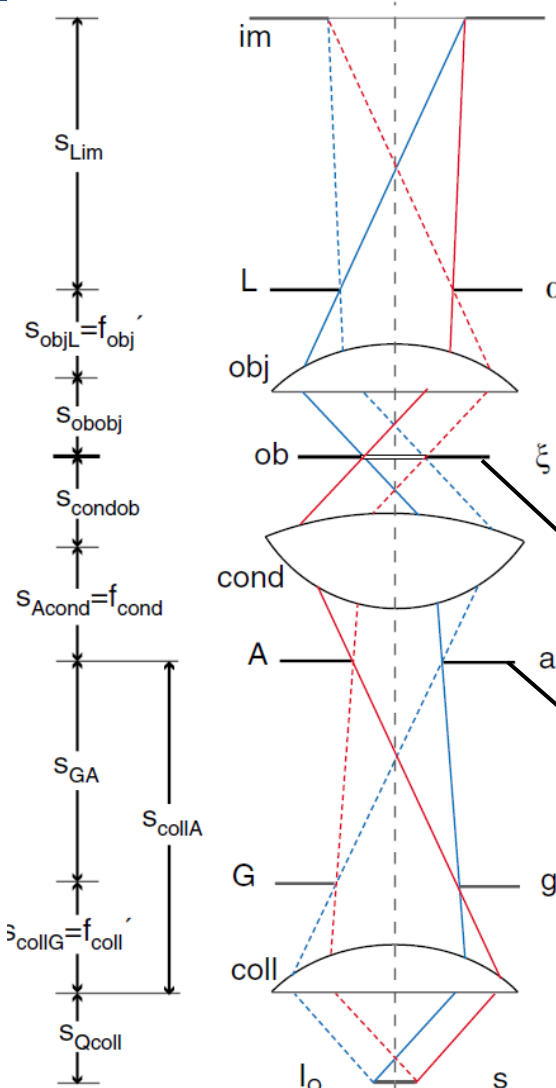


Köhler's and critical illumination

"object –image light path": Along the dashed or solid line pairs

"pupil light path": along the **red** and **blue** pairs of lines, respectively

Köhler Illumination



Principle of Köhler illumination (1893):

- Alternating field and pupil
- No source structure in object field
- Light source conjugated to system pupil

Coherence function in object plane:

$$\Gamma_{ob}(\xi_1 - \xi_2) = \iint da Q(a) \exp(-i2\pi\sigma_w a \cdot (\xi_1 - \xi_2))$$

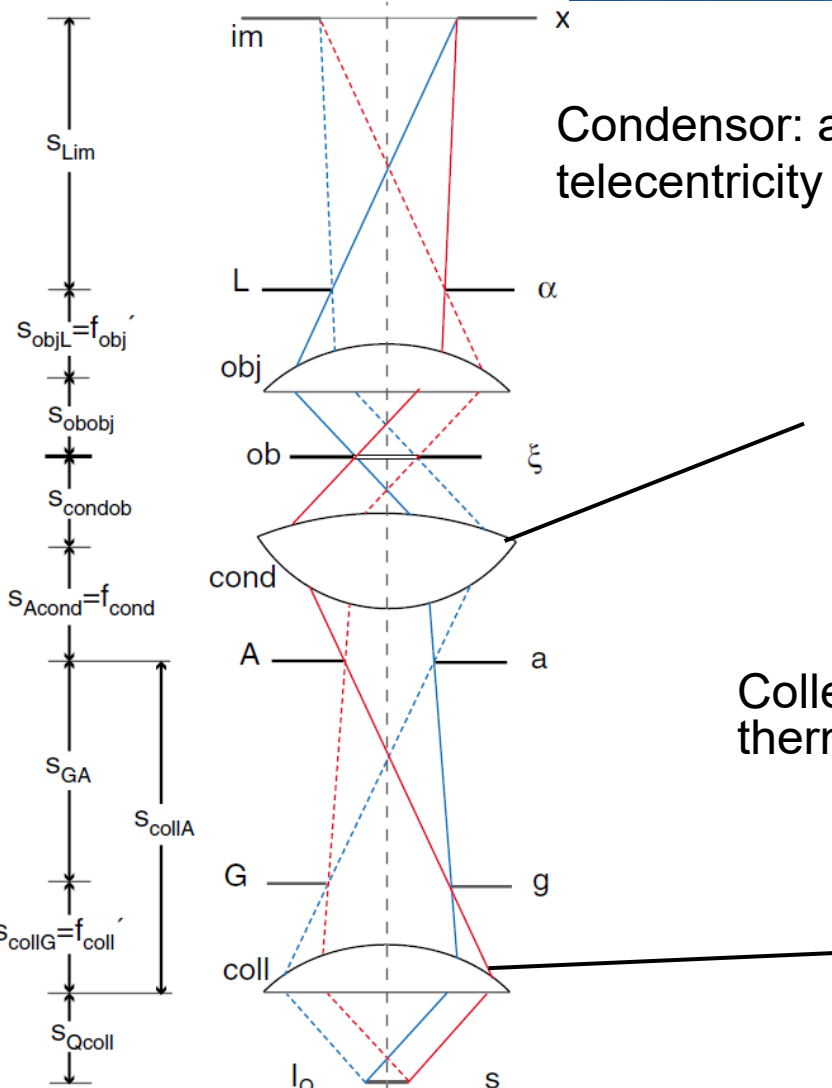
$$\Gamma_Q(a_1, a_2) = Q(a_1)\delta(a_1 - a_2) \quad \text{Effective light source in illumination pupil}$$

$$\Gamma_Q(s_1, s_2) = \frac{\lambda^2}{\pi} I_Q(s_1) \delta(s_1 - s_2)$$

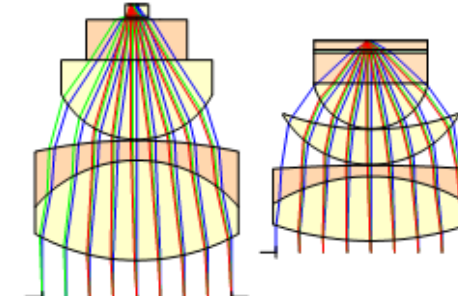
Spatially incoherent light source

Köhler illumination

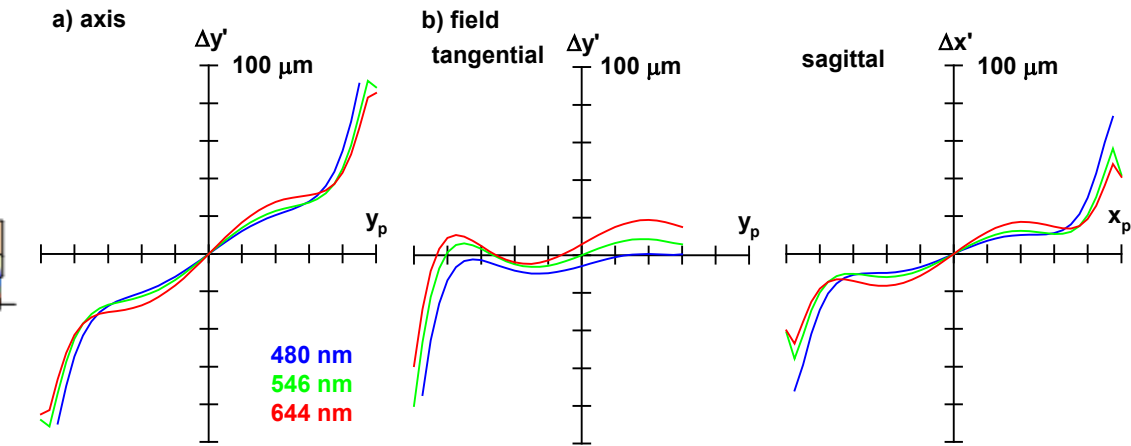
Optical design examples condenser, collector for microscope illumination system



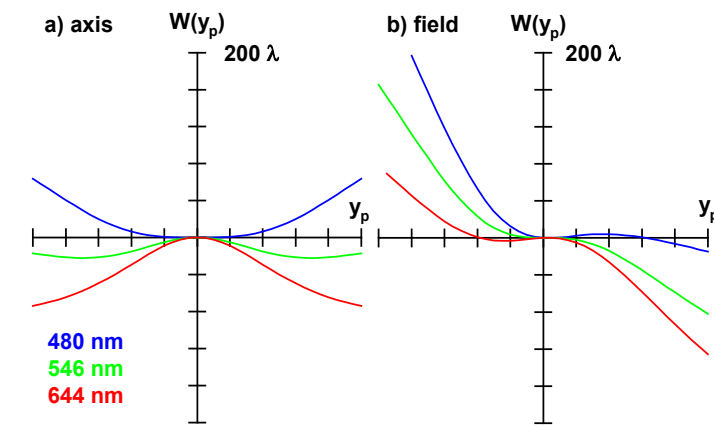
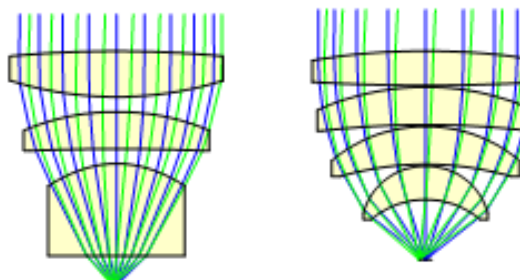
Condensor: aplanatic, achromatic, pupil matching / telecentricity



Design examples (H. Gross)

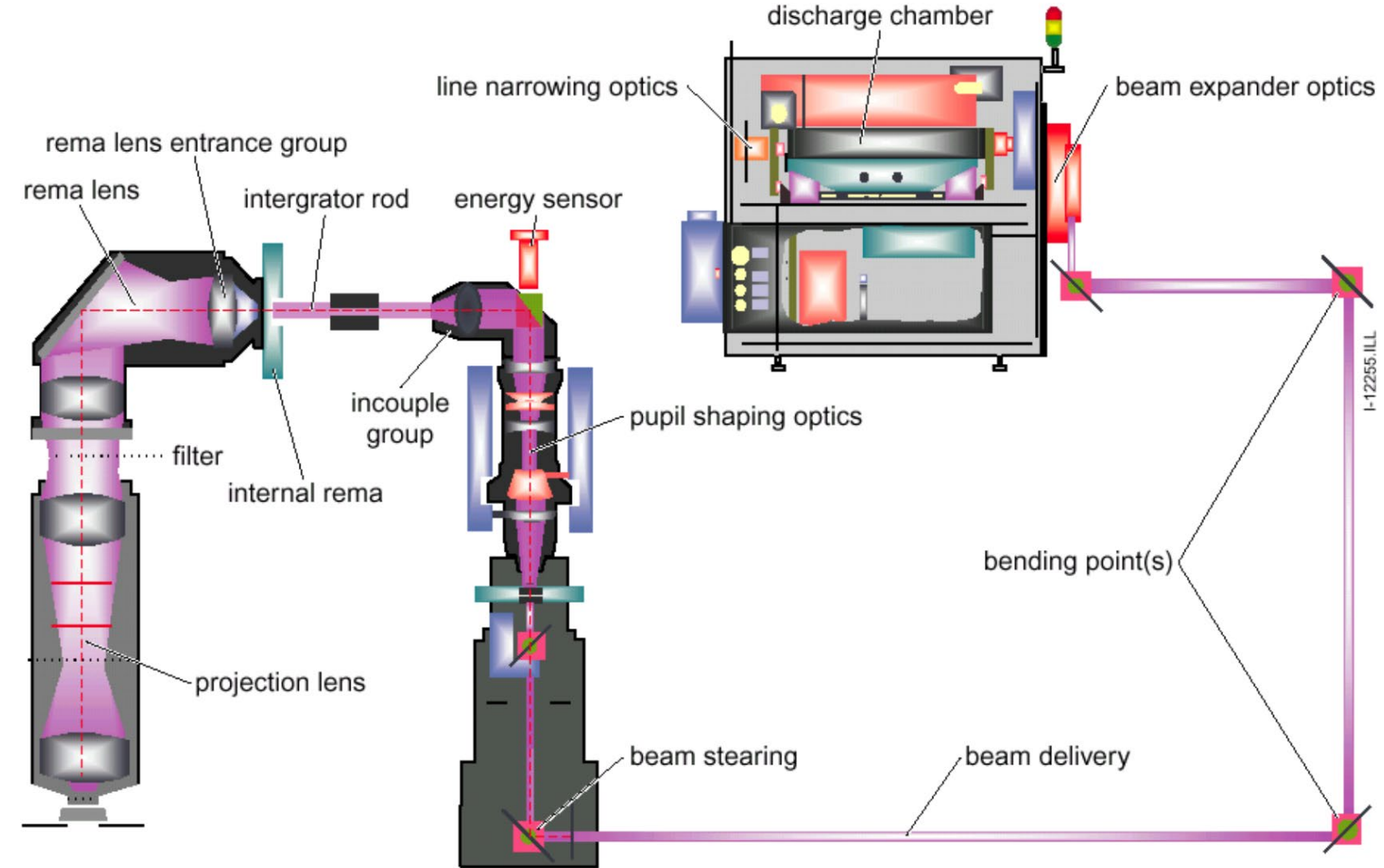


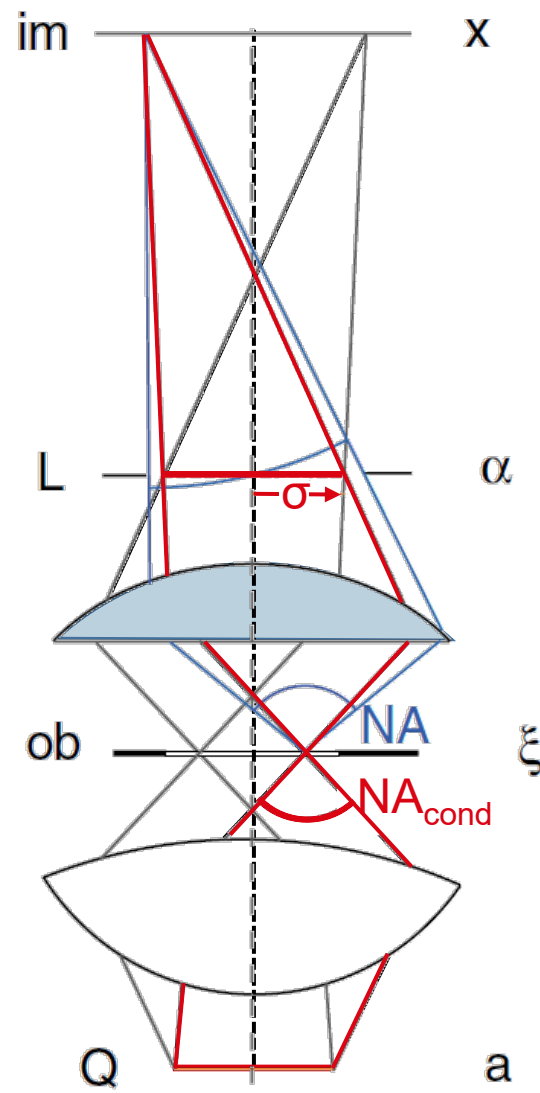
Collectors characteristics: Large collecting solid angle and large thermal load; Correction not critical

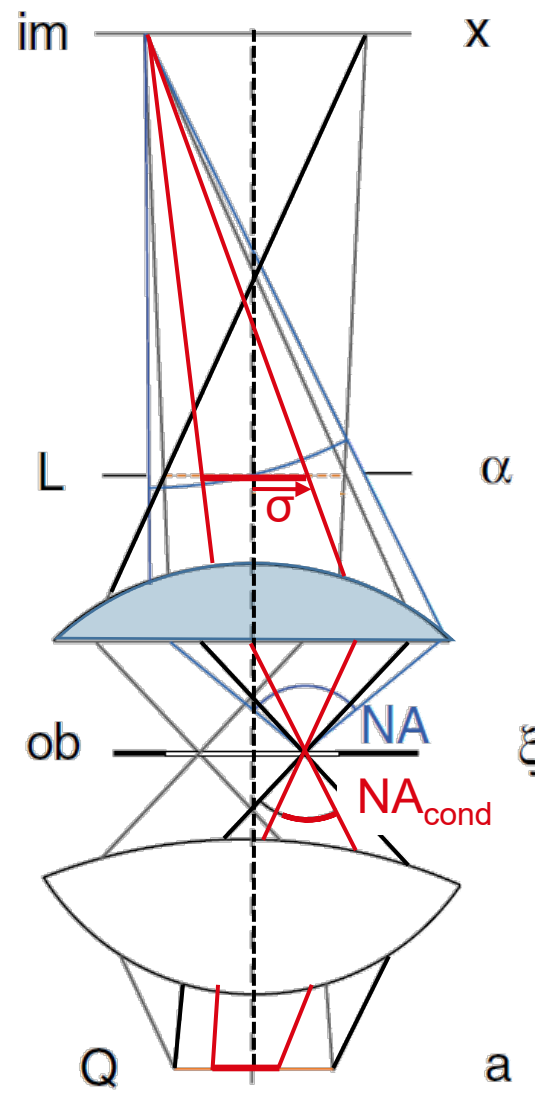


Köhler illumination

Optical Projection Lithography







Most practical:

object ξ and image coordinates x in units of length [mm]
illumination pupil a and lens pupil α in dimensionless coordinates

We normalize the pupil coordinates of the system α and the source a :

$$0 \leq |\alpha| \leq 1,$$

$$0 \leq |a| \leq 1.$$

We define the coherence parameter σ as the ratio of the illumination to the projection system aperture on the object side

$$\sigma = \frac{NA_{cond}}{NA}.$$

This parameter corresponds to the relative size of the effective light source in the system pupil.

In addition, we define another parameter w , which is directly linked to the object-side resolution: $w = \frac{NA}{\lambda}$.

General form of the imaging equation

Inserting the coherence function in the object plane

$$\Gamma_{ob}(\xi_1 - \xi_2) = \iint da Q(a) \exp(-i2\pi\sigma w a \cdot (\xi_1 - \xi_2)).$$

in the general form of the partially coherent imaging equation

$$I(x) = \iint d\xi_1 d\xi_2 \Gamma_{ob}(\xi_1, \xi_2) A_{ob}(\xi_1) A_{ob}^*(\xi_2) K(x, \xi_1) K^*(x, \xi_2)$$

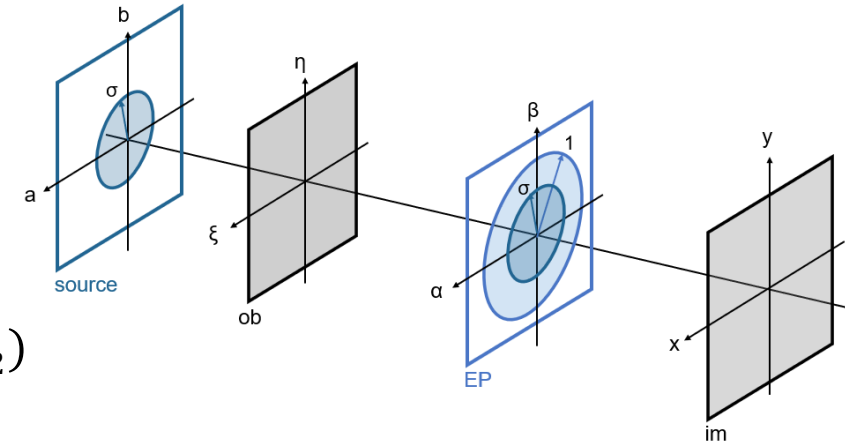
with the amplitude point spread function:

$$K(x, \xi) = \iint d\alpha L(\alpha, \xi) \exp(-i2\pi w \alpha \cdot (x/m - \xi))$$

$$I(x) = \iint da Q(a)$$

$$\times \iint d\alpha_1 \exp(-i2\pi w \alpha_1 \cdot x/m) \iint d\xi_1 A_{ob}(\xi_1) L(\xi_1, \alpha_1) \exp(i2\pi w \xi_1 \cdot (\alpha_1 - \sigma a))$$

$$\times \iint d\alpha_2 \exp(i2\pi w \alpha_2 \cdot x/m) \iint d\xi_2 A_{ob}^*(\xi_2) L^*(\xi_2, \alpha_2) \exp(-i2\pi w \xi_2 \cdot (\alpha_2 - \sigma a))$$



$$0 \leq |\alpha| \leq 1,$$

$$0 \leq |a| \leq 1.$$

$$\sigma = \frac{NA_{cond}}{NA}.$$

$$w = \frac{NA}{\lambda}.$$

General form of the imaging equation: 3 alternative forms

We have the freedom to **interchange the orders of integration** between source, object and lens pupil.
In principle this gives $3! = 6$ permutations. Only 3 of those are useful for further considerations:

1.

$$I(x) = \iint \iint d\alpha_1 d\alpha_2 \exp(-i2\pi w(\alpha_1 - \alpha_2) \cdot x/m) \iint \iint d\xi_1 d\xi_2 A_{ob}(\xi_1) A_{ob}^*(\xi_2) C(\xi_1, \xi_2, \alpha_1, \alpha_2) \exp(i2\pi w(\xi_1 \cdot \alpha_1 - \xi_2 \cdot \alpha_2))$$

with $C(\xi_1, \xi_2, \alpha_1, \alpha_2) = \iint da Q(a) L(\xi_1, \alpha_1 + \sigma a) L^*(\xi_2, \alpha_2 + \sigma a)$.

2.

$$I(x) = \iint da Q(a) \left| \iint d\alpha AL(\alpha, a) \exp(-i2\pi w\alpha \cdot x) \right|^2$$

with the amplitude spectrum in the pupil coupled with the pupil function $L(\xi, \alpha)$:

$$AL(\alpha, a) = \iint d\xi A_{ob}(\xi) L(\xi, \alpha) \exp(i2\pi w(\alpha - \sigma a) \cdot \xi),$$

3.

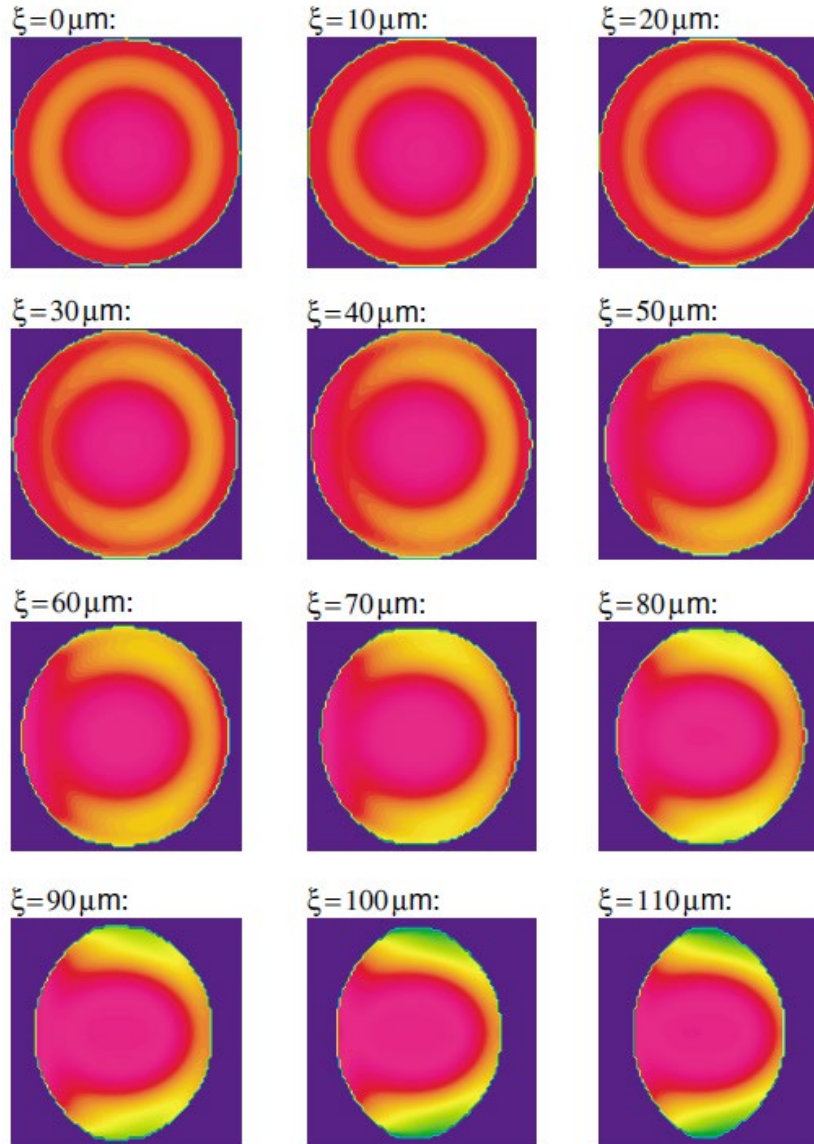
$$I(x) = \iint da Q(a) \left| \iint d\xi A_{ob}(\xi, a) K(x, \xi) \exp(-i2\pi \sigma w a \cdot \xi) \right|^2$$

with the amplitude point spread function

$$K(x, \xi) = \iint d\alpha L(\alpha, \xi) \exp(-i2\pi w \alpha \cdot (x/m - \xi))$$

- Compared with the original general form in 2. and 3. the number of integrations is reduced from 10 to 6.
- Equation 1. and 2. would considerably simplify with the assumption of **spatial stationarity**: $L(\xi, \alpha) = L(\alpha)$

Spatial stationarity (“Isoplanatic”)



Pupil function $L(\alpha, \beta, \xi, \eta)$ of a microscope lens.

Variation over field gives rise to varying performance.

Critical for assumption of **spatial stationarity**

$$L(\xi, \alpha) = L(\alpha) :$$

Is the performance variation over image field critical for the object sizes of interest?

Partially coherent imaging equations

(assuming spatially incoherent light source & spatially invariant (isoplanatic) optical system transfer)

Order of integrations	Imaging equation	remark
1. source object 2. pupil (α, ξ, a)	$I(x) = \iint \iint d\alpha_1 d\alpha_2 \exp(-i2\pi w(\alpha_1 - \alpha_2) \cdot x)$ $\times HTF(\alpha_1, \alpha_2) FT(A_{ob})(\alpha_1) FT(A_{ob}^*)(\alpha_2)$ $C(\alpha_1, \alpha_2) = \iint da Q(a) L(\alpha_1 + \sigma a) L^*(\alpha_2 + \sigma a)$ $FT(A_{ob})(\alpha) = \iint d\xi A_{ob}(\xi) \exp(i2\pi w \alpha \cdot \xi)$	Hopkins transfer function (HTF) enables Fourier analysis and synthesis of spatial frequency transfer in lens pupil; Analytical transfer function for ideal cases, e.g., no aberrations and circular or annular source & pupil Analytical calculation of object spectrum e.g., for periodic (or aliased) structures → Fourier series of intensity distribution
1. object 2. pupil 3. source (ξ, α, a)	$I(x) = \iint da Q(a) \left \iint d\alpha L(\alpha) FT(A_{ob})(\alpha - \sigma a) \exp(-i2\pi w \alpha \cdot x) \right ^2$ $FT(A_{ob})(\alpha - \sigma a) = \iint d\xi A_{ob}(\xi) \exp(i2\pi w (\alpha - \sigma a) \cdot \xi)$	suitable if object spectrum analytical, e.g., periodic (aliased) objects & complex lens pupil functions (Litho-simulators Solid-C, Prolith)
1. pupil 2. object 3. source (α, ξ, a)	$I(x) = \iint da Q(a) \left \iint d\xi A_{ob}(\xi) K(x - \xi) \exp(-i2\pi \sigma w \alpha \cdot \xi) \right ^2$ $K(x - \xi) = \iint d\alpha L(\alpha) \exp(-i2\pi w \alpha \cdot (x - \xi))$	aPSF analytical or efficiently stored (non-isoplanatic case Karhunen-Loewe)

Spatially stationary (isoplanatic) imaging

Microscope Lens Design

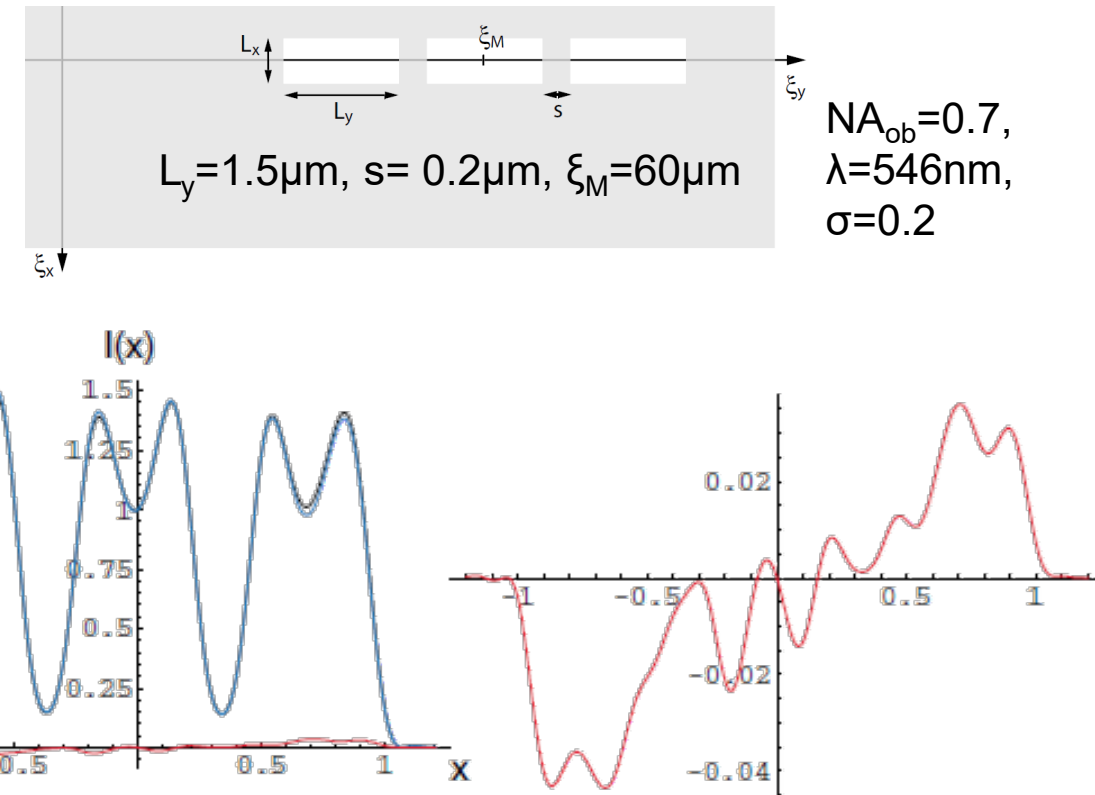
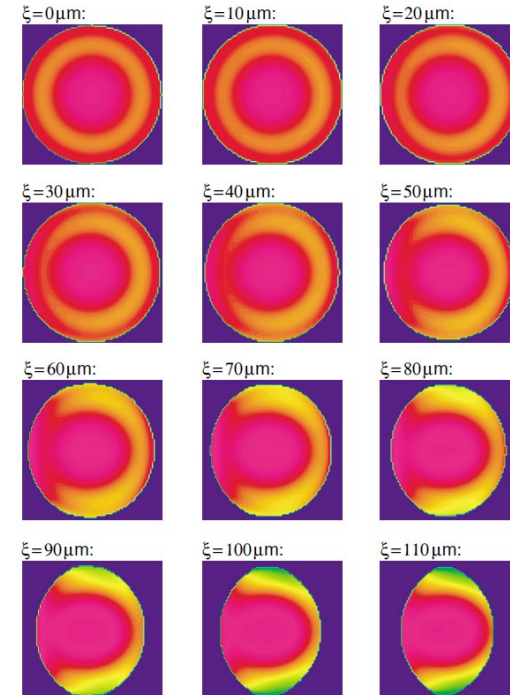

 $NA_{ob}=0.7$
 Magnification 1:40
 Object field radius 0.11mm

Imaging equation

$$I(x) = \iint da Q(a) \left| \iint d\xi A_{ob}(\xi) K(x, \xi) \exp(-i2\pi\sigma w a \cdot \xi) \right|^2$$

$$K(x, \xi) = \iint d\alpha L(\xi, \alpha) \exp(-i2\pi w \alpha \cdot (x - \xi))$$

Microscope lens pupil (wavefront deformation, shape) over field



Comparison of space-variant vs stationary computation of image intensity of bar chart object

Partially coherent imaging equations

(assuming spatially incoherent light source & spatially invariant (isoplanatic) optical system transfer)

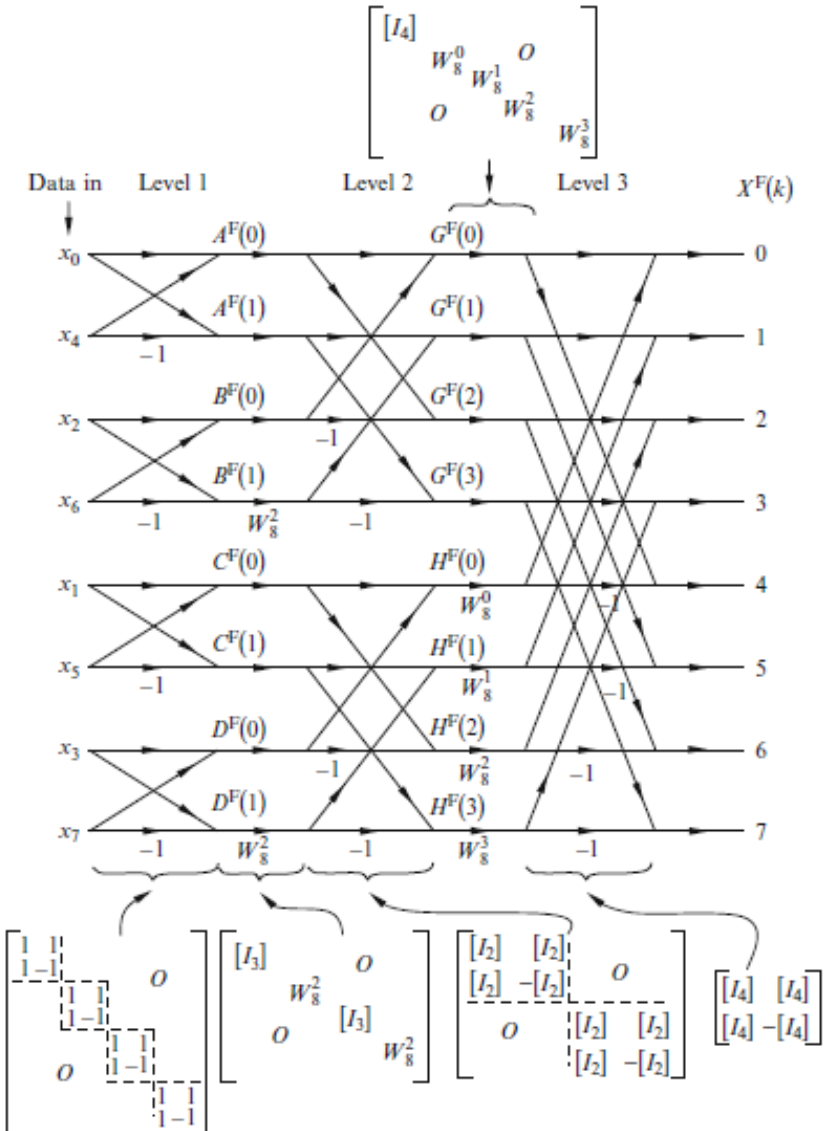
Order of integrations	Imaging equation	remark
1. source object 2. pupil (α, ξ, a)	$I(x) = \iint \iint d\alpha_1 d\alpha_2 \exp(-i2\pi w(\alpha_1 - \alpha_2) \cdot x)$ $\times HTF(\alpha_1, \alpha_2) FT(A_{ob})(\alpha_1) FT(A_{ob}^*)(\alpha_2)$ $C(\alpha_1, \alpha_2) = \iint da Q(a) L(\alpha_1 + \sigma a) L^*(\alpha_2 + \sigma a)$ $FT(A_{ob})(\alpha) = \iint d\xi A_{ob}(\xi) \exp(i2\pi w \alpha \cdot \xi)$	Hopkins transfer function (HTF) enables Fourier analysis and synthesis of spatial frequency transfer in lens pupil; Analytical transfer function for ideal cases, e.g., no aberrations and circular or annular source & pupil Analytical calculation of object spectrum e.g., for periodic (or aliased) structures → Fourier series of intensity distribution
1. object 2. pupil 3. source (ξ, α, a)	$I(x) = \iint da Q(a) \left \iint d\alpha L(\alpha) FT(A_{ob})(\alpha - \sigma a) \exp(-i2\pi w \alpha \cdot x) \right ^2$ $FT(A_{ob})(\alpha - \sigma a) = \iint d\xi A_{ob}(\xi) \exp(i2\pi w (\alpha - \sigma a) \cdot \xi)$	suitable if object spectrum analytical, e.g., periodic (aliased) objects & complex lens pupil functions (Litho-simulators Solid-C, Prolith)
1. pupil 2. object 3. source (α, ξ, a)	$I(x) = \iint da Q(a) \left \iint d\xi A_{ob}(\xi) K(x - \xi) \exp(-i2\pi \sigma w \alpha \cdot \xi) \right ^2$ $K(x - \xi) = \iint d\alpha L(\alpha) \exp(-i2\pi w \alpha \cdot (x - \xi)) = FT(L)(x - \xi)$	aPSF analytical or efficiently stored (non-isoplanatic case Karhunen-Loewe)

Fast Fourier Transform

- Reducing the computation time from $O(n^2)$ “by almost a factor n” (large n) to $O(n \log(n))$
- There are several possible procedures: all have in common, that
 - the FT is a linear transformation of a n-dim vector (“object” in our context) to a n-dim vector (“image”); n preferably $2k$, k
 - The transformation matrix is a n x n-matrix consisting of equidistant phase factors
 - The input-data are rearranged such that phase factors can be shortened so that matrices can be diagonalized, reducing the amount of operations

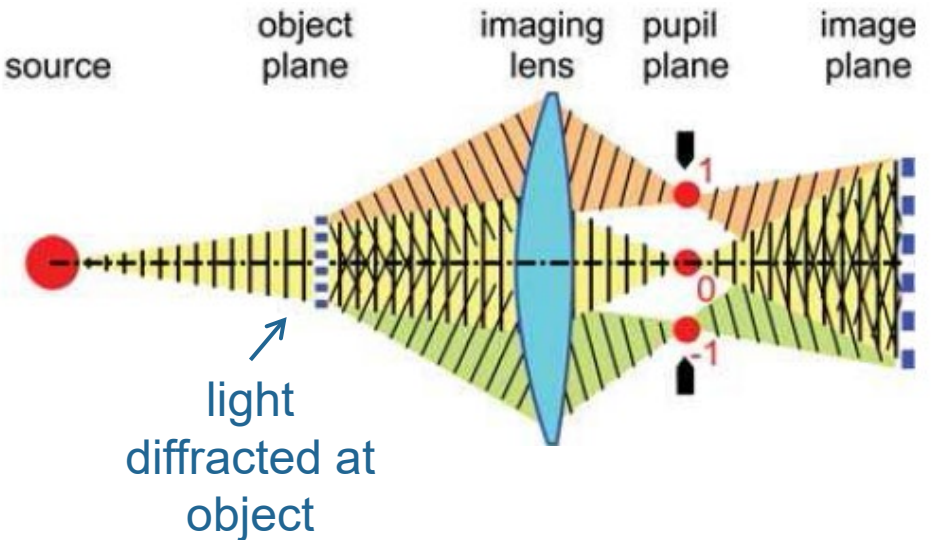
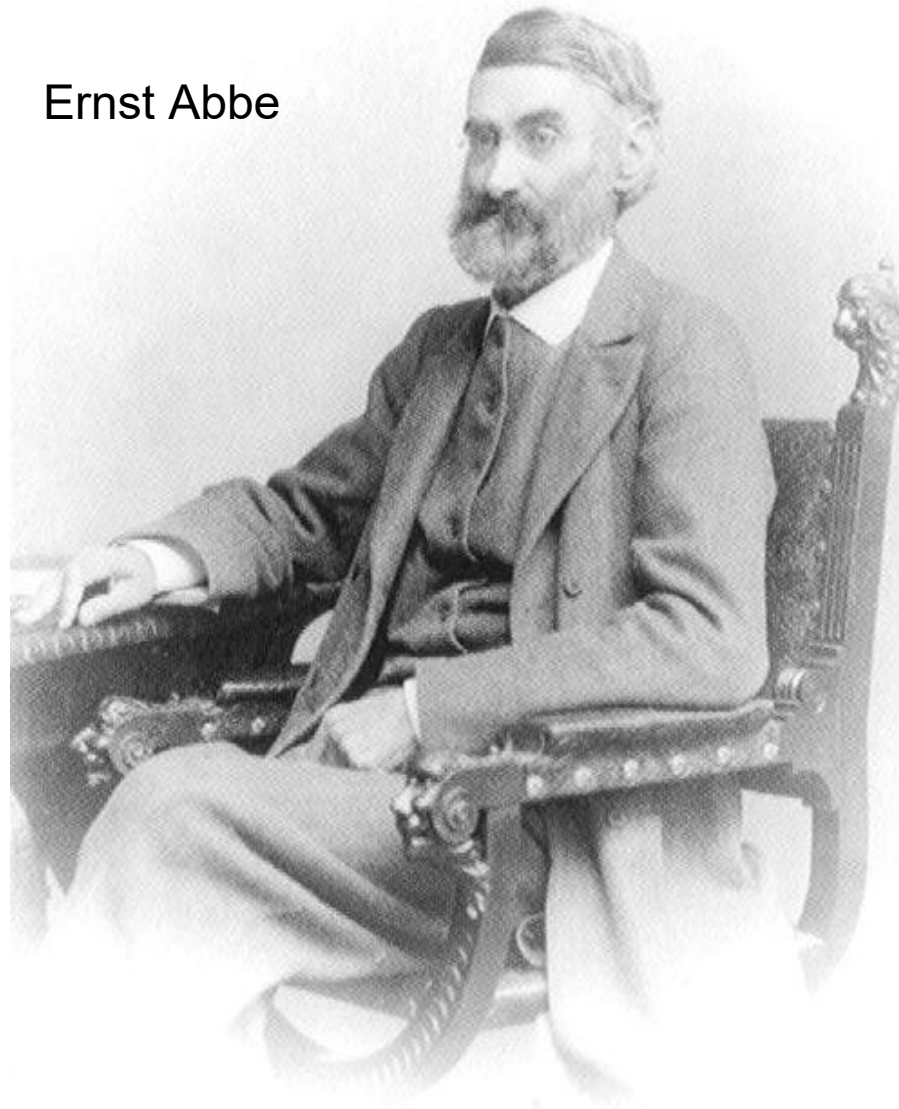
Speed at the expense of flexibility!

(a Fourier-Transform integration w/o FFT allows for different dimension input and output vector and non-equidistant phase steps)

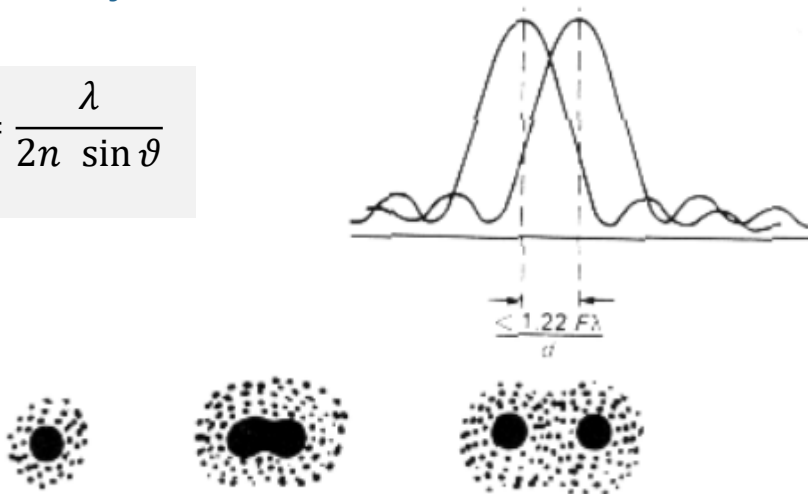


Abbe's theory of optical image-formation

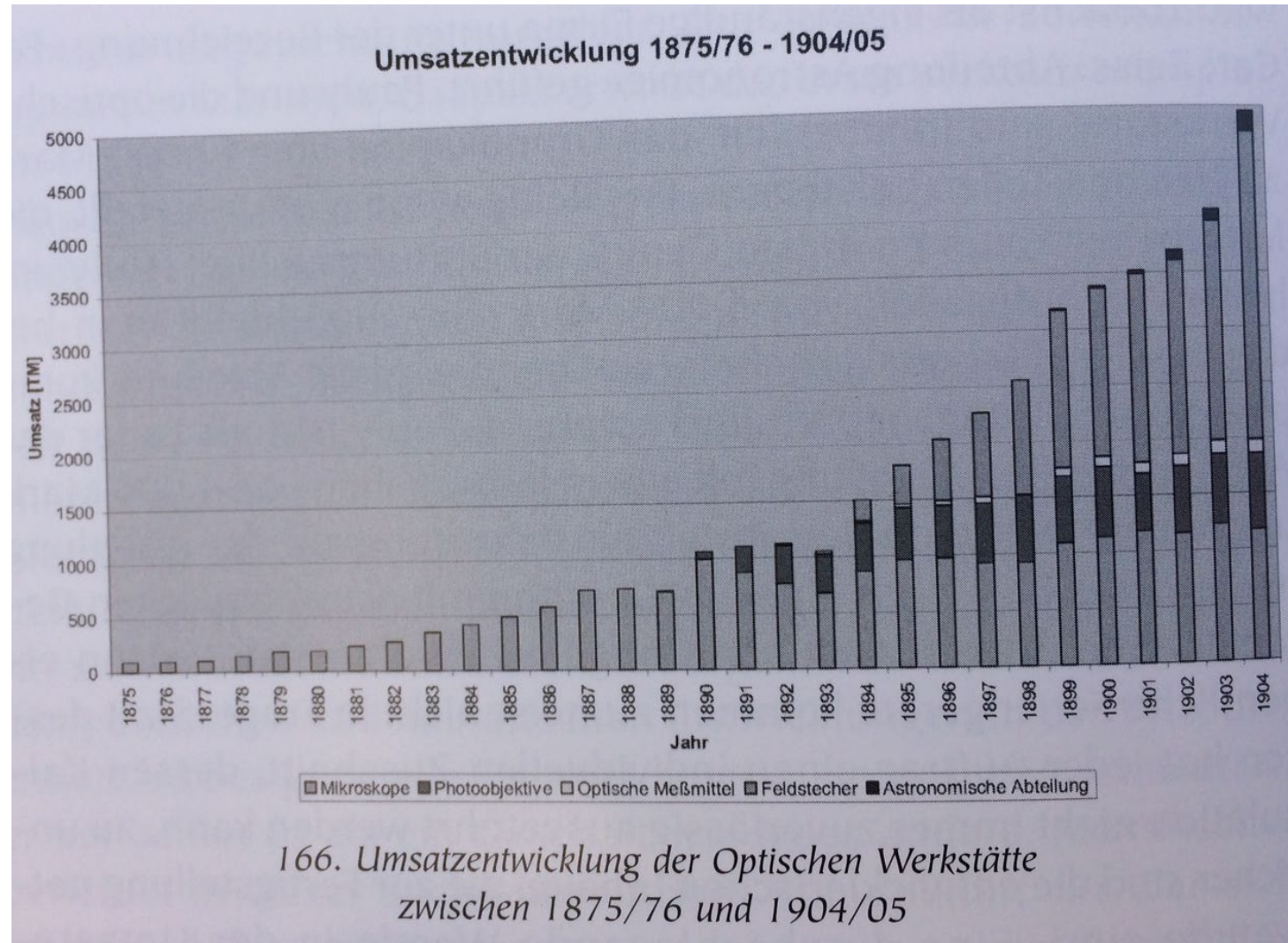
Ernst Abbe



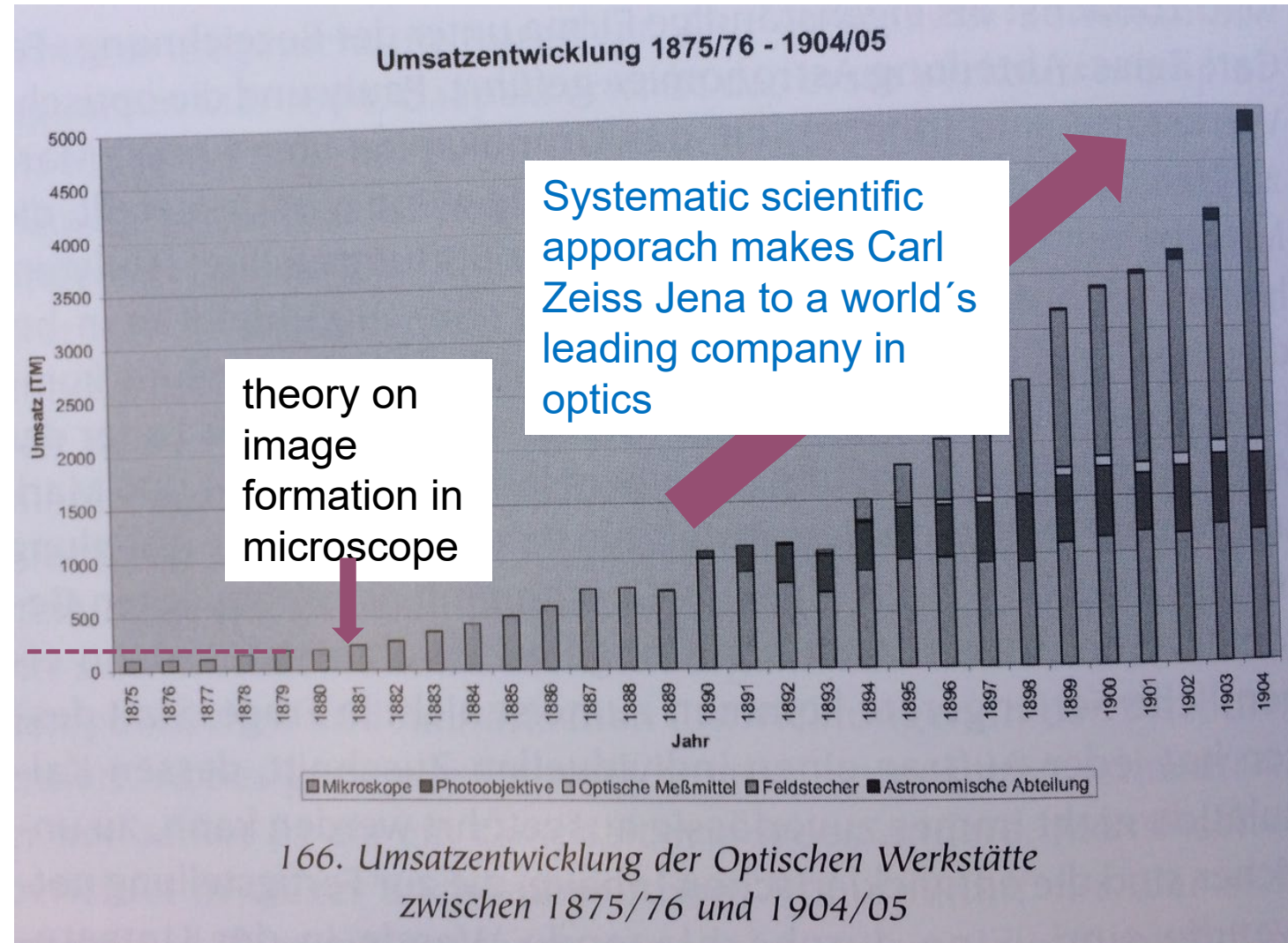
$$d = \frac{\lambda}{2n \sin \vartheta}$$



Zeiss revenue 1875 – 1905 (during Ernst Abbe's time in Zeiss company)



Zeiss revenue 1875 – 1905 (during Ernst Abbe's time in Zeiss company)



Source:
ZEISS-Archiv

Imaging with periodic structures (grating)

We consider a periodic 1D-object function

$$t_{ob}(\xi) = \sum_{j=-\infty}^{\infty} T_j \exp\left(i2\pi \frac{j}{p}\right)$$

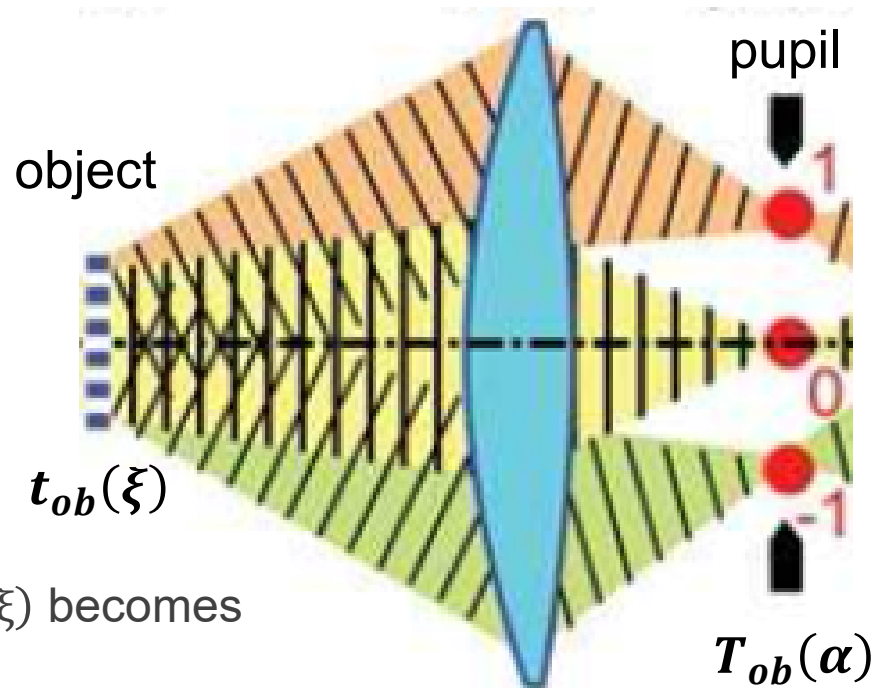
where the Fourier coefficients are computed by

$$T_j = \frac{1}{p} \int_{-\frac{p}{2}}^{\frac{p}{2}} t_{ob}(\xi) \exp\left(-i2\pi \xi \frac{j}{p}\right) d\xi$$

The amplitude spectrum in the lens pupil, the Fourier Transform of $t_{ob}(\xi)$ becomes

$$T_{ob}(\alpha) = FT(t_{ob})(\alpha) = \int_{-\infty}^{\infty} t_{ob}(\xi) \exp(-i2\pi w \alpha \xi) d\xi$$

$$= \frac{1}{p} \int_{-\frac{p}{2}}^{\frac{p}{2}} \sum_{j=-\infty}^{\infty} T_j \exp\left(i2\pi \xi \left(\frac{j}{p} - w\alpha\right)\right) d\xi = \frac{1}{p} \sum_{j=-\infty}^{\infty} T_j \delta\left(w\alpha - \frac{j}{p}\right)$$



Diffraction at a periodic amplitude-phase structure (grating)

Let's look at an amplitude-phase rectangular lattice with the amplitudes $0 \leq A_1, A_2 \leq 1$ and the relative phase shift φ . The transparency function of a phase slit of width B is

$$t_{ob}(\xi) = A_1 + [A_2 \exp(i\varphi) - A_1] \mathfrak{I}_{\{|\xi| \leq B/2\}}(\xi) \text{ with the indicator function } \mathfrak{I}_{\{|\xi| \leq B/2\}}(\alpha) = \begin{cases} 1, & \text{if } |\xi| \leq B/2 \\ 0, & \text{else} \end{cases}$$

The slit is chosen symmetrically to the optical axis. The object function is part of a grating with periodicity $p > B$. The Fourier coefficients are in general calculated according to:

$$T_j = \frac{1}{p} \int_{-\frac{p}{2}}^{\frac{p}{2}} t_{ob}(\xi) \exp\left(-i2\pi \xi \frac{j}{p}\right) d\xi$$

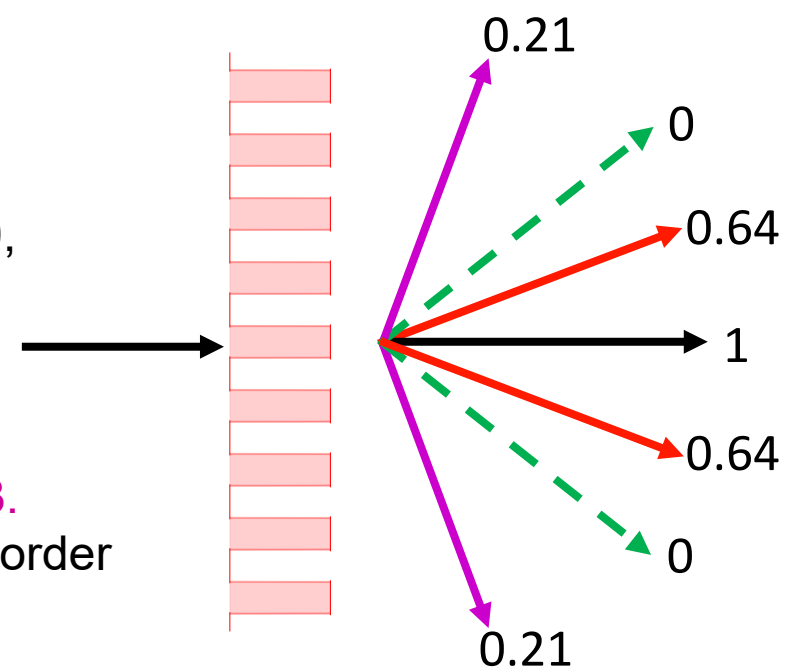
For our example we obtain

$$T_0 = A_1 + [A_2 \exp(i\varphi) - A_1] \frac{B}{p}$$

$$T_j = [A_2 \exp(i\varphi) - A_1] \operatorname{sinc}\left(\pi \frac{B}{p} j\right) \frac{B}{p} \quad \text{with } \operatorname{sinc}(x) \equiv \frac{\sin x}{x}$$

Example:
 $A_1=1, A_2=0,$
 $B/p=0.5$

0., 1., 2., 3.
diffraction order



Partially coherent imaging with periodic object

$$I(\mathbf{x}) = \iint d\mathbf{a} Q(\mathbf{a}) \left| \iint d\alpha L(\alpha) FT(t_{ob})(\alpha - \sigma \mathbf{a}) \exp(-i2\pi w \alpha \cdot \mathbf{x}) \right|^2$$

$$T_{ob}(\alpha - \sigma \mathbf{a}) = FT(t_{ob})(\alpha - \sigma \mathbf{a}) = \iint d\xi t_{ob}(\xi) \exp(i2\pi w (\alpha - \sigma \mathbf{a}) \cdot \xi)$$

For a periodic object $T_{ob}(\alpha - \sigma \mathbf{a}) = \frac{1}{p} \sum_{j=-\infty}^{\infty} T_j \delta\left(w(\alpha - \sigma \mathbf{a}) - \frac{j}{p}\right)$ the integral,

$$\left| \iint d\alpha L(\alpha) FT(t_{ob})(\alpha - \sigma \mathbf{a}) \exp(-i2\pi w \alpha \cdot \mathbf{x}) \right|^2 = \left| \iint d\alpha L(\alpha) \frac{1}{p} \sum_{j=-\infty}^{\infty} T_j \delta\left(w(\alpha - \sigma \mathbf{a}) - \frac{j}{p}\right) \exp(-i2\pi w \alpha \cdot \mathbf{x}) \right|^2$$

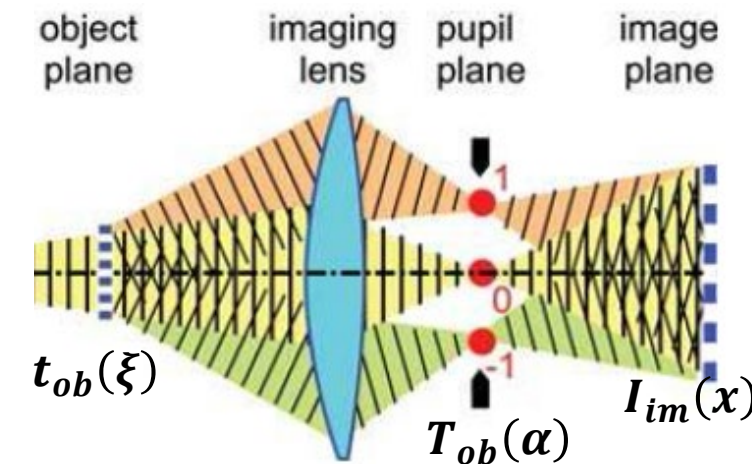
$$= \frac{1}{p^2} \left| \sum_{j=-\infty}^{\infty} L\left(\frac{\sigma}{w} \mathbf{a} + \frac{j}{w p}\right) T_j \exp\left(-i2\pi w \left(\sigma \mathbf{a} + \frac{j}{p}\right) \cdot \mathbf{x}\right) \right|^2$$

Interpretation:

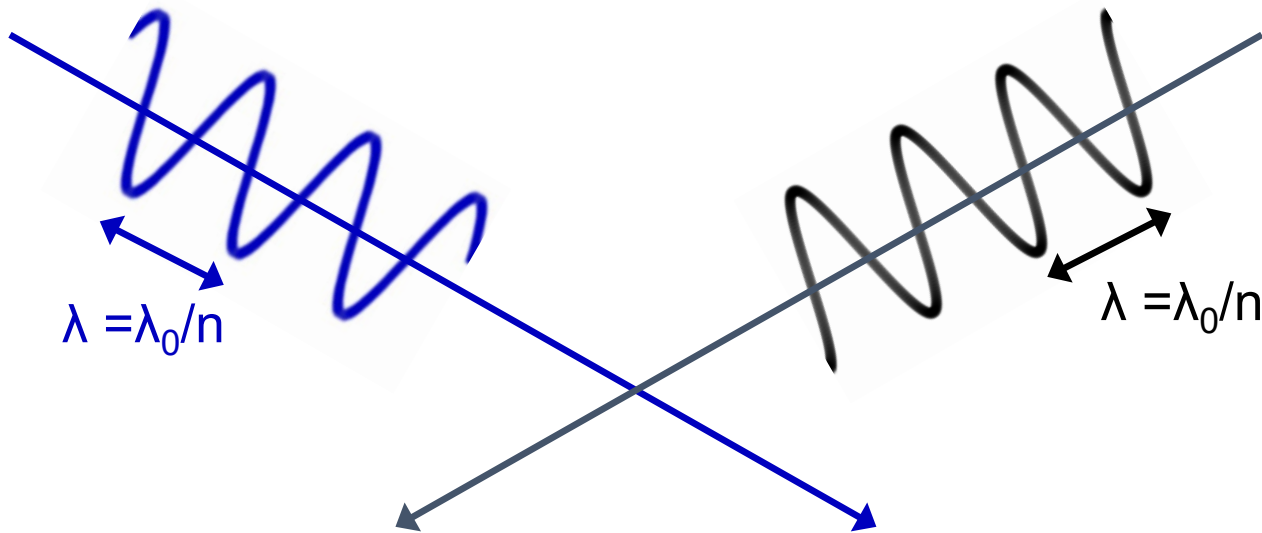
Finite pupil truncates
number of diffraction orders j
illumination direction

Plane waves from diffraction orders
enter the image plane and...

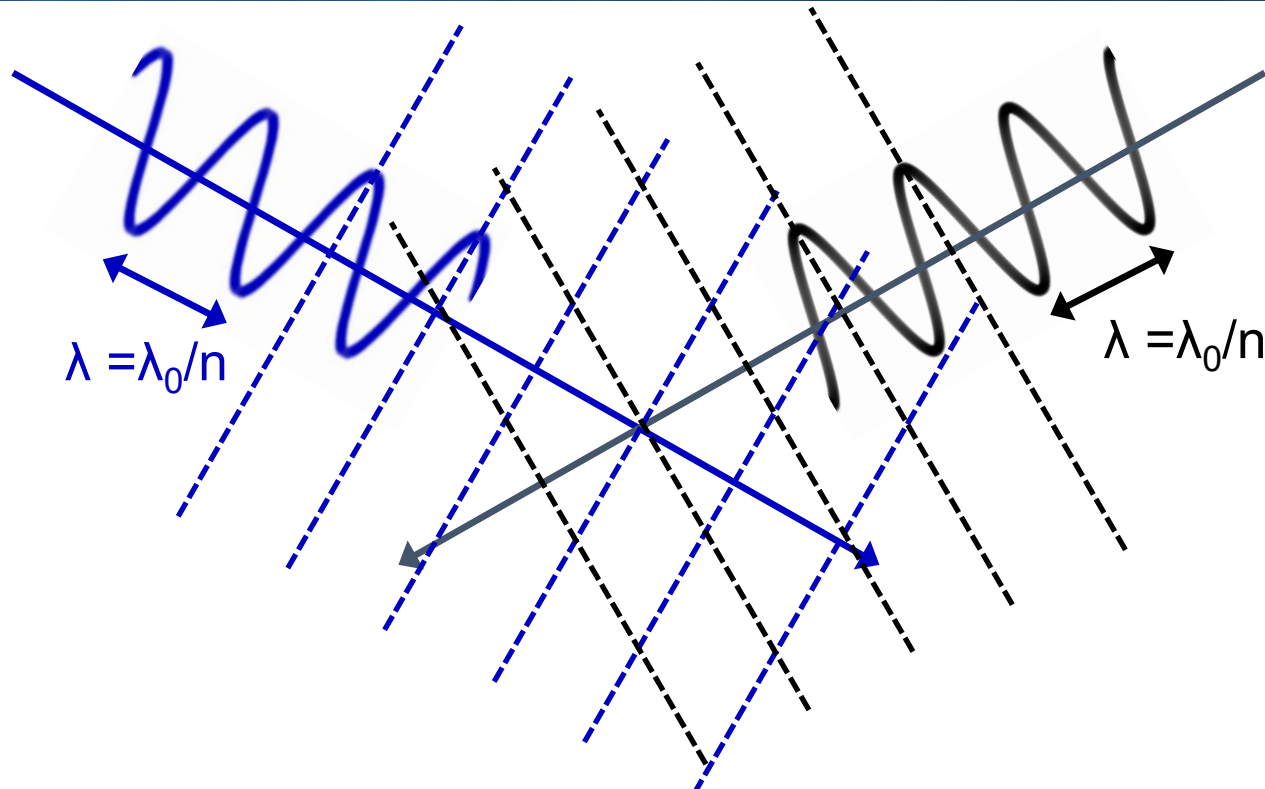
...and interfere
coherently
according to $| \dots |^2$



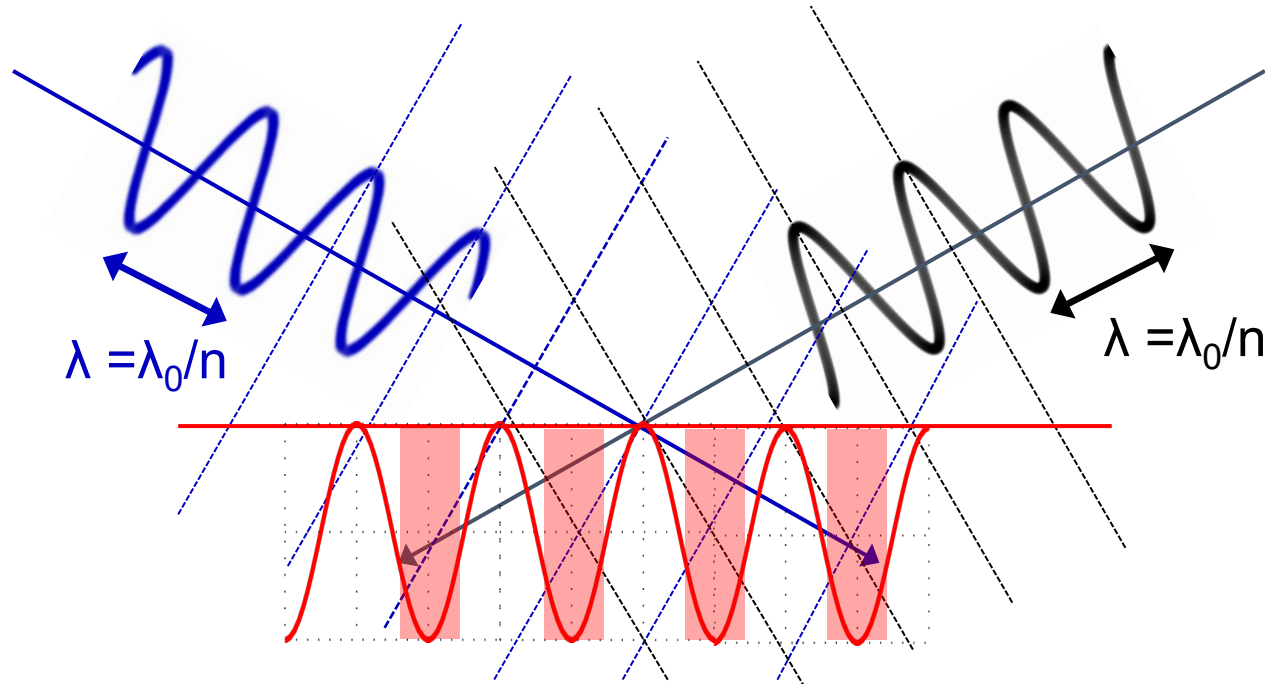
Periodic light intensity distribution by superposition of two light waves



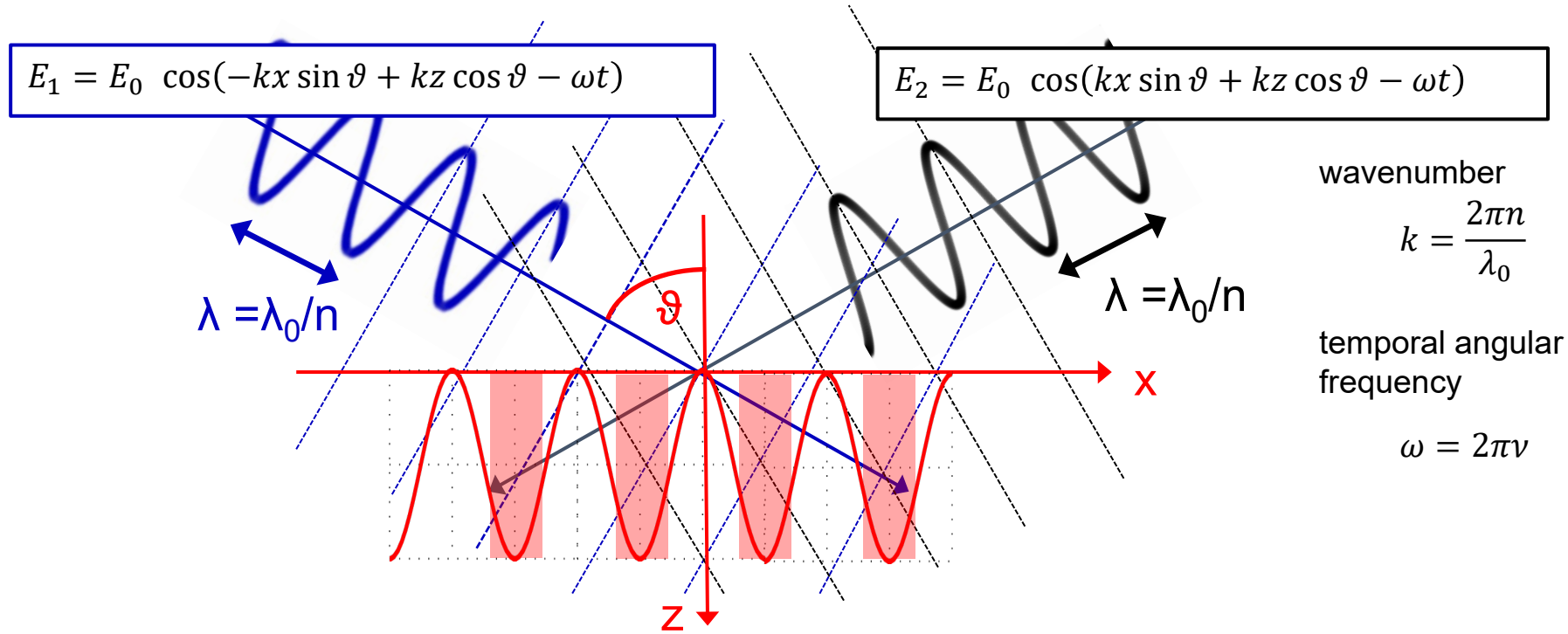
Periodic light intensity distribution by superposition of two light waves



Periodic light intensity distribution by superposition of two light waves



Periodic light intensity distribution by superposition of two light waves



$$E_{total} = E_1 + E_2 = E_0 \{ \cos(-kx \sin \vartheta + kz \cos \vartheta - \omega t) + \cos(kx \sin \vartheta + kz \cos \vartheta - \omega t) \}$$

intensity

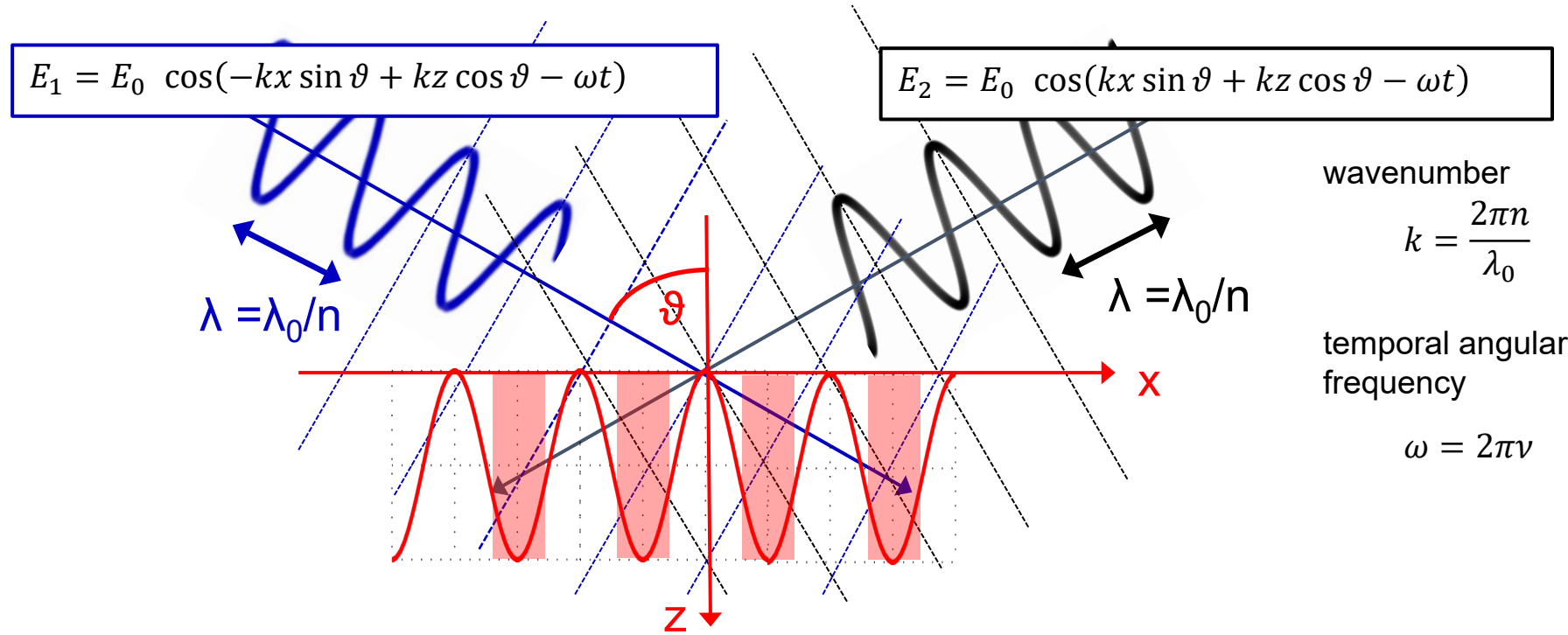
$$\langle E_{total}^2 \rangle = E_0^2 (1 + \cos(2kx \sin \vartheta)) = E_0^2 \left(1 + \cos \left(2\pi x \frac{2n \sin \vartheta}{\lambda_0} \right) \right)$$

$$(\cos \alpha \pm \cos \beta)^2 = \left(\frac{e^{i\alpha} + e^{-i\alpha}}{2} \pm \frac{e^{i\beta} + e^{-i\beta}}{2} \right)^2 = \frac{1}{2} (\cos 2\alpha + 1) + \frac{1}{2} (\cos 2\beta + 1) \pm \cos(\alpha + \beta) \pm \cos(\alpha - \beta)$$

wavenumber
 $k = \frac{2\pi n}{\lambda_0}$

temporal angular frequency
 $\omega = 2\pi\nu$

Periodic light intensity distribution by superposition of two light waves



$$E_{total} = E_1 + E_2 = E_0 \{ \cos(-kx \sin \vartheta + kz \cos \vartheta - \omega t) + \cos(kx \sin \vartheta + kz \cos \vartheta - \omega t) \}$$

intensity

$$\langle E_{total}^2 \rangle = E_0^2 (1 + \cos(2kx \sin \vartheta)) = E_0^2 \left(1 + \cos \left(2\pi x \frac{2n \sin \vartheta}{\lambda_0} \right) \right)$$

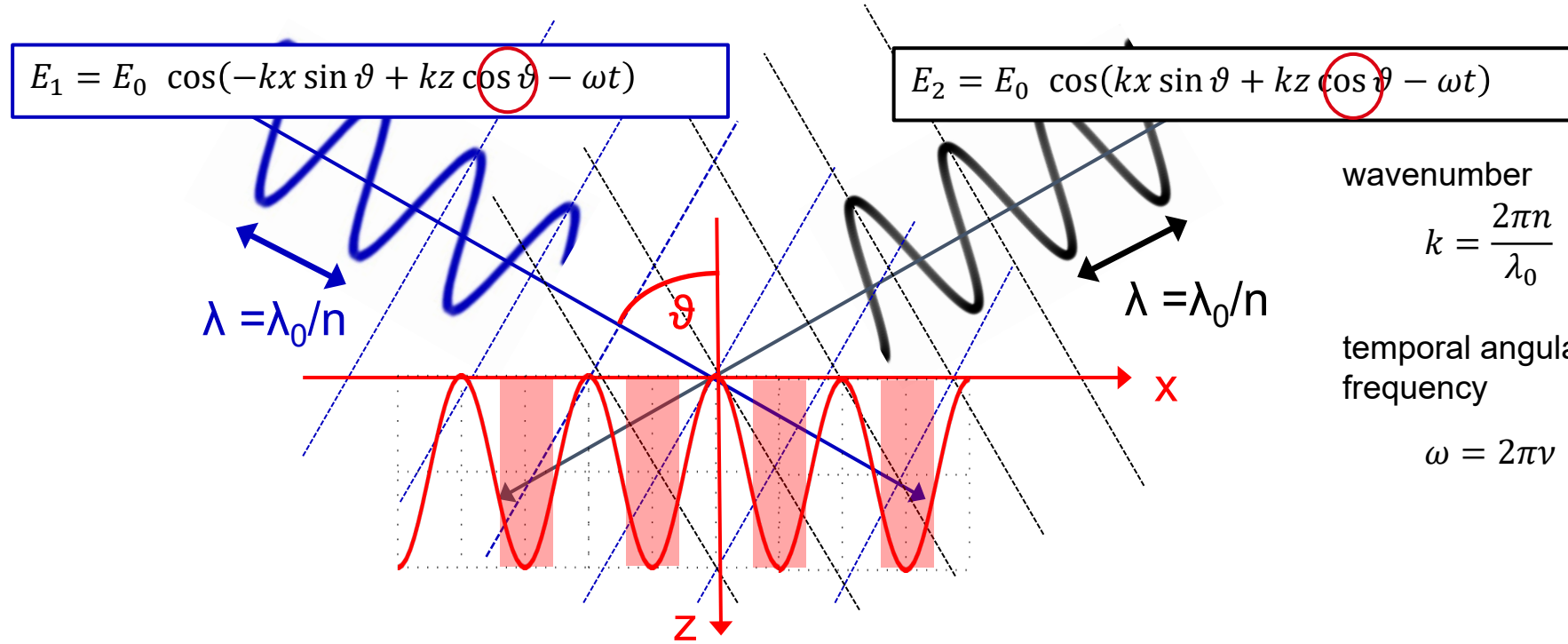
„half-pitch“

$$\frac{p}{2} = 0.25 \frac{\lambda_0}{n \sin \vartheta}$$

$$p = \frac{\lambda_0}{2n \sin \vartheta}$$

$$\frac{1}{p}$$

Periodic light intensity distribution by superposition of two light waves



$$E_{total} = E_1 + E_2 = E_0 \{ \cos(-kx \sin \vartheta + kz \cos \vartheta - \omega t) + \cos(kx \sin \vartheta + kz \cos \vartheta - \omega t) \}$$

3D intensity distribution

$$\langle E_{total}^2 \rangle = E_0^2 (1 + \cos(2kx \sin \vartheta)) = E_0^2 \left(1 + \cos \left(2\pi x \frac{2n \sin \vartheta}{\lambda_0} \right) \right)$$

wavenumber
 $k = \frac{2\pi n}{\lambda_0}$

temporal angular frequency
 $\omega = 2\pi\nu$

In general depth-of-field is object structure dependant!

The result does not depend on z ! We have infinite depth-of-field!

Coherent imaging with periodic object

$$I(\mathbf{x}) = \iint d\mathbf{a} Q(\mathbf{a}) \left| \sum_{j=-\infty}^{\infty} L\left(\frac{\sigma}{w} \mathbf{a} + \frac{j}{w p}\right) T_j \exp\left(-i2\pi w\left(\sigma \mathbf{a} + \frac{j}{p}\right) \cdot \mathbf{x}\right) \right|^2$$

Extended light source gives rise to diffraction orders which interfere and also to those (portions) which do not interfere – that expresses partially coherent imaging

We will come back to the partial coherent case soon, first let us assume, that the source is „infinitely small“:

$$Q(\mathbf{a}) = \delta(\mathbf{a} - \mathbf{a}_0).$$

For $\mathbf{a}_0=0$ we have on-axis illumination, otherwise off-axis illumination.

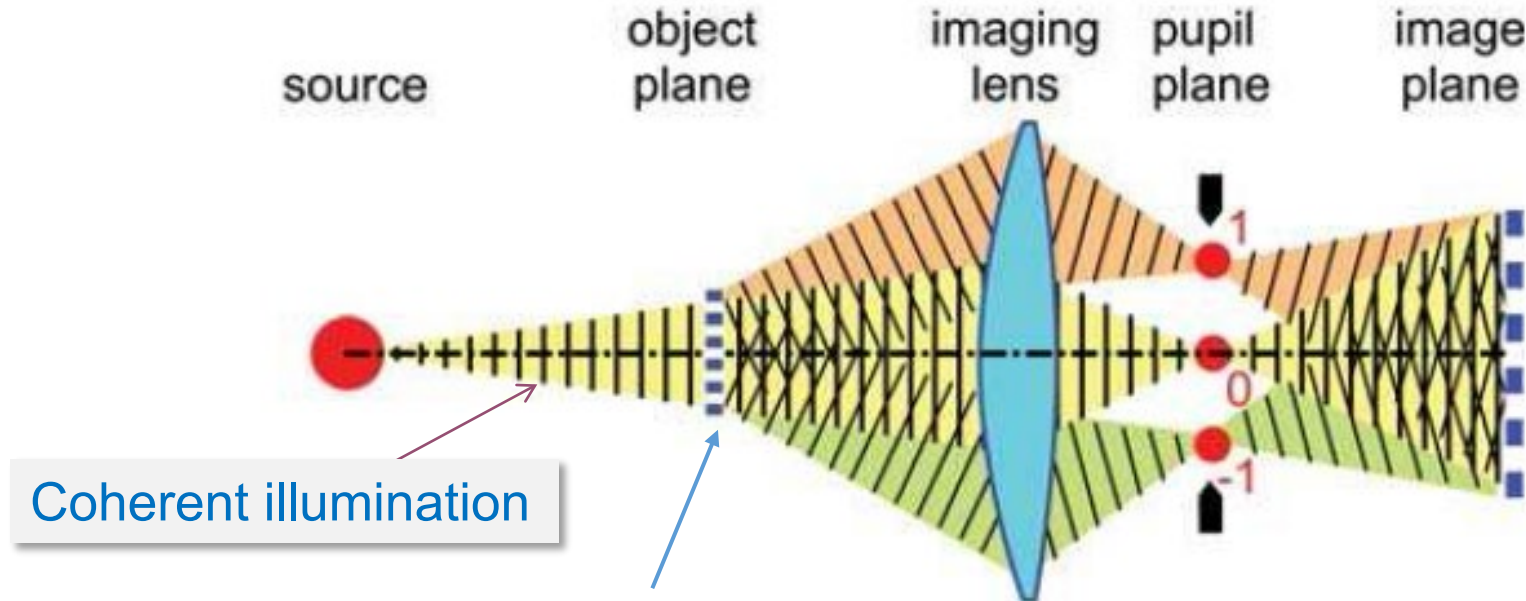
For on-axis illumination the intensity distribution is

$$I(\mathbf{x}) = \left| \sum_{j=-\infty}^{\infty} L\left(\frac{j}{w p}\right) T_j \exp\left(-i2\pi w \frac{j}{p} \mathbf{x}\right) \right|^2$$

The zeroth diffraction order is obviously located at $\alpha=0$, the first at $\alpha = \frac{1}{w p} = \frac{\lambda}{NA p}$.

As the pupil coordinates are normalized

Image formation in microscope (Abbe)



periodic object $t_{ob}(\xi) = \sum_{j=-\infty}^{\infty} T_j \exp\left(i2\pi \xi \frac{j}{p}\right)$

Image formation in microscope (Abbe)

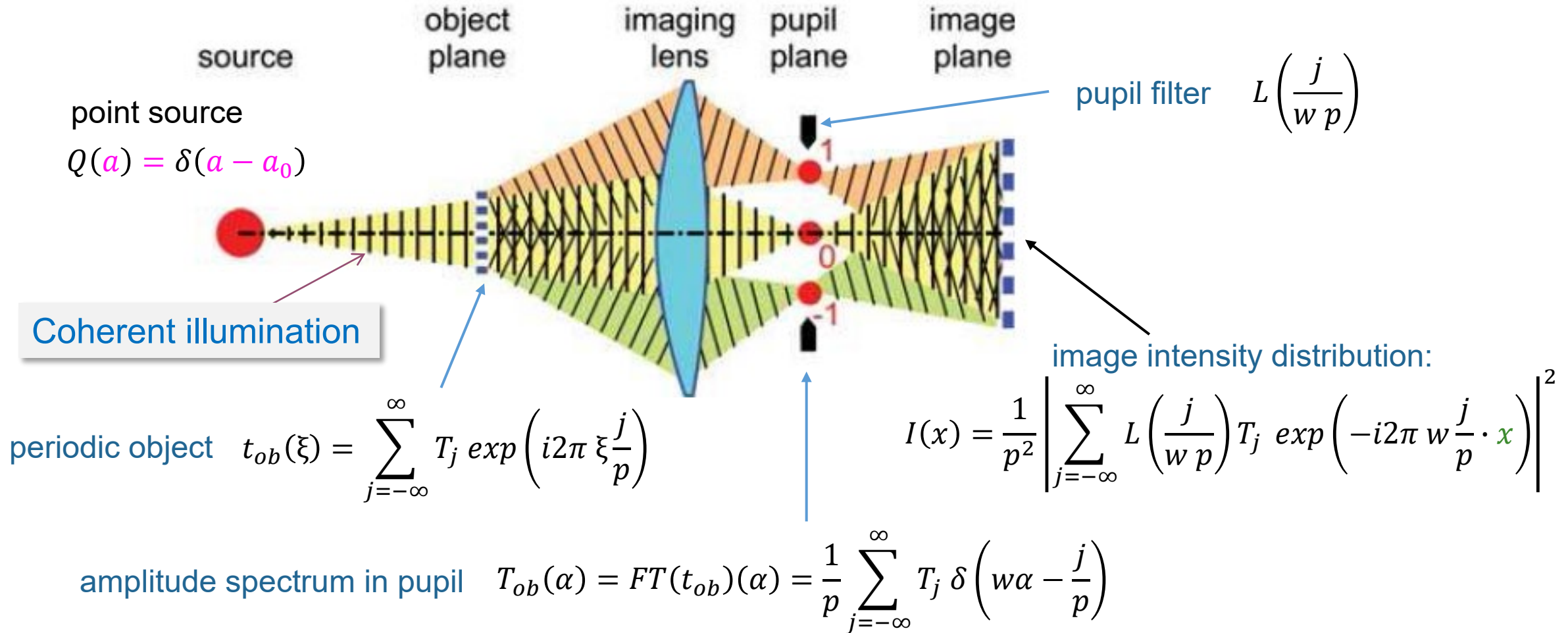


Image formation in microscope (Abbe)

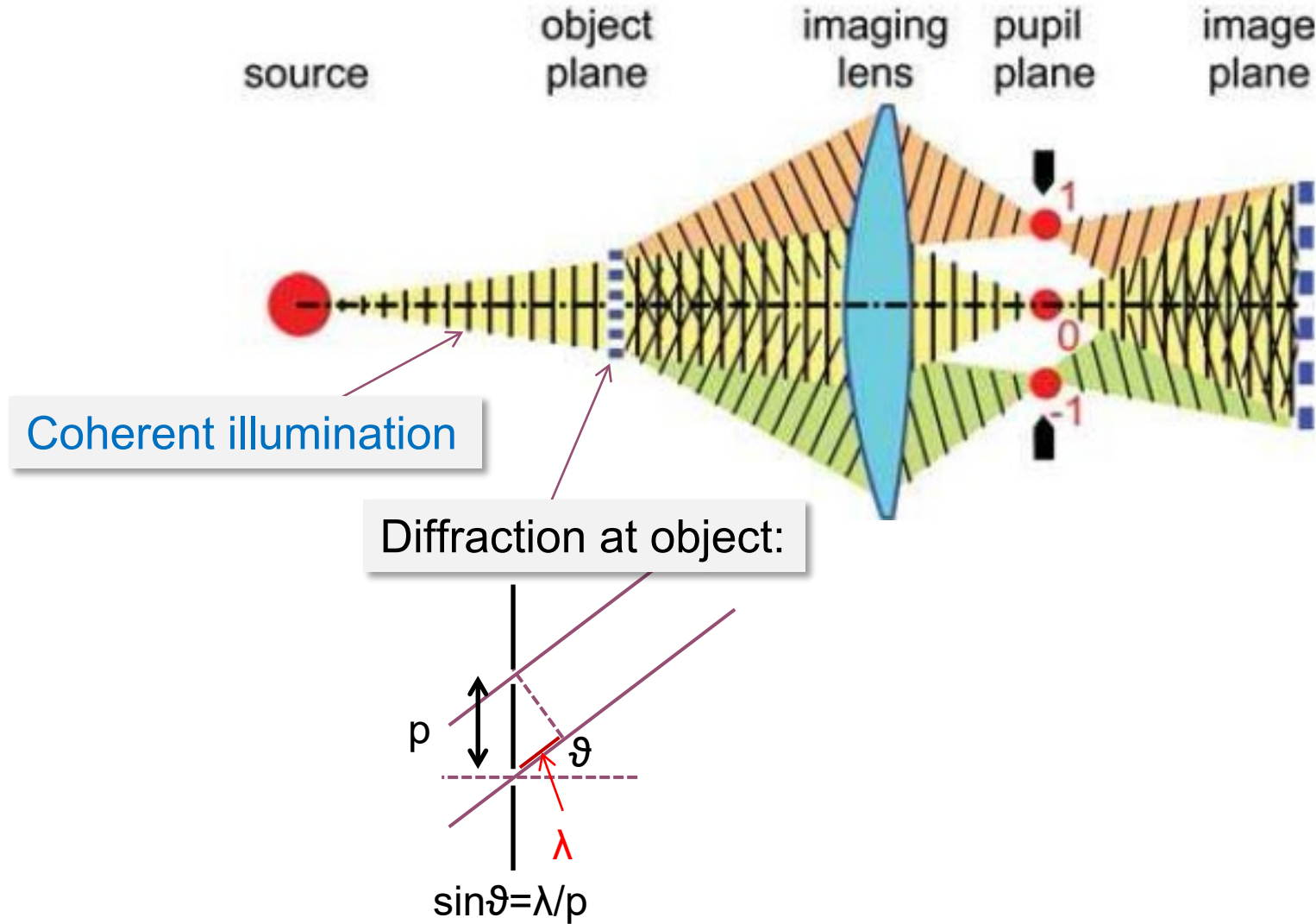


Image formation in microscope (Abbe)

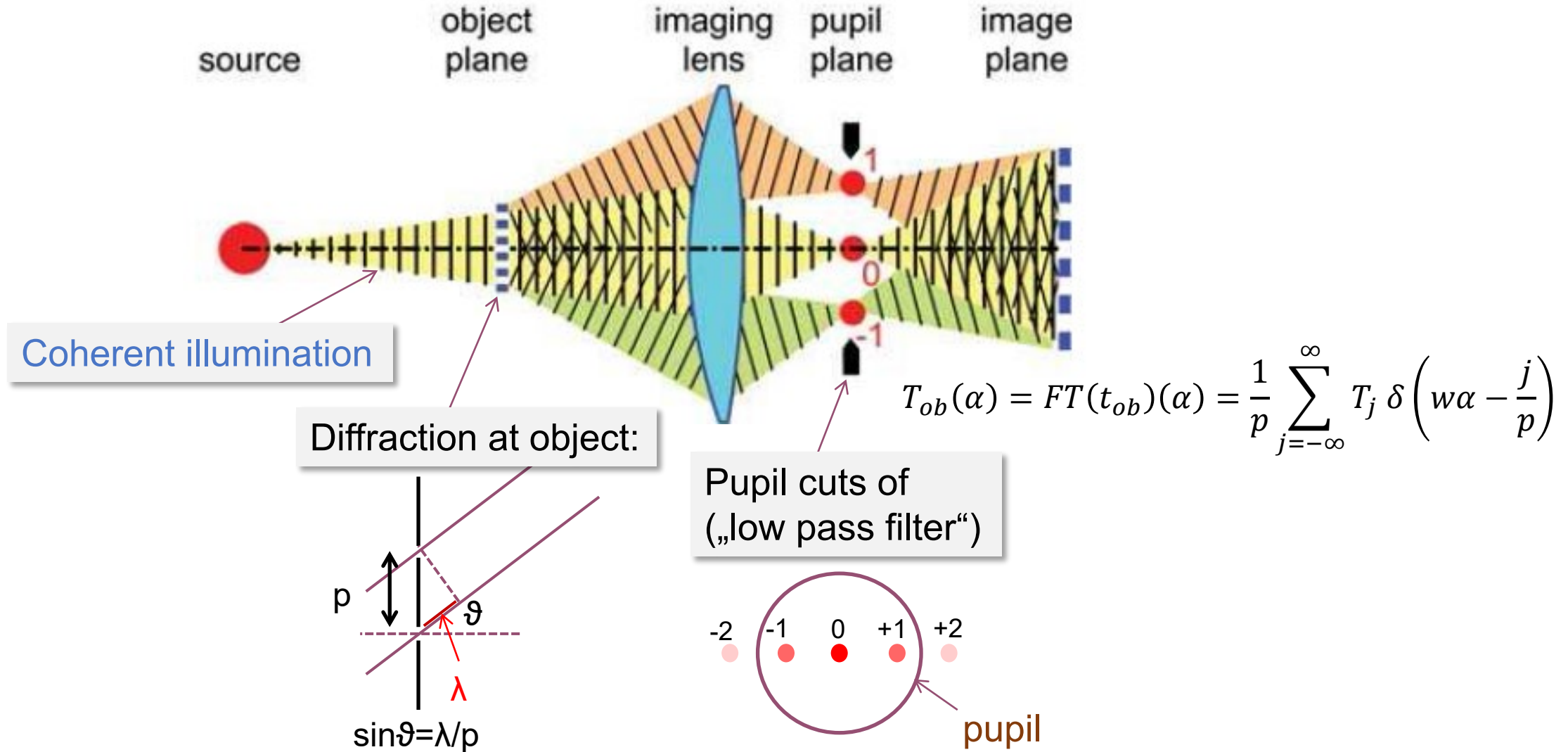


Image formation in microscope (Abbe)

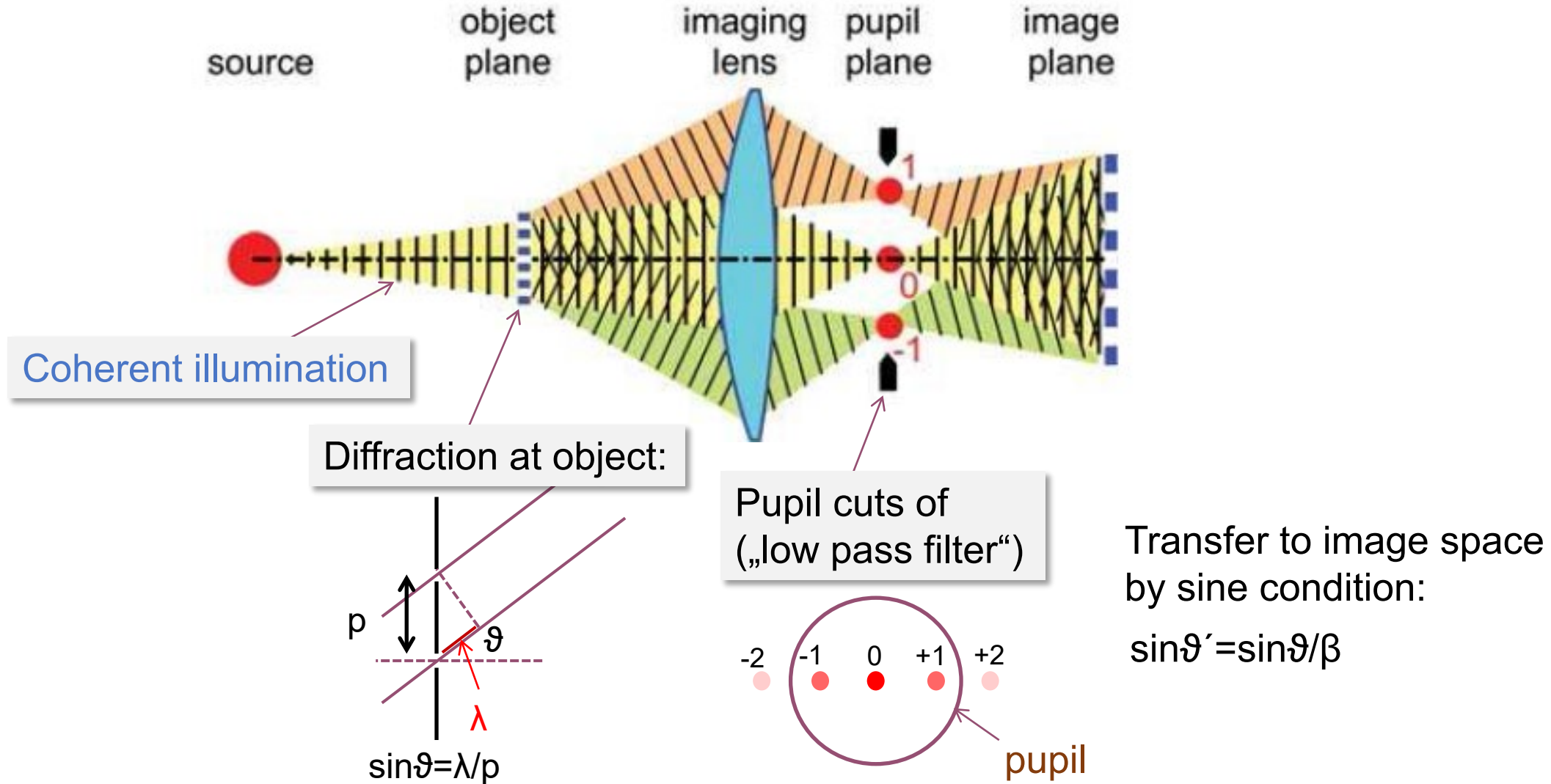


Image formation in microscope (Abbe)

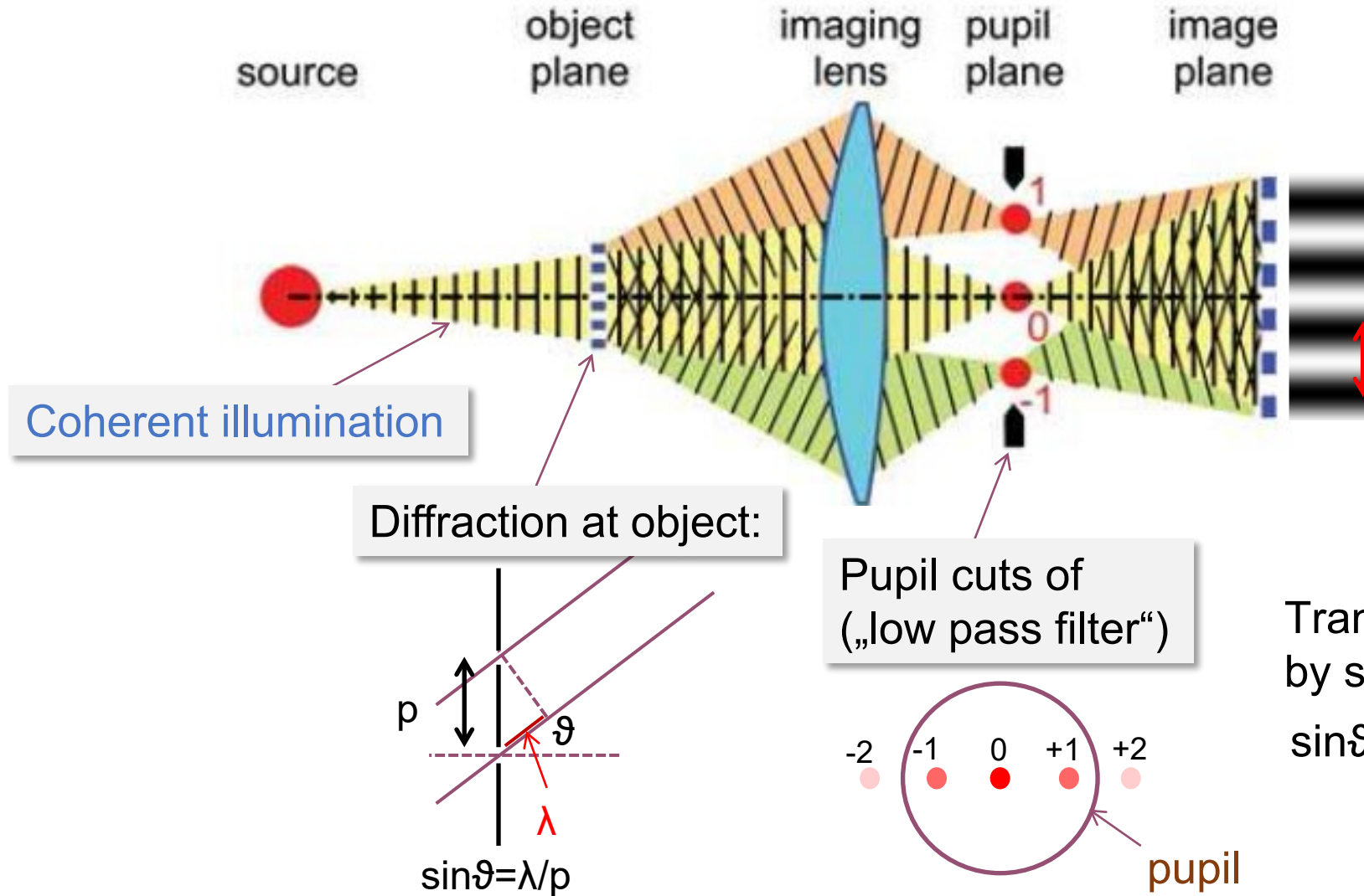


Image forms by interference
of waves in image space

Min. achievable
periodicity*: $p \geq \frac{\lambda}{\sin\vartheta'_{\max} \frac{\lambda}{NA'}}$

(coherent image formation)

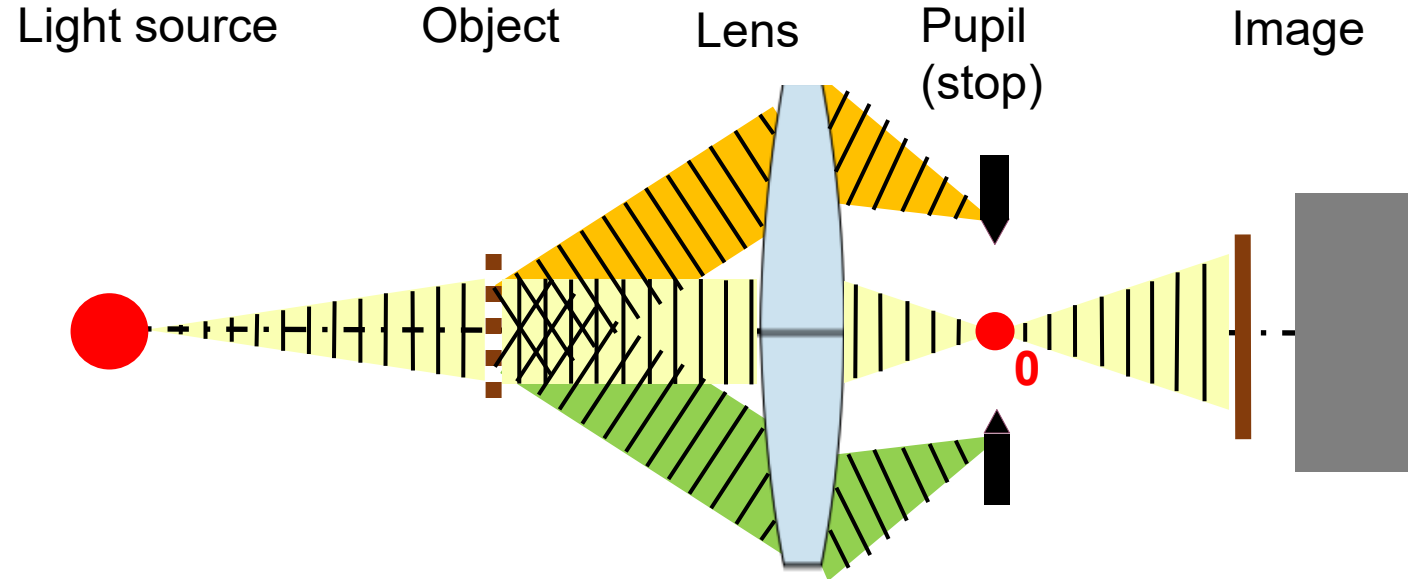
$$p \geq 2 \frac{\lambda}{\sin\vartheta'_{\max} \frac{\lambda}{NA'}}$$

(incoherent/ partially
coherent image formation.)

Transfer to image space
by sine condition:
 $\sin\vartheta' = \sin\vartheta/m$

*limited due min. two diffraction
orders need to pass the pupil

Image formation in microscope (Abbe)



If only one diffraction order arrives at the image there is no structure visible!

Image formation in microscope (Abbe)

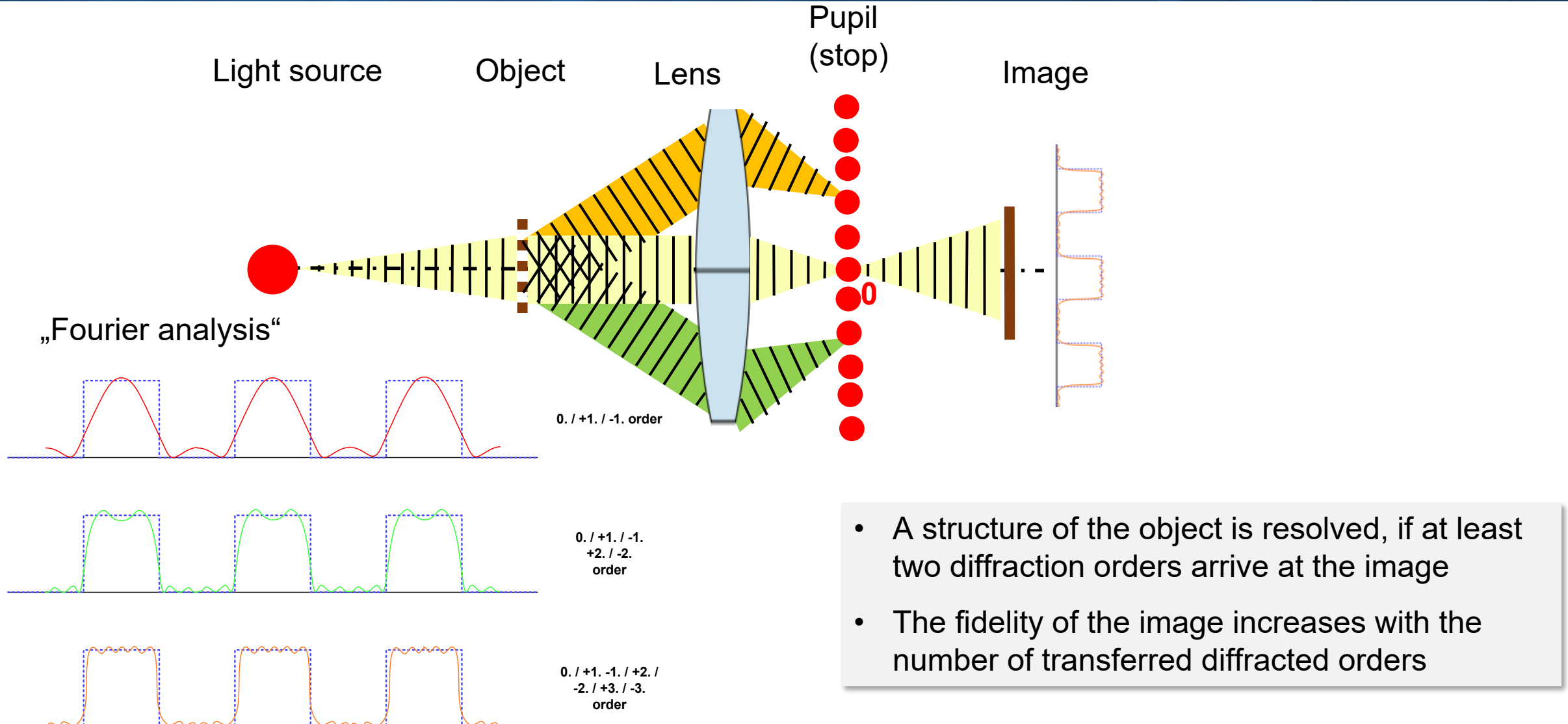
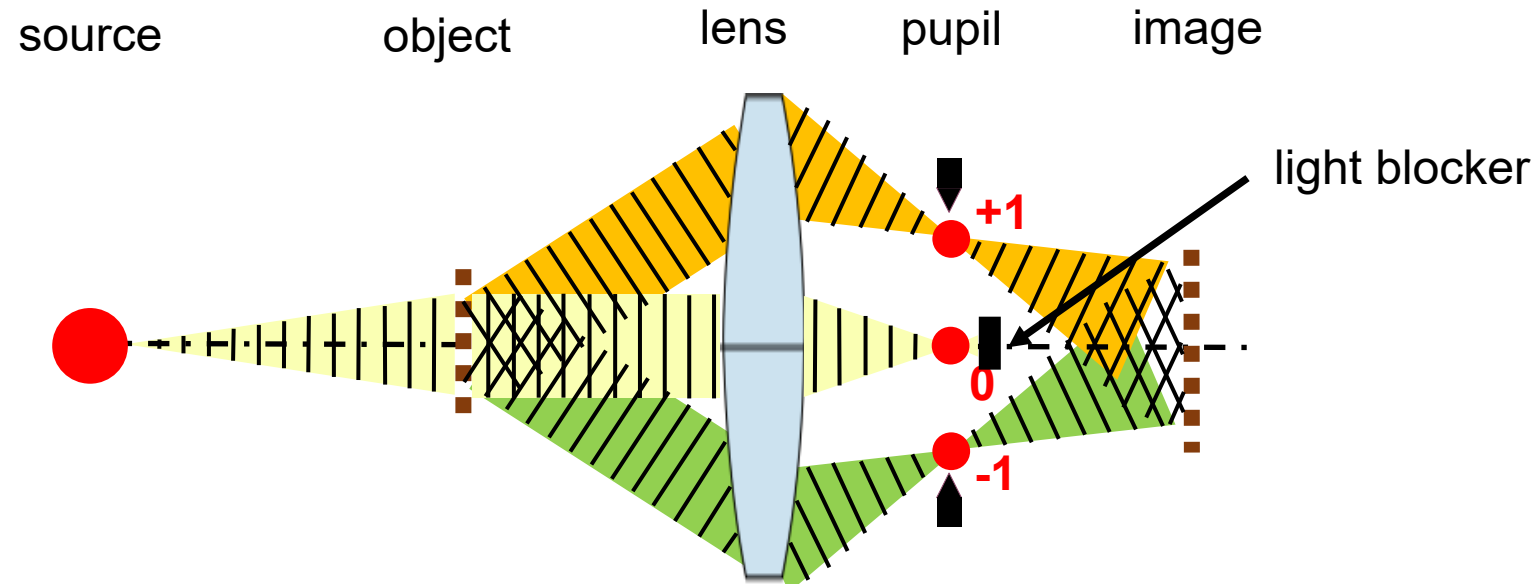


Image formation in microscope (Abbe)

Blocking 0th diffraction order in pupil



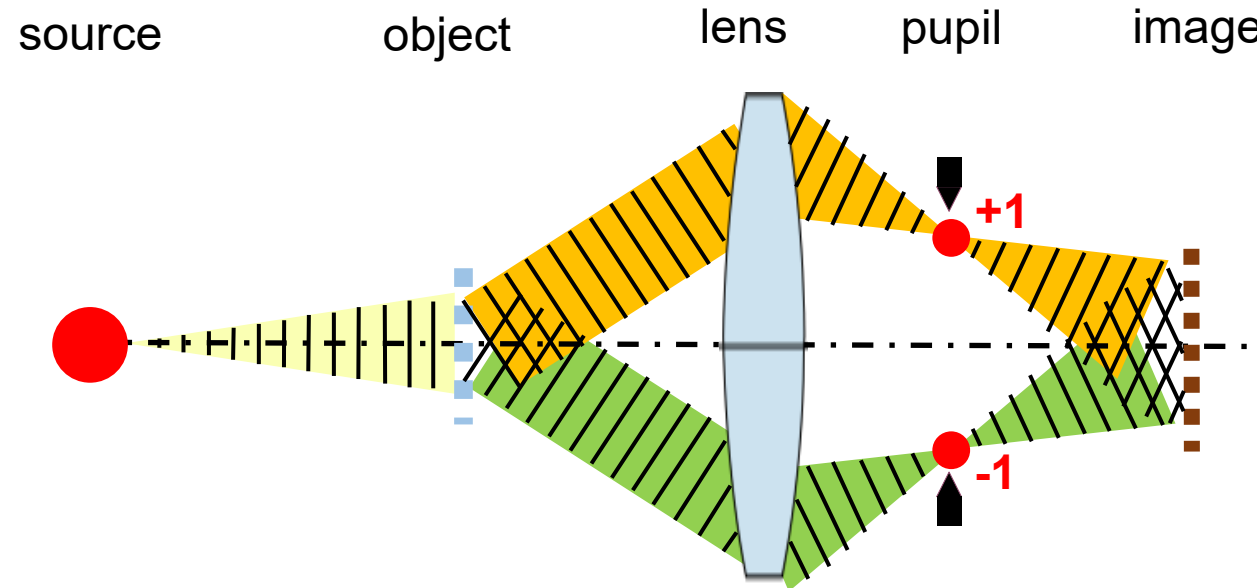
The intensity distribution in the image plane can be modified by modifications in the lens pupil plane (blocking light, transmission or phase distributions).

In given example we removed the 0th diffraction order by blocking light at the center of the pupil. Only +1st and -1st diffraction order contribute to image formation.

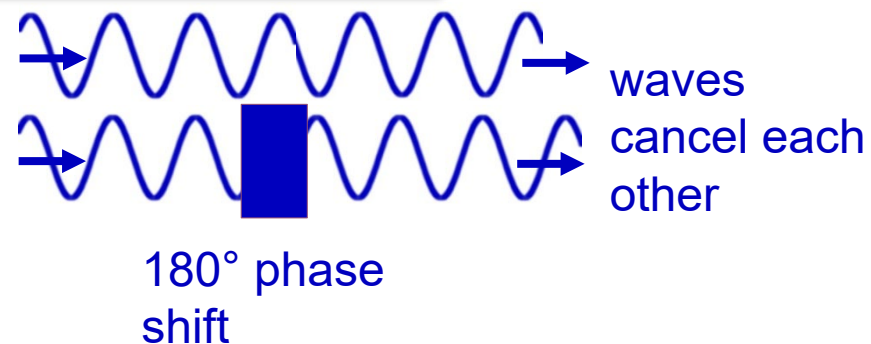
Mathematically light distributions in object or image plane to the pupil plane are related by Fourier Transforms. This is the basis for Fourier Optics.

Image formation in microscope

Phase object (180° phase shift)

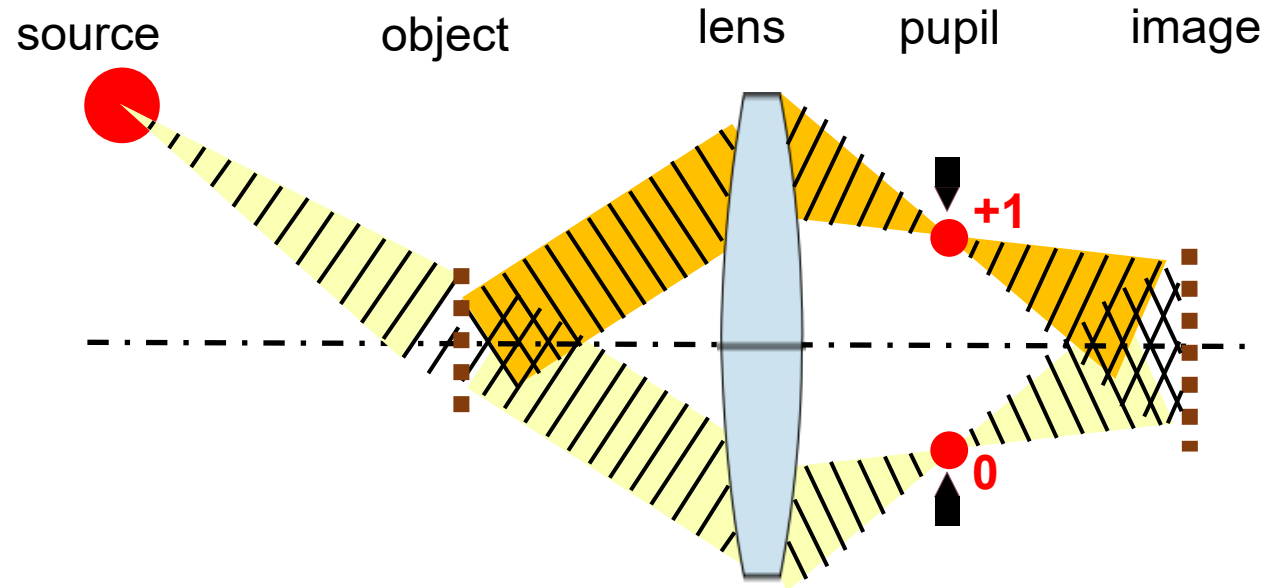


0th order vanishes:



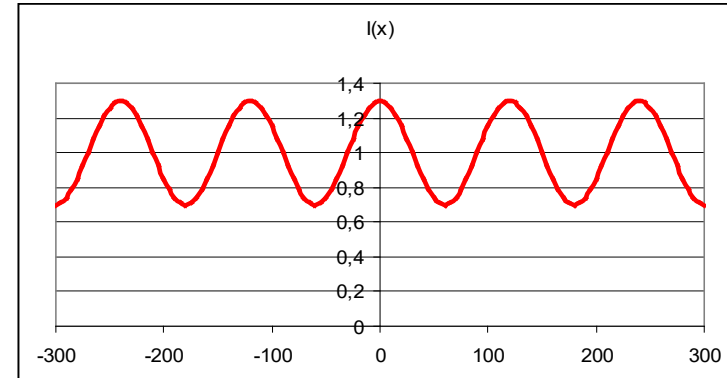
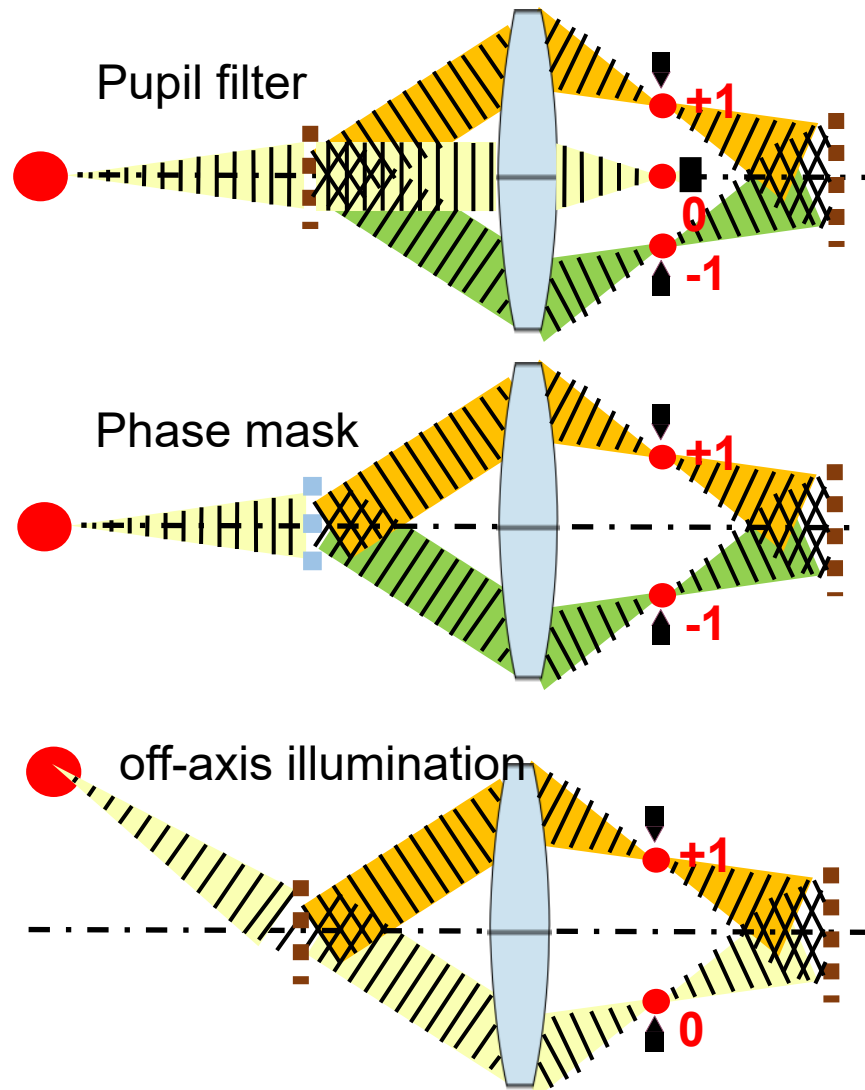
If the pitch of the phase grating is chosen two times the pitch of the transmission grating the ± 1 st diffraction orders enter the lens with the same angle.

Image formation Off-axis illumination



With off-axis illumination and a transmission grating two-beam interference in image plane is also realizable. (Intensity of 1st and 0th order can be made equal with attenuated phase shift masks giving maximum contrast).

Same intensity distribution with different methods



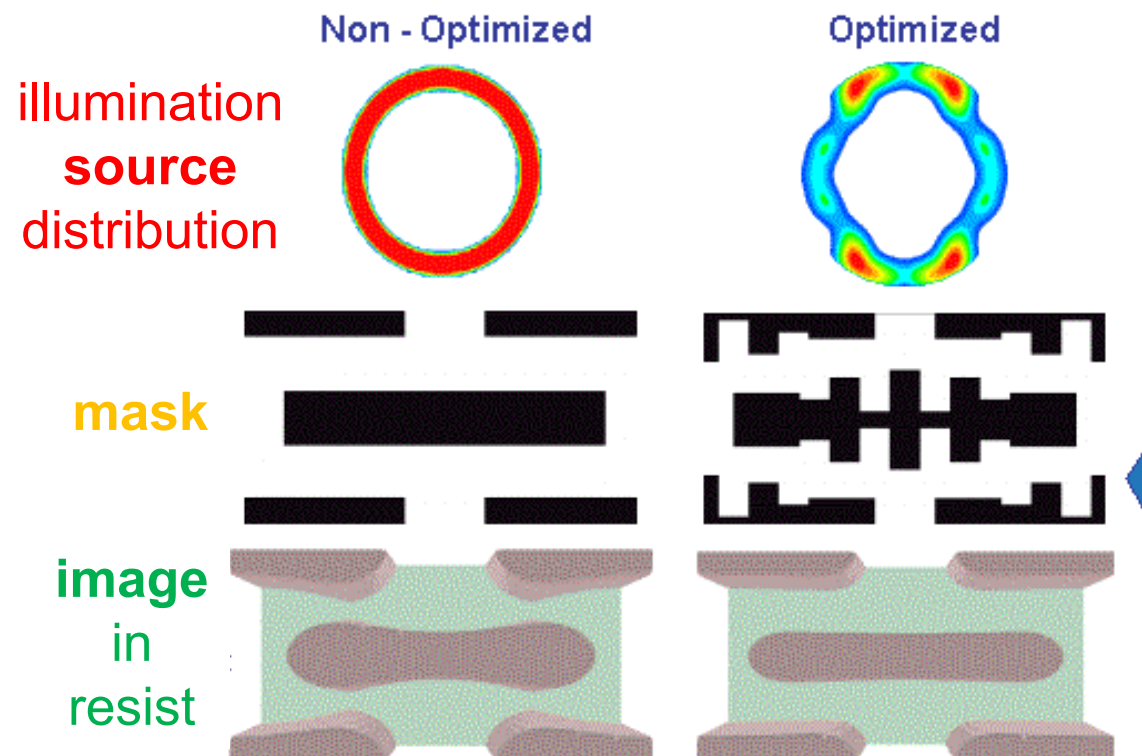
$$I(x)=I_0+I_1*\cos(2\pi x/p)$$

With all these different methods it is possible to achieve the same intensity distribution.

Combined mask and illumination source optimization in optical lithography

$$I(x, z) = \int da Q(a) \left| \int d\alpha L(\alpha, z) T_{ob}(\alpha - \sigma a) \exp(-i2\pi w\alpha \cdot x) \right|^2$$

image intensity illumination
distribution (desired source
pattern known) distribution
lens pupil (spectrum
of) mask



Optical Lithography for Chipmaking:
Inverse partially coherent imaging
problem to enabling and process-
optimizing printing of electronic
structures onto microchip.

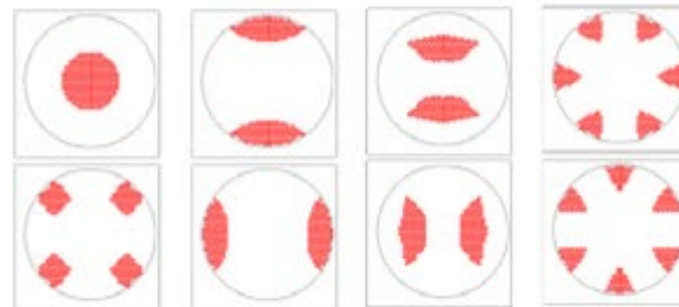
Note that for partially coherent imaging near diffraction limit the similarity of object and image structure is limited, typical undesired effects:

- corner rounding
- structure shortening
- undesired bridging
- variation of structure width

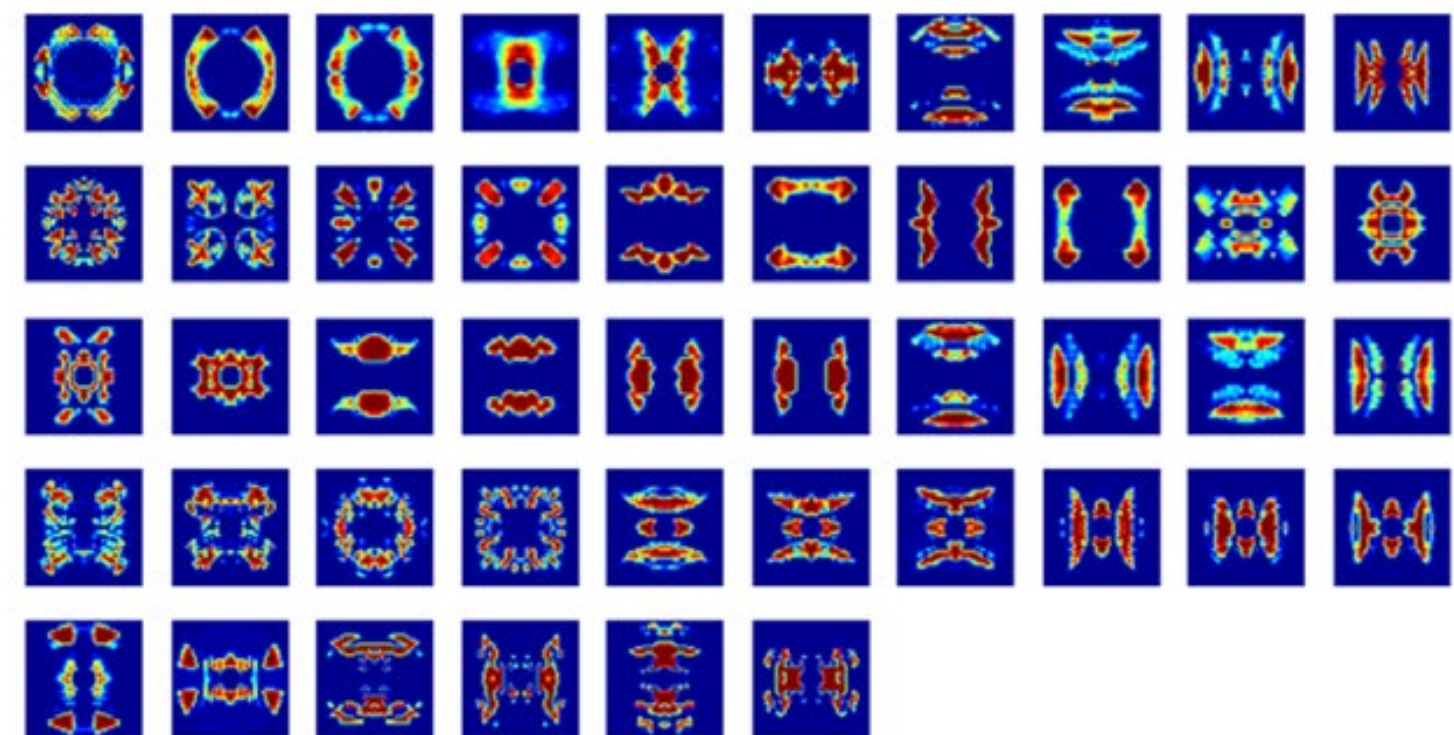
Complex illumination distributions for source-mask optimization in optical lithography

Lithography: “illumination settings” = intensity distribution in the illuminator pupil

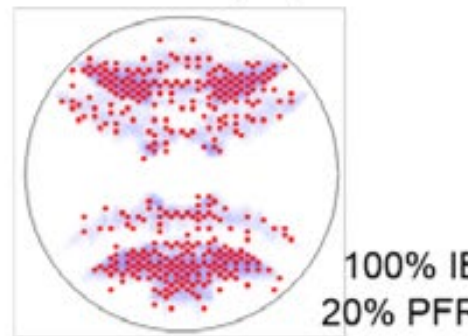
a) Sub-set of ‘standard settings’



c) Further examples of free-form pupil shapes

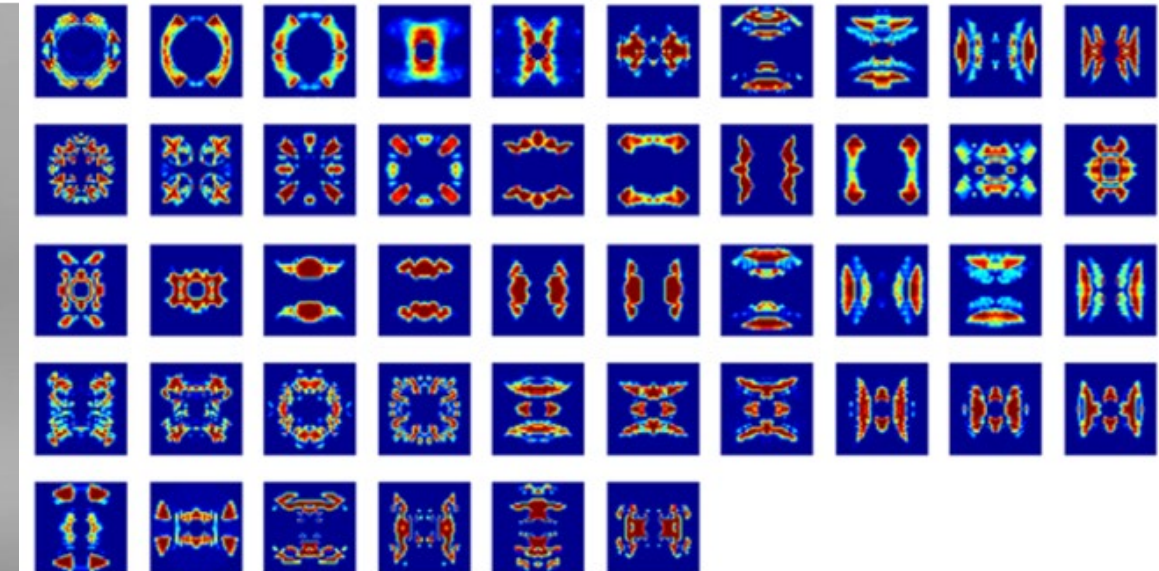
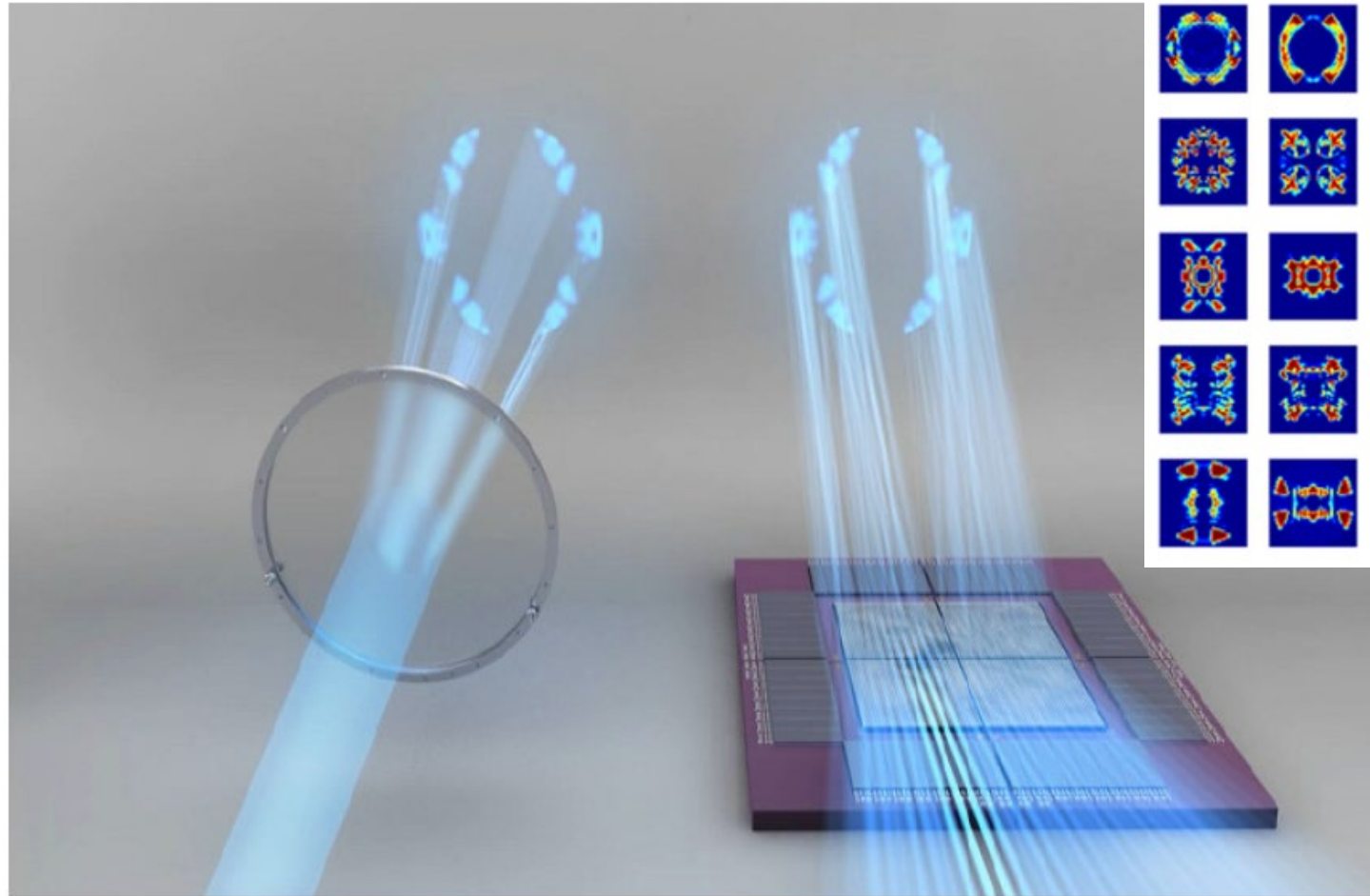


b) SMO free-form pupil



Realization principle of complex illumination distributions

Flexible illumination:
from Diffractive Optical Element (DOE)
to programmable illuminator using MEMs



- Born, M. / Wolf, E. (1999). *Principles of Optics*, Cambridge University Press. (1st ed. 1959)
- Goodman, J. W. (1985). *Statistical Optics*, J. Wiley & Sons, New York.
- Goodman, J. W. (1996). *Introduction to Fourier Optics*, McGraw-Hill, San Francisco (1st ed. 1968).
- Hopkins, H. H. (1951). *The concept of partial coherence in optics*, Proc. Roy. Soc. (London) A **208**, S. 263-277.
- Hopkins, H. H. (1953). *On the diffraction theory of optical images*, Proc. Roy. Soc. (London) A **217**, S. 408-432.
- Lohmann, A. W. (2006). *Optical Information Processing*. Universitätsverlag Ilmenau.
- Marathay, A. S. (1982). *Elements of Optical Coherence Theory*, J. Wiley&Sons, New York.
- Nasse, H. H. (2008/09). How to read MTF curves I & II. ZEISS Lenspire.
- Singer, W., Totzeck, M., Gross, H.: Handbook of Optical Systems, Bd. 2
- Zernike, F. (1934). *Beugungstheorie des Schneidenverfahrens und seiner verbesserten Form, der Phasenkontrastmethode*, Physica (The Hague) **1**, S. 689-704.
- Zernike, F. (1938). *The concept of degree of coherence and its application to optical problems*, Physica (The Hague) **5** (8), S. 785-795.

- Imaging models and their software implementation exist both purely based on ray-tracing (without diffraction) and including diffraction for partially coherent , coherent and non-coherent illumination
- The principle of ray path duality allows for alternative interpretation of optical system layouts from the perspective of either field or pupil characteristics
- In coherence theory the optical field $V(r,t)$ is modeled as random variable of a stochastic process
- It is convenient to use complex instead of real functions to represent the optical field as phase operations of the system can explicitly be expressed as linear operators (multiplication of complex exponentials)
- The analytical signal of Gabor represents the field $V(r,t)$ as decomposition of its harmonics by a Fourier Transform physically meaningful with positive frequencies only
- The coherence function, $\Gamma(P_1, t_1, P_2, t_2) = \left\langle \vec{E}(P_1, t_1) \cdot \overline{\vec{E}(P_2, t_2)} \right\rangle$, the correlation function of the electrical field includes the intensity as $I = \Gamma(P_1, t_1, P_1, t_1) = \left\langle \vec{E}(P_1, t_1) \cdot \overline{\vec{E}(P_1, t_1)} \right\rangle$. The brackets are either time averages or ensemble averages over all realizations of the stochastic variables. Unlike the electrical field, Γ and I are measurable

- As the field itself, the coherence function also fulfills the Helmholtz-equations and therefore propagation laws obtain the same form as in diffraction models for the electric field (e.g., Rayleigh-Sommerfeld diffraction theory)
- Approximations need to be made to in general propagate the coherence function coherence function via complex optical system
- In Fresnel approximation the phase function of the field is approximated up to second order
- An optical system can be modeled in Fresnel approximation using the paraxial focus conditions in the quadratic phase terms
- For a focused optical system the transfer between object to pupil and pupil to image is a (inverse) Fourier Transform respectively and the diffraction in the pupil (stop of finite size) acts as a low pass filter
- The transition to high aperture systems is to generalize the pupil to large angles with sine scaling of the pupil coordinates for aplanatic, incorporating a field-and pupil dependent pupil function $L(\xi, \alpha)$ and eventually also a Jones pupil including all electrical field components
- Partially coherent imaging to model image formation in microscopy or lithography requires at least 6 integrals

- A significant simplification in computational effort of the imaging equations is done by assuming spatial stationarity, that is that either $L(\xi, \alpha) = L(\alpha)$ or $K(x, \xi) = K(x - \xi)$, which is in general only valid for limited regions within the field-of-view
- Special cases of Abbe's imaging theory which yield the famous resolution criteria of resolvable feature size dependence of $\frac{\lambda}{NA}$ result as well as a Filter model that discrete diffraction orders passing the pupil giving rise to harmonic components of the intensity distribution $I(\textcolor{green}{x}) = \left| \sum_{j=-\infty}^{\infty} L\left(\frac{j}{w p}\right) T_j \exp\left(-i2\pi w \frac{j}{p} \textcolor{green}{x}\right) \right|^2$
- The combination of different light source distribution and object distribution (e.g. parameters of amplitude/phase gratings) can be varied to achieve the same intensity distribution; an optimization of both can also improve the image towards a desired distribution (e.g. source-mask optimization in optical lithography)